9-1-2016

Grid Integration of Intermittent Renewable Generation: Markovian and Interval Optimization Approaches

Yaowen Yu
University of Connecticut - Storrs, yuyaowen1988@gmail.com

Grid Integration of Intermittent Renewable Generation: Markovian and Interval Optimization Approaches

Yaowen Yu, PhD

University of Connecticut, 2016

With major initiatives promoting renewable energy, effective and robust integration of intermittent renewable generation into the grid becomes an important issue. The problem is challenging in view of renewable uncertainty, possible transmission congestions, and unexpected transmission and generator outages (contingencies). To overcome the above difficulties, this dissertation focuses on two critical operation processes in wholesale electricity markets: unit commitment (UC) and economic dispatch (ED). Three novel Markovian and interval approaches for UC problems and one new contingency filtering approach for the ED problem have been developed:

1. *A pure Markovian approach for stochastic UC without transmission constraints.* A stochastic UC problem has been innovatively formulated based on renewable states instead of scenarios. The advantage of this formulation is that the state at a time instant summarizes the information of all previous instants in a probabilistic sense for reduced complexity.

2. *A hybrid Markovian and interval approach for transmission-constrained UC.* To avoid the complexity of explicitly considering a large number of combinations of distributed renewable states, interval optimization has been synergistically integrated with the Markovian approach. Constraints are innovatively formulated to guarantee solution feasibility for all possible combinations of states without much complexity and over-conservativeness.

3. *An interval optimization approach for contingency-constrained UC.* A large number of transmission contingencies are innovatively described by treating corresponding generation shift factors (GSFs) as

uncertain parameters varying within intervals. To ensure solution robustness, bounds of GSFs and renewables in different types of constraints are captured based on interval optimization.

4. *A contingency filtering approach for corrective security-constrained ED.* Our approach, consisting of the decomposition and coordination method, and enhancements by novel warm-start of subproblem models and by parallel computing, is scalable for corrective security-constrained ED problems. Instead of always removing conflicting contingencies as in existing papers, our approach offers system operators an important option to keep them for increased reliability, enabled by identifying multiple conflicting contingencies simultaneously.

Grid Integration of Intermittent Renewable Generation: Markovian and Interval Optimization Approaches

Yaowen Yu

B.S., Huazhong University of Science and Technology, Wuhan, China, 2011

M.S., University of Connecticut, Storrs, CT, 2014

A Dissertation

Submitted in Partial Fulfillment of the

Requirements for the Degree of

Doctor of Philosophy

at the

University of Connecticut

2016

APPROVAL PAGE

Doctor of Philosophy Dissertation

Grid Integration of Intermittent Renewable Generation: Markovian and Interval Optimization Approaches

Presented by

Yaowen Yu, B.S., M.S.

Major Advisor _____
Peter B. Luh

Associate Advisor _____
Peng Zhang

Associate Advisor _____
Eugene Litvinov

University of Connecticut
2016

ACKNOWLEDGMENTS

First, I would like to express my deepest gratitude to my adviser, Prof. Peter. B. Luh for his continuous support of my doctoral study at the University of Connecticut. His guidance, encouragement, and immense knowledge helped me in all the time of research and paved the way for my successful dissertation.

I would also like to express my gratitude to Dr. Eugene Litvinov of ISO New England for his support and insightful guidance. My sincere thanks to Prof. Peng Zhang for joining my advisory committee and providing useful suggestions.

I gratefully acknowledge Dr. Tongxin Zheng, Mr. Izudin Lelic, Dr. Feng Zhao, Dr. Jinye Zhao, and Dr. Dane A. Schiro of ISO New England for insightful discussions and invaluable comments on our collaborated research works. My sincere thanks to Dr. Eugene Litvinov, Dr. Tongxin Zheng, and Mr. Izudin Lelic for providing me an internship opportunity for beneficial industry experience.

I would like to thank all my labmates for the pleasant study and research experience. The discussions and exchanges of knowledge enriched my experience. My special thanks to Mr. Mikhail Bragin for improving the Surrogate Lagrangian Relaxation module.

And last but not least, I would like to thank my parents, other family members, and friends for their love and support throughout writing this thesis and my life.

Table of Contents

List of Figures viii
List of Tables ix
Publications Related to this Thesis x
1 Introduction 1
1.1 Motivations 1
1.2 Major Contributions 3
1.3 Organization of this Thesis 4
References 4
2 Grid Integration of Intermittent Wind Generation: A Markovian Approach 6
2.1 Introduction 7
2.2 Literature Review 9
2.3 Formulation of Wind Generation 11
2.4 Unit Commitment Problem Formulation 13
2.4.1 Integration of Wind Generation into System Demand 14
2.4.2 The Markovian Stochastic Unit Commitment Problem Formulation 15
2.5 Solution Methodology 18
2.5.1 Solving the Markovian Problem by Using Branch-and-cut 18
2.5.2 Monte Carlo Simulation 19
2.5.3 Simulating Rare Events by Using Importance Sampling 19
2.5.4 Comparison of Different Approaches 20
2.6 Numerical Results 22
2.6.1 Example 1 22
2.6.2 Example 2 24
2.7 Conclusion 29
References 30
3 Grid Integration of Distributed Wind Generation: Hybrid Markovian and Interval Unit Commitment 33
3.1 Introduction 34
3.2 Literature Review 37
3.3 Problem Formulation 41
3.3.1 Wind Model and the UC Problem 41

3.3.2 Pure Markov-based Optimization and Its Complexity 43
3.3.3 Hybrid Markovian and Interval UC Formulation 44
3.3.4 Discussion on Reducing the Wind Uncertainty 49
3.4 Solution Methodology 51
3.4.1 Transformation of the Min/Max Operations 51
3.4.2 Comparison of Approaches 52
3.5 Numerical Results 53
3.5.1 Example 1 54
3.5.2 Example 2 56
3.5.3 Example 3 58
3.6 Conclusion 59
Appendix 3.A 60
Appendix 3.B 61
References 62
4 Transmission Contingency-Constrained Unit Commitment with High Penetration of Renewables via Interval Optimization 66
4.1 Nomenclature 67
4.2 Introduction 68
4.3 Interval CCUC Formulation 72
4.3.1 The CCUC Problem and the Deterministic Model 72
4.3.2 Interval CCUC Formulation with Expected Net Demand 73
4.3.3 Interval CCUC Formulation with Uncertain Net Demand 76
4.3.4 Improved Interval Computation 80
4.4 Alleviation of Conservativeness 82
4.5 Solution Methodology 84
4.6 Numerical Results 87
4.6.1 Example 1 88
4.6.2 Example 2 91
4.6.3 Example 3 95
4.7 Conclusion 98
References 98
5 Scalable Corrective Security-constrained Economic Dispatch Considering Conflicting Contingencies 101
5.1 Introduction 102
5.1.1 Motivations of Corrective SCED 102

5.1.2 Literature Review 103
5.1.3 Contributions and Organization of this Paper 105
5.2 Problem Formulation 106
5.2.1 Real-time Corrective SCED Formulation 106
5.2.2 Infeasible Contingencies 109
5.3 Solution Methodology 110
5.3.1 Key Points and the Flow Control of our Approach 110
5.3.2 The Master SCED Problem 112
5.3.3 Contingency subproblems 113
5.4 Performance Enhancements 115
5.4.1 Warm-start of subproblem models 115
5.4.2 Parallel Computing 117
5.5 Numerical Results 119
5.5.1 Example 1 120
5.5.2 Example 2 121
5.6 Conclusion 125
References 126

List of Figures

Fig. 2.1. Net system demand state transition. 14
Fig. 3.1. The three-bus transmission network for Example 1 54
Fig. 4.1. Illustration of the interval contingency model. 74
Fig. 4.2. Flowchart of the combined SLR and B&C method. 87
Fig. 4.3. GSF intervals of Line 1 at six buses of Case 1 in Example 1. 88
Fig. 4.4. Optimization and simulation results of Case 1 in Example 1. 89
Fig. 4.5. Sensitivity of optimization and simulation costs with respect to $\alpha^E(t)$. 94
Fig. 4.6. Comparison between pure B&C and the SLR+B&C method for solving the interval CCUC model with the redundant constraint identification. 97
Fig. 5.1. Flowchart of our contingency filtering approach. 111
Fig. 5.2. Contingency screening procedure of our contingency filtering approach in serial computing. . 116
Fig. 5.3. Warm-start between two subproblems of transmission contingencies. 116
Fig. 5.4. Contingency screening procedure of our contingency filtering approach in parallel computing. 119

List of Tables

Table 2.1. Non-winter Wind Transition Matrix for New England 13
Table 2.2. Comparison of the Markovian Formulation, the Deterministic Formulation and the Stochastic Programming Formulation 21
Table 2.3. Unit Parameters for Example 1 23
Table 2.4. Results for Example 1 by using the Markovian Approach 23
Table 2.5. Dispatch Decisions in Scenario 10 for Example 1 by using Stochastic Programming 24
Table 2.6. Penalty Curves for Load Shedding and Over Generation for Example 2 25
Table 2.7. Results for Case 1 26
Table 2.8. Results for Case 2 27
Table 2.9. Results for Case 3 without Rate Events 28
Table 2.10. Results for Case 3 with Rate Events 29
Table 3.1. Comparison of the Complexity of the Three Approaches 52
Table 3.2. Unit Parameters for Example 1 54
Table 3.3. Optimization Results for Example 1 Using the Markovian and Interval approach 55
Table 3.4. Simulation Results for Example 1 55
Table 3.5. Results for Case 1 of Example 2 57
Table 3.6. Results for Case 2 of Example 2 58
Table 3.7. Results for Example 3 59
Table 4.1. Optimization and Simulation Results of Case 2 in Example 1 90
Table 4.2. Optimization and Simulation Results of Example 2 93
Table 4.3. Optimization and Simulation Results of Example 3 96
Table 5.1 Comparison between Our Warm-Start of Subproblem Models and Creating All Subproblem Models in Serial Computing 117
Table 5.2. Comparison between Our Warm-Start of Subproblem Models and Creating All Subproblem Models in Parallel Computing 119
Table 5.3. Optimization and Simulation Results of Case 1 in Example 3 121
Table 5.4. Computational Performance on Laptop of Case 3 in Example II 123
Table 5.5. Computational Performance on HPC of Case 3 in Example 2 125

Publications Related to this Thesis

Journal Articles

[1] **Y. Yu**, P. B. Luh, E. Litvinov, T. Zheng, F. Zhao, J. Zhao, D. A. Schiro, and I. Lelic, "Scalable Corrective Security-constrained Economic Dispatch Considering Conflicting Contingencies," Submitted.

[2] **Y. Yu**, P. B. Luh, E. Litvinov, T. Zheng, J. Zhao, F. Zhao, and D. A. Schiro, "Transmission Contingency-constrained Unit Commitment with High Penetration of Renewables via Interval Optimization," *IEEE Transactions on Power Systems*, published online June 2016, DOI: 10.1109/TPWRS.2016.2585521.

[3] **Y. Yu**, P. B. Luh, E. Litvinov, T. Zheng, F. Zhao, and J. Zhao, "Grid Integration of Distributed Wind Generation: Hybrid Markovian and Interval Unit Commitment," *IEEE Transactions on Smart Grid*, vol. 6, no. 6, pp. 3061-3072, Nov. 2015

[4] P. B. Luh, **Y. Yu**, B. Zhang, E. Litvinov, T. Zheng, F. Zhao, J. Zhao, and C. Wang, "Grid Integration of Intermittent Wind Generation: a Markovian Approach," *IEEE Transactions on Smart Grid*, vol.5, no.2, pp. 732-741, March 2014

[5] B. Yan, H. Fan, P. B. Luh, K. Moslehi, X. Feng, C. N. Yu, M. A. Bragin, and **Y. Yu**, "Grid Integration of Wind Generation Considering Remote Wind Farms: Hybrid Markovian and Interval Unit Commitment," to appear in *IEEE/CAA Journal of Automatica Sinica*.

Conference Proceedings

[6] **Y. Yu**, P. B. Luh, E. Litvinov, T. Zheng, J. Zhao, and F. Zhao, "Transmission contingency-constrained unit commitment with uncertain wind generation via interval optimization," in *Proceedings of the 2015 IEEE Power and Energy Society General Meeting* (in Session ***Best Conference Papers on Integration of Renewable & Intermittent Resources***), Denver, Colorado, July 2015.

[7] **Y. Yu**, P. B. Luh, E. Litvinov, T. Zheng, J. Zhao, and F. Zhao, "Markov-based Stochastic Multi-period Market Settlement with Wind Uncertainties," in *Proceedings of the 2014 IEEE Power and Energy Society General Meeting*, National Harbor, Maryland, July 2014.

[8] **Y. Yu**, P. B. Luh, E. Litvinov, T. Zheng, F. Zhao, and J. Zhao, "Markov-Based Stochastic Unit Commitment Considering Wind Power Forecasts," in *Proceedings of the 2013 IEEE Power and Energy Society General Meeting* (in Session ***Best Conference Papers on Integrating Wind, Solar, and Energy Storage***), Vancouver, BC, Canada, July 2013.

[9] **Y. Yu**, P. B. Luh, E. Litvinov, T. Zheng, F. Zhao, and J. Zhao, "Unit Commitment with Intermittent Wind Generation via Markovian Analysis with Transmission Capacity Constraints," in *Proceedings of the 2012 IEEE Power and Energy Society General Meeting*, San Diego, California, July 2012.

Chapter 1

Introduction

1.1 Motivations

Renewable energy can help reduce the dependence on fossil fuels and greenhouse gas emissions, and the global wind industry has been growing rapidly. In 2012, nearly 45 GW of wind capacity was brought online, and the global wind capacity was increased by 19% to almost 283 GW [1]. The U.S. Department of Energy sets the target to increase wind energy's contribution to 20% of electricity by 2030 [2]. President Obama's goal is to generate 80% of US electricity by 2035 from clean energy sources, including wind, solar, nuclear, clean coal and natural gas [3]. Nevertheless, the intermittent nature of wind and solar brings major challenges in meeting system demand. For example, it is not uncommon to see in Spain that a drop of wind generation within just a few hours is equivalent to the shutdown of four nuclear units, and this has presented major challenges to system operators [4]. Another example is the calling for an emergency electric curtailment plan by the Electric Reliability Council of Texas in February 2008 caused by a sudden drop of wind [5]. To ensure grid-wide reliability, substantial reserves from conventional generation are usually required. Such large reserves, however, are the dark secret behind intermittent renewable generation as they induce significant costs. The issues would become more severe as the level of renewable penetration increases.

A critical operational process for renewable integration is unit commitment (UC) in which the Independent System Operator (ISO) determines the most cost-effective set of online/offline decisions for conventional generators (units) one day ahead or hours ahead to meet the forecasted demand while satisfying unit-level and transmission constraints. UC with high penetrations of renewable generation, however, is challenging because of the uncertain nature of renewable generation and possible congestions in transmission lines. It is difficult for existing approaches, including the deterministic approach [6], [7], stochastic programming [8]-[14], robust optimization [15]-[17] and interval optimization [14], [18], to balance modeling accuracy, simulation costs, solution feasibility and computational efficiency.

Moreover, an important practical requirement for system reliability is that UC solutions have to be feasible under contingencies. A contingency is caused by a sudden failure of a generator or a transmission line. The North American Electric Reliability Corporation's "*N*-1" criterion requires that no such single failure should lead to system infeasibility [19]. The resulting contingency-constrained unit commitment (CCUC) satisfying the "$N-1$" criterion is extremely complex, and the issue is now compounded by the drastic increase in renewable generation. Contingencies and sudden renewable generation changes can happen together to push a system further away from its nominal operating point, leading to system infeasibility. Consequently, an integrated consideration of contingencies and intermittent renewable generation is thus critical and urgent. This issue, however, has mostly been overlooked, perhaps because of problem complexity or because of solution conservativeness.

The "$N-1$" criterion is also considered in economic dispatch (ED), a central operational process for real-time wholesale electricity markets. ED is conducted every five minutes to decide how much MW of power each online unit should produce to minimize the total generation cost. The version of ED considering the "$N-1$" criterion and corrective actions that can be taken after contingencies is known as corrective security-constrained economic dispatch (SCED) [20]. The problem is difficult because of a large number

of contingencies and the strict time limit for real-time operations. The existence of conflicting contingencies further complicates the problem [21], [22].

1.2 Major Contributions

To overcome the above difficulties, this dissertation develops three novel Markovian and interval approaches for UC problems and one new contingency filtering approach for the ED problem:

1. *A pure Markovian approach for stochastic UC without transmission constraints.* A stochastic UC problem has been innovatively formulated based on renewable states instead of scenarios. The advantage of this formulation is that the state at a time instant summarizes the information of all previous instants in a probabilistic sense for reduced complexity.

2. *A hybrid Markovian and interval approach for transmission-constrained UC.* To avoid the complexity of explicitly considering a large number of combinations of distributed renewable states, interval optimization has been synergistically integrated with the Markovian approach. Constraints are innovatively formulated to guarantee solution feasibility for all possible combinations of states without much complexity and over-conservativeness.

3. *An interval optimization approach for CCUC.* The novel idea lies in using intervals to describe transmission contingencies based on generation shift factors (GSFs), as opposed to analyzing contingencies one at a time. To ensure solution robustness under contingencies and uncertain renewable realizations, bounds of GSFs and renewable generation in different types of constraints are captured based on interval optimization.

4. *A contingency filtering approach for corrective SCED.* Our approach, consisting of the decomposition and coordination method, and enhancements by novel warm-start of subproblem models and by parallel computing, is scalable for corrective SCED problems. Instead of always removing conflicting contingencies as in existing papers, our approach offers system operators an

important option to keep them for increased reliability, enabled by identifying multiple conflicting contingencies simultaneously.

1.3 Organization of this Thesis

The rest of this thesis is organized as follows. Chapter 2 introduces the pure Markovian approach for stochastic UC without transmission constraints. Chapter 3 presents the hybrid Markovian and interval approach for transmission-constrained UC. Chapter 4 discusses the interval optimization approach for CCUC. Chapter 5 reports the contingency filtering approach for corrective SCED.

For the rest of this dissertation, wind generation is used as an example of intermittent renewables. Solar generation can be modeled and solved in ways similar to those for wind generation. The reason is that even though wind and solar have different diurnal patterns – peak wind generation usually occurs in the morning and evening while that of solar usually occurs in the middle of a day [23], they share the similar uncertain nature.

References

[1] Global Wind Energy Council, "Global wind report – Annual market update 2012," Brussels, Belgium, April 2013 [Online]. Available: http://www.gwec.net/wp-content/uploads/2012/06/Annual_report_2012_LowRes.pdf

[2] U.S. Department of Energy, "20% wind energy by 2030: Increasing wind energy's contribution to U.S. electricity supply", DOE/GO-102008-2567, July 2008 [Online]. Available: http://www.nrel.gov/docs/fy08osti/41869.pdf

[3] B. H. Obama, State of the Union address, 2011 [Online]. Available: http://www.whitehouse.gov/the-press-office/2011/01/25/remarks-president-barack-obama-state-union-address

[4] A. J. Conejo, "Scheduling Energy and Reserve in Systems with High Wind Penetration," seminar presentation at the University of Illinois at Urbana-Champaign, May 2012 [Online]. Available: http://energy.ece.illinois.edu/Guest_Speakers/Conejo/1%20Scheduling.pdf

[5] E. Ela and B. Kirby, "ERCOT Event on February 26, 2008: Lessons Learned," NREL, CO, Tech. Rep. NREL/TP-500-43373, July 2008 [Online]. Available: http://www.nrel.gov/docs/fy08osti/43373.pdf

[6] M. Black and G. Strbac, "Value of bulk energy storage for managing wind power fluctuations," *IEEE Transactions on Energy Conversion*, vol.22, no.1, pp.197-205, March 2007.

[7] M. A. Ortega-Vazquez and D. S. Kirschen, "Estimating the spinning reserve requirements in systems with significant wind power generation penetration," *IEEE Transactions on Power Systems*, vol.24, no.1, pp. 114-124, Feb. 2009.

[8] F. Bouffard and F. D. Galiana, "Stochastic security for operations planning with significant wind power generation," *IEEE Transactions on Power Systems*, vol. 23, no. 2, pp. 306-316, 2008.

[9] J. Wang, M. Shahidehpour, and Z. Li, "Security-constrained unit commitment with volatile wind power generation," *IEEE Transactions on Power Systems*, vol. 23, no. 3, Aug. 2008.

[10] V. S. Pappala, I. Erlich, K. Rohrig, and J. Dobschinski, "A stochastic model for the optimal operation of a wind-thermal power system," *IEEE Trans. Power Syst.*, vol. 24, no. 2, pp. 940–950, May 2009.

[11] P. Ruiz, P. C. Philbrick, E. Zak, K. W. Cheung, and P. Sauer, "Uncertainty management in the unit commitment problem," *IEEE Transactions on Power Systems*, vol. 24, no. 2, pp. 642–651, May 2009.

[12] C. Weber, P. Meibom, R. Barth, and H. Brand, "WILMAR: A stochastic programming tool to analyze the large-scale integration of wind energy," *Optimization in the Energy Industry*, Chapter 19, pp. 437–458, Berlin, Germany, Springer, 2009.

[13] A. Papavasiliou, S. Oren, and R. P. O'Neill, "Reserve requirements for wind power integration: A scenario-based stochastic programming framework," *IEEE Trans. on Power Syst.*, vol. 26, no. 4, pp. 2197-2206, Nov. 2011.

[14] L. Wu, M. Shahidehpour, and Z. Li, "Comparison of scenario-based and interval optimization approaches to stochastic SCUC," *IEEE Transactions on Power Systems*, vol. 27, no. 2, pp. 913-921, May 2012.

[15] D. Bertsimas, E. Litvinov, X. A. Sun, J. Zhao, and T. Zheng, "Adaptive robust optimization for the security constrained unit commitment problem," *IEEE Trans. Power Syst.*, vol. 28, no. 1, pp. 52-63, Feb. 2013.

[16] L. Zhao and B. Zeng, "Robust unit commitment problem with demand response and wind energy," in *Proc. of the 2012 IEEE Power and Energy Soc. Gen. Meet.*, San Diego, California, July 2012.

[17] R. Jiang, J. Wang, Y. Guan, "Robust unit commitment with wind power and pumped storage hydro," *IEEE Transactions on Power Systems*, vol. 27, no. 2, pp.800-810, May 2012.

[18] Y. Wang, Q. Xia, and C. Kang, "Unit commitment with volatile node injections by using interval optimization," *IEEE Transactions on Power Systems*, vol. 26, no. 3, pp. 1705-1713, 2011.

[19] A. J. Wood, B. F. Wollenberg, and G. B. Sheble, *Power Generation, Operation and Control (3rd ed.)*, Wiley, 2013.

[20] A. Monticelli, M. V. F. Pereira, and S. Granville, "Security-constrained optimal power flow with post-contingency corrective rescheduling," *IEEE Trans. Power Syst.*, vol. 2, no. 1, pp. 175-180, 1987.

[21] Q. Jiang and K. Xu, "A novel iterative contingency filtering approach to corrective security-constrained optimal power flow," *IEEE Trans. Power Syst.*, vol. 29, no. 3, pp. 1099-1109, May 2014.

[22] Y. Liu, M. C. Ferris, and F. Zhao, "Computational study of security constrained economic dispatch with multi-stage rescheduling," *IEEE Trans. Power Syst.*, vol. 30, no. 2, pp. 920-929, March 2015.

[23] NERC, *Special report: Accommodating high levels of variable generation*, April, 2009, [Online]. Available: http://www.nerc.com/files/IVGTF_Report_041609.pdf

Chapter 2

Grid Integration of Intermittent Wind Generation: A Markovian Approach

Although the unique characteristics of intermittent wind generation have been acknowledged and drastic impacts of sudden wind drops have been experienced, no effective integration approach has been developed. In this chapter, without considering transmission capacity constraints for simplicity, aggregated wind generation is modeled as a discrete Markov process with state transition matrices established based on historical data. Wind generation is then integrated into system demand with multiple net demand levels at each hour. To accommodate the uncertain net demand, a stochastic unit commitment problem is formulated based on states instead of scenarios. The objective is to minimize the total commitment cost of conventional generators and their total expected dispatch cost while satisfying all possible net demand levels. The advantage of this formulation is that the state at a time instant summarizes the information of all previous instants in a probabilistic sense for reduced complexity. With state transition probabilities given, state probabilities calculated before optimization, and the objective function and constraints formulated in a linear manner, the problem is effectively solved by using branch-and-cut. Numerical testing shows that the new Markovian approach is effective and robust through the examined cases, resembling the sudden wind drop in Texas in February 2008.

2.1 Introduction

With major initiatives promoting wind generation, effective and robust integration of wind into the grid becomes a critical issue. Wind generation cannot be dispatched as conventional generation because of its intermittent and uncertain nature. Sudden drops in wind generation may have drastic impacts on system security if the system ramping capability of dispatchable resources is not large enough to respond. One example is the event on February 26, 2008 in which the Electric Reliability Council of Texas (ERCOT) called for an Emergency Electric Curtailment Plan (EECP) because of worsening imbalance between generation and load. One of the major reasons behind was a large 3.5-hour ramp-down in wind generation from 2,000 MW to 360 MW. Even though the curtailment plan resolved the imbalance issue, there was a decline in system frequency from 60 Hz to 59.85 Hz [1]. Although the intermittent and volatile characteristics of wind generation have been acknowledged and the drastic impacts of sudden drops in wind generation have been experienced, no effective integration approach has yet been developed to address these issues.

In this chapter, a Markov-based stochastic unit commitment model is presented based on states instead of scenarios to integrate intermittent and uncertain wind generation in the day-ahead unit commitment process. With state transition probabilities given, state probabilities calculated before optimization, and the objective function and constraints formulated in a linear manner, the problem can be effectively solved by using the branch-and-cut method. The approach developed here can be applied to reliability assessment commitment performed in real-time. In Section 2.2, the deterministic approach, stochastic programming approach, and robust optimization approach are reviewed. For the deterministic approach, the uncertainty of wind generation is not explicitly captured, so solutions are not robust against realizations of wind generation. On the other hand, the stochastic programming approach explicitly models uncertainty by considering the possible scenarios and the probability information. Scenario reduction techniques are commonly used to reduce the number of scenarios for computational efficiency. However, it is difficult to

balance the computational effort and the ability to manage low-probability high-impact events by selecting an appropriate number of representative scenarios. The robust optimization approach models uncertainty by using a deterministic uncertainty set, rather than the probability information as is used in the stochastic programming approach. The robust optimization approach considers the worst-case realization, and it is difficult to choose an appropriate uncertainty set that balances the tradeoff between low-probability high-impact events and the resulting costs.

To overcome the above difficulties, discrete Markov processes are used in Section 2.3 to model intermittent and uncertain wind generation, with state transition matrices established based on historical data. In Section 2.4, discretized wind generation is aggregated into system demand, which itself is assumed to be deterministic for simplicity. The net system demand for each hour thus has many possible states, each corresponding to one wind generation level. The stochastic unit commitment problem is to minimize the total expected cost by selecting a single set of unit commitment decisions over a given period (e.g., 24 hours), and multiple sets of economic dispatch decisions, one per net system demand level at each hour. Constraints considered include generator capacities, ramp rates, minimum up/down times, and system demand constraints. For simplicity, transmission capacity constraints, demand bids and ancillary services are not considered. Since the performance of the branch-and-cut method depends heavily on problem linearity, the objective function, constraints and the state transitions are formulated in a linear manner. The advantage of the proposed Markovian formulation is that the state at a time instant summarizes the information of all previous instants in a probabilistic sense, resulting in reduced complexity of the overall problem.

In Section 2.5, the problem is solved by using the branch-and-cut method. Although commercial packages such as CPLEX [2] or GUROBI [3] do not provide infrastructure to explicitly describe stochastic processes, with state transition probabilities given, state probabilities calculated before optimization, and the objective function and constraints formulated in a linear manner, the problem can be effectively solved.

For reliability assessment commitment performed in real-time, wind generation may maintain an increasing (or a decreasing) trend over several consecutive timeframes. With this trend, the stochastic process representing wind generation is driven by a colored noise, and pre-whitening can be performed [4]. In Section 2.6, two examples are provided. In Example 1, a simple two-unit three-hour problem is used to illustrate the differences between the Markovian approach and the standard stochastic programming approach. In Example 2, a problem with 309 units based on ISO-New England data is tested to demonstrate the computational efficiency, the effectiveness to accommodate high levels of wind penetration, and the ability to capture low-probability high-impact events.

The preliminary results for a simplified unit commitment model were presented in [5]. In this chapter, testing using an ISO-NE's data set is added, and the comparison with the deterministic approach and the stochastic programming approach is made through Monte Carlo simulation. The ability to capture low-probability events, resembling the sudden wind drop happened in Texas in February 2008, is also demonstrated. In addition, the overall presentation has been significantly improved.

2.2 Literature Review

Most of the practical applications, either in day-ahead or real-time market, adopt **the deterministic approach**. In this approach, intermittent and uncertain wind generation is represented by its mean value without explicitly considering uncertainties. The problem is then solved by existing methods, e.g., Lagrangian relaxation to exploit the separability of a formulation [6], [7], or branch-and-cut to solve linear mixed-integer formulations [8]-[10]. Since uncertainties are not explicitly considered, the solutions of deterministic models are not robust against realizations of wind generation. On the research side, **stochastic programming** has recently been explored by many to address the intermittent and uncertain nature of wind generation based on representative scenarios in unit commitment problems [11]-[17]. Generally, a large number of scenarios are generated based on distributions of wind generation [11], [12] or wind speed [15], [16] over a day. The number of scenarios could be prohibitively large. For example, a distribution with

seven discretized values per hour over a time horizon of 24 hours will result in 724 (=1.9×1020) scenarios if all possible inter-hour transitions are considered [11]. Scenario reduction techniques are therefore commonly used to eliminate scenarios with very low probability, or to aggregate "close" scenarios based on probability metrics [18]-[20]. The reduced set of scenarios is then used in the unit commitment process. To mimic the operation of the day-ahead market, the scenario-based stochastic unit commitment model looks for a single set of unit commitment decisions to satisfy all scenarios, while generation levels of committed units are scenario dependent to satisfy individual net demand levels. In addition, individual unit constraints should be satisfied for all scenarios. The objective of the stochastic unit commitment problem is to minimize the expected total cost. The scenario-based stochastic unit commitment problem is non-deterministic polynomial-time hard (NP-hard) [17], i.e., it is not proved to be solvable within polynomial time and is at least as hard as NP-complete problems [21]. Thus, decomposition methods are often used for near-optimal solutions. For example, Benders' decomposition is used to decompose the problem into one master problem and multiple subproblems for each scenario [12], [17]. Subproblems are linear and can be solved by using branch-and-cut. The number of scenarios is a critical consideration. If too few scenarios are selected, low-probability but high-impact events, such as the sudden wind drop happened to ERCOT on the February 26, 2008, may not be captured, and this may lead to severe consequences. If too many scenarios are included, the computational effort will be prohibitive. In a recent study, it took 35 minutes to solve the modified IEEE 118-bus system with 54 thermal units, three wind farms, and 186 branches with 100 scenarios using CPLEX 12.1 on an Intel Core i7 2.67-GHz personal computer [17]. The stochastic programming approach thus has limited success and questionable scalability.

Robust optimization seeks the optimal solution feasible for any realization in a given uncertainty set without requiring a specific probabilistic description. This is equivalent to find the optimal solution for the worst-case realization [22], [23]. Robust optimization was investigated to address demand uncertainty in [24] and uncertainties on both demand and supply sides in power grids in [25], [26]. A two-stage robust

adaptive model for the security constrained unit commitment problem with uncertain net injections was discussed in [27]. In their paper, the first stage is to find optimal unit commitment decisions feasible for any realizations in the given uncertainty set of net injections, while the second stage is to find the worst-case dispatch under the fixed unit commitment decisions obtained from the first stage. This problem is solved by using a Benders' decomposition type cutting plane algorithm. A real world system operated by ISO New England was tested. In [28], wind generation uncertainties and pumped-storage units to partially absorb the uncertainties were considered in robust unit commitment, and the problem was solved by using Benders' decomposition. For the robust optimization approach, it is difficult to choose an appropriate uncertainty set that balances the tradeoff between low-probability high-impact events and the resulting costs.

2.3 Formulation of Wind Generation

In this section, to overcome the above difficulties, discrete Markov processes are used to model intermittent and uncertain wind generation, with state transition matrices established based on historical data.

In the formulation, since transmission capacity constraints are ignored, wind generation from all wind farms can be aggregated, and the resulting generation is assumed to be a discrete Markov process [29], [30]. In this Markov process, the capacity of wind generation is evenly divided into N intervals. The mean of each interval is represented by a state, and the states are arranged in the ascending order of the means. The state transition matrix, of which the elements are state transition probabilities, can be established based on historical data. The $(m, n)^{th}$ element is the ratio of the number of observed transitions from state m to state n to the number of occurrences of state m [31]:

$$\pi_{mn} = \frac{observed\ transitions\ from\ state\ m\ to\ n}{occurrences\ of\ state\ m}. \tag{2.1}$$

The average hourly wind generation for the year 2000 of the Lake Benton wind farm was analyzed in [29], and it was shown that the generation had a weak diurnal pattern but with noticeable changes from winter to non-winter. Furthermore, wind generation in New England over the years 2004, 2005, and 2006 had the highest values in winter seasons [31]. Therefore, a winter wind transition matrix is developed using data from winter seasons, and a non-winter wind transition matrix is constructed from non-winter seasons. The advantage of formulating aggregated wind generation as discrete Markov processes is that according to the Markov property, the state at a time instant summarizes the information of all previous instants in a probabilistic sense, resulting in reduced complexity of the stochastic unit commitment problem to be formulated in Section 2.4.

For example, National Renewable Energy Laboratory's Eastern Wind Dataset from April to September 2006 [32] is used to establish the summer wind transition matrix for an aggregation of 113 onshore and 666 offshore wind farms in New England with a total capacity of 24 GW. With wind generation discretized into ten equally divided states, the non-winter wind transition matrix is obtained in Table 2.1. This transition matrix is block diagonal, indicating that the probabilities for sudden increases or decreases of wind generation are generally very small. The block diagonal characteristic is common for aggregated wind farms over large regions. The analysis from [33] shows that the reduction of wind power forecasting error is mainly determined by the size of the region, e.g., for the size of a typical large utility (~370 km in diameter), less than 50 sites are sufficient to obtain 63% of the error of single sites. If the wind generation is more volatile, there will be more nonzero transition rates in the off-diagonal positions. Our approach can still incorporate the transition matrix with more nonzero off-diagonal elements, since the approach is not based on the block diagonal characteristic. Also, the number of states N (= 10 in Table 2.1) should be determined as a balance between modeling accuracy and computational efficiency when solving the unit commitment problem. A detailed state transition matrix, which is derived from the same data set but with

a larger number of states, is used to produce random scenarios for simulating the real-time dispatch process to evaluate the performance of the new approach in Section 2.6.

Table 2.1. Non-winter Wind Transition Matrix for New England

State	1	2	3	4	5	6	7	8	9	10
1	0.785	0.215	0	0	0	0	0	0	0	0
2	0.115	0.711	0.168	0.006	0	0	0	0	0	0
3	0	0.167	0.652	0.169	0.012	0	0	0	0	0
4	0	0.005	0.204	0.604	0.176	0.012	0	0	0	0
5	0	0	0.016	0.204	0.599	0.174	0.007	0	0	0
6	0	0	0	0.002	0.210	0.631	0.148	0.008	0	0
7	0	0	0	0	0.007	0.187	0.679	0.126	0	0
8	0	0	0	0	0	0	0.205	0.700	0.095	0
9	0	0	0	0	0	0	0	0.184	0.776	0.041
10	0	0	0	0	0	0	0	0	0.171	0.829

It should be noted that more refined state transition matrices can be established as needed, e.g., based on monthly patterns, and incorporated in our approach. Also, to describe daily wind generation probabilities more accurately, day-ahead wind power forecasts can be considered. However, this is beyond the scope of this thesis. Also, although battery storage technology can help reduce the uncertainty of wind generation, large-scale battery storage remains expensive [34], and no practical solution to completely eliminate the uncertainty of wind generation is expected [35].

2.4 Unit Commitment Problem Formulation

Since wind generation cannot be dispatched as conventional generation, it is integrated into system demand following [11]-[16] in subsection 2.4.1. In subsection 2.4.2, the Markovian stochastic unit commitment problem is formulated based on states instead of scenarios, considering generator capacities, ramp rates,

minimum up/down time, and system demand. For simplicity, demand bids and ancillary services (e.g., regulation and reserves) are not considered. The objective function, constraints and state transitions are formulated in a linear manner so that branch-and-cut can be effectively used.

2.4.1 Integration of Wind Generation into System Demand

It is known that day-ahead load forecasting is much more accurate than wind forecasting. For example, the Mean Absolute Error (MAE) of day-ahead load forecasts is 1% to 3% of the load, while the MAE of the state-of-the-art day-ahead wind forecasts is 15% to 20% of wind generation [31]. Therefore, for simplicity, the uncertainty of load forecasting is ignored. The resulting net system demand is the forecasted system demand minus the aggregated wind generation, and is a discrete Markov process with N states at each hour. For this Markov process, state transitions are illustrated in Fig. 2.1.

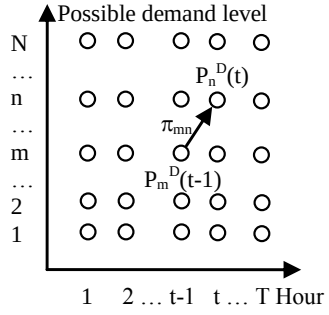

Fig. 2.1. Net system demand state transition.

The range of power levels at the same net system demand state can vary at different hours, given that the forecasted system demand is time varying. For convenience, the order of net demand states is reversed from that of wind generation states. The probability that the net system demand is at state *n* at time *t*, denoted as $\varphi_n(t)$, is the sum of probabilities at time *t*-1 weighted by different transitions:

$$\varphi_n(t) = \sum_{m=1}^{N} \pi_{mn} \varphi_m(t-1) . \qquad (2.2)$$

The probabilities of net demand levels for future time instants can thereby be derived based on the initial wind generation state and the transition matrix obtained in Section 2.3.

2.4.2 The Markovian Stochastic Unit Commitment Problem Formulation

The stochastic unit commitment problem is to minimize the total expected cost by selecting a single set of unit commitment decisions over a 24-hour period and multiple sets of economic dispatch decisions depending on net system demand levels. Building on our previous formulation [5], [6], consider a day-ahead energy market with I conventional units indexed by i ($1 \le i \le I$) over T (=24) operational hours indexed by t ($1 \le t \le T$). Unit i submits a multi-block bid that includes bid block price $C_{i,b}$ (\$/MWh) for block b ($1 \le b \le B$) with size $p_{i,b\max}$ (MW), no-load cost S_i^{NL} (\$/hr), startup cost S_i (\$/Start), and minimal and maximal generation levels $p_{i\min}$ (MW) and $p_{i\max}$ (MW), respectively. The bid block price is monotonically increasing. For unit i, the ramp rate is denoted as Δ_i (MW/h), the minimum-up time $\bar{\tau}_i$ (h), and the minimum-down time $\underline{\tau}_i$ (h). The net system demand at state n of hour t is $P_n^D(t)$ (MW) with probability $\varphi_n(t)$. As for decision variables, the startup decision is denoted by a binary decision variable $u_i(t)$, with "1" representing the starting up of the unit and "0" otherwise. The commitment status is denoted by a binary variable $x_i(t)$, with "1" meaning online and "0" offline. The generation level is denoted by $p_{i,n}(t)$ (MW) when the net system demand is at state n at time t, with $p_{i,b,n}(t)$ (MW) representing the generation of block b. As a Markov decision problem, the dispatch decision at time t depends on the state at time t only.

Constraints include individual unit constraints (startup, generator capacities, ramp rates, and minimum up/down times) and system demand constraints as presented below.

Startup constraints. The binary startup variable $u_i(t)$ equals 1 if and only if the unit is turned on from offline at hour t, i.e.,

$$u_i(t) \ge x_i(t) - x_i(t-1), \forall i, \forall t \,. \tag{2.3}$$

Generation limits for each block. The generation level for each block of unit *i* cannot exceed the block size, i.e.,

$$0 \le p_{i,b,n}(t) \le p_{i,b\max}, \forall i, \forall b, \forall n, \forall t. \tag{2.4}$$

The sum of generation levels for all the blocks is equal to the generation level of this unit, i.e.,

$$\sum_{b=1}^{B} p_{i,b,n}(t) = p_{i,n}(t), \forall i, \forall n, \forall t. \tag{2.5}$$

Generator capacities. The generation level of a unit is limited by its minimum and maximum values if the unit is committed. Otherwise, the generation level should be zero, i.e.,

$$x_i(t) p_{i\min} \le p_{i,n}(t) \le x_i(t) p_{i\max}, \forall i, \forall n, \forall t. \tag{2.6}$$

Ramp rates. If unit *i* is online at both *t-1* and *t* hours, then the change of generation levels of the unit cannot exceed its ramp rate. Since the net system demand can be at different states at these two hours, ramp rates should be satisfied for all possible state transitions, i.e.,

$$p_{i,m}(t-1) - \Delta_i \le p_{i,n}(t) \le p_{i,m}(t-1) + \Delta_i, \forall i, \forall n, \forall t, \forall m \in \left\{ m \mid \pi_{mn} \ne 0 \right\}, \text{ if } x_i(t-1) = 1 \text{ and } x_i(t) = 1. \tag{2.7}$$

Upon starting up or at shutting down, the generation level cannot exceed its $p_{i\min}$ plus 30-minute ramp rate. i.e.,

$$p_{i,n}(t) \le p_{i\min} + \frac{\Delta_i}{2}, \forall i, \forall n, \forall t,$$
$$\text{if } x_i(t-1) = 0 \text{ and } x_i(t) = 1,$$
$$\text{or if } x_i(t) = 1 \text{ and } x_i(t+1) = 0. \tag{2.8}$$

The above constraints (2.7) and (2.8) contain logical conditions, and are transformed into linear constraints (2.9) and (2.10) by following [8]:

1) Ramp-up constraints:

$$p_{i,n}(t) - p_{i,m}(t-1) \le \Delta_i x_i(t-1) + \left(p_{i\min} + \frac{\Delta_i}{2} \right) \left(x_i(t) - x_i(t-1) \right), \forall i, \forall n, \forall t, \forall m \in \{ m \mid \pi_{mn} \ne 0 \}. \quad (2.9)$$

Upon starting up, (2.9) becomes (2.8); when the unit is kept online, (2.9) becomes (2.7); and (2.9) is redundant otherwise.

2) Ramp-down constraints:

$$p_{i,m}(t-1) - p_{i,n}(t) \le \Delta_i x_i(t) + \left(p_{i\min} + \frac{\Delta_i}{2} \right) \left(x_i(t-1) - x_i(t) \right), \forall i, \forall n, \forall t, \forall m \in \{ m \mid \pi_{mn} \ne 0 \}. \quad (2.10)$$

Minimum Up/Down Time. Unit *i* must be kept online until its minimum up time is reached, or be kept offline until the minimum down time is reached. A linear formulation from [8] (Equations (21)-(26)) is used.

System demand constraints. Net system demand needs to be satisfied at every hour for each state of which the probability is nonzero, i.e.,

$$\sum_{i=1}^{I} p_{i,n}(t) = P_n^D(t), \forall t, \forall n \in \{ n \mid \varphi_n(t) \ne 0 \}. \quad (2.11)$$

If net demand cannot be satisfied, penalties will be added based on convex piecewise linear penalty functions for load shedding or over generation/wind curtailment.

Objecive Function. The objective is to minimize the total expected cost, which consists of dispatch cost, no-load cost and startup cost, i.e.,

$$J = \sum_{t=1}^{T} \sum_{i=1}^{I} \left\{ \sum_{n=1}^{N} \sum_{b=1}^{B} \varphi_n(t) C_{i,b} p_{i,b,n}(t) + x_i(t) S_i^{NL} + u_i(t) S_i \right\}. \quad (2.12)$$

The above stochastic unit commitment problem (2.3)-(2.6), (2.9), (2.10), minimum up/down time, (2.11), (2.12) is a linear mixed-integer optimization problem with binary decision variables $\{u_i(t)\}$ and $\{x_i(t)\}$ and continuous variables $\{p_{i,b,n}(t)\}$, with uncertainty described by the net demand levels $\{P_n^D(t)\}$, state probabilities $\{\varphi_n(t)\}$, and transition probabilities $\{\pi_{mn}\}$.

2.5 Solution Methodology

The above problem is solved by using the branch-and-cut method in subsection 2.5.1. Monte Carlo simulation is used to evaluate the solution quality as presented in subsection 2.5.2. To effectively simulate rare events, importance sampling is used as presented in subsection 2.5.3. Our Markovian approach is then compared with the deterministic approach as well as the stochastic programming approach as presented in subsection 2.5.4.

2.5.1 Solving the Markovian Problem by Using Branch-and-cut

The branch-and-cut method combines the branch and bound algorithm and the cutting-plane method. After relaxing integrality constraints, branch-and-cut starts with cuts trying to obtain the convex hull of feasible solutions of the original problem. After the convex hull is obtained, the linear programming simplex method then efficiently optimizes the relaxed problem over the convex hull and obtains an optimal solution, which is also the optimal solution to the original problem. Since obtaining the convex hull itself is NP-hard for NP-hard problems, branching operations may be needed to decompose the problem as in the branch and bound algorithm.

The branch-and-cut method is efficient in solving deterministic linear mixed-integer problems, and has been widely used by ISOs, utility companies and semiconductor manufacturers. Also, the existence of commercial packages such as CPLEX [2] or GUROBI [3] reduces the time to code and the time to debug. However, these packages do not provide infrastructure to explicitly describe stochastic processes. For our formulation, note that state probabilities are included in the objective function (2.12) as weights, and system

demand constraints (2.11) only have to hold for those states with nonzero probabilities. Also, ramp rate constraints (2.9) and (2.10) only have to hold for those transitions with nonzero probabilities. With state transition probabilities given, state probabilities calculated before optimization based on (2.2), and the objective and constraints formulated in a linear manner, the overall problem is a linear mixed-integer problem and can be effectively solved by using branch-and-cut.

2.5.2 Monte Carlo Simulation

After the problem is solved, the optimization cost can be calculated according to (2.12). The cost for a particular scenario can also be evaluated by solving the dispatch problem with commitment decisions fixed by optimization. Monte Carlo simulation runs can be conducted to obtain the simulation cost, which is the ensemble average of simulated costs. In the process, a scenario can be produced by sampling from the detailed transition matrix sequentially from Hour 1 to Hour *T*. The dispatch problem uses the deterministic counterpart of (2.4)-(2.6) and (2.9)-(2.12) following [14], [27] for simplicity instead of solving dispatch problems sequentially for each hour as in the real-time dispatch process, and is a linear programming problem with dispatch decisions as decision variables. Since the simulation is based on scenarios and the optimization is based on states, there are discrepancies between the simulation cost and the optimization cost. Moreover, since a simplified state transition matrix is used in optimization as presented in Section 2.3, the simulation cost for scenarios obtained from the detailed transition matrix could be further different from the optimization cost.

2.5.3 Simulating Rare Events by Using Importance Sampling

If there are low-probability events captured by the state transition matrix, a very large number of scenarios will be needed in the Monte Carlo simulation for the results to be meaningful. To increase simulation efficiency, *Importance Sampling* [36], [37] is used to make rare events occur more frequently. This technique modifies the transition probability distributions, and then adjusts the cost of each scenario. More specifically, let j be the index of scenarios ranging from 1 to J. For scenario j, let cost(j) be the cost, $p_{ori}(j)$

the scenario probability calculated as the product of a sequence of original state transition probabilities, $p_{new}(j)$ the scenario probability calculated based on the new transition matrix with importance sampling. The expected cost based on the original transition matrix, E[cost], is:

$$E[\text{cost}] = \frac{1}{J}\sum_{j=1}^{J}\text{cost}(j)\frac{p_{ori}(j)}{p_{new}(j)}. \tag{2.13}$$

Similarly, the original variance of costs, *var*[cost], is:

$$\text{var}[\text{cost}] = \frac{1}{J}\sum_{j=1}^{J}\left[\left(\text{cost}(j) - \frac{1}{J}\sum_{j=1}^{J}\text{cost}(j)\right)\frac{p_{ori}(j)}{p_{new}(j)}\right]^2. \tag{2.14}$$

and the standard deviation is the square root of the variance.

2.5.4 Comparison of Different Approaches

Our Markovian approach is compared with the deterministic approach as well as the stochastic programming approach. The deterministic formulation can be viewed as a special case of the Markovian formulation with only one state at each time instant, and can be efficiently solved by using branch-and-cut [8]-[10]. As shown in the first two columns in Table 2.2, the numbers of decision variables and constraints of the Markovian formulation are not drastically larger than those of the deterministic formulation. More importantly, the Markovian formulation does not change the fundamental linear mixed-integer programming problem structure of the deterministic formulation. According to Section 3 of [10], the branch-and-cut method is efficient to solve deterministic unit commitment problems of different sizes. The Markovian formulation can therefore be effectively solved by using the branch-and-cut method as will be demonstrated in the next section.

Table 2.2. Comparison of the Markovian Formulation, the Deterministic Formulation and the Stochastic Programming Formulation

	Deterministic	Markovian	Stochastic programming
Generation levels	$I \times T$	$I \times T \times N$	$I \times T \times J$
Demand constraints	T	$T \times N$	$T \times J$
Ramp Constraints	$2 \times I \times T$	$2 \times I \times [N+(T-1) \times N^2]$	$2 \times I \times T \times J$

For the stochastic programming formulation, there are $J = N^T$ total number of possible scenarios, and the numbers of decision variables and constraints are shown in the third column of Table 2.2. When J is reduced by using scenario reduction techniques, say to N for easy comparison, the numbers of decision variables and system demand constraints are equal to those of the Markovian formulation. However, since only a limited number of scenarios are considered in making unit commitment decisions, high penalties may incur during simulation, and the simulation cost may not be significantly lower than that of the Markovian formulation as will be shown in Case 3 of Example 2 in the next section.

It is interesting to note that with J reduced to N, the number of ramp constraints for the stochastic programming formulation is smaller than that of the Markovian formulation, since ramp rate constraints are enforced differently. For the stochastic programming formulation, since state transition from hour t-1 to t is fixed for each scenario, a unit should satisfy only two ramp constraints, and the total number of constraints is $2 \times I \times T \times J$. For the Markovian formulation, from each state, N possible transitions can occur from hour t - 1 to t, and the total number of constraints is about $2 \times I \times T \times N^2$. With more ramp rate constraints considered, the Makovian approach is more conservative, and can result in higher optimization cost than that of the stochastic programming approach.

In above, wind generation in the day-ahead unit commitment process is modeled as a Markov process driven by a white noise. For the reliability assessment commitment process performed in real-time,

however, wind generation may maintain an increasing (or a decreasing) trend over several consecutive timeframes. With this trend, the stochastic process representing wind generation is driven by a colored noise. Nevertheless, the colored noise can be pre-whitened and treated as the output of a pre-whitening system driven by a white noise. This augmented state is a Markov process [4], and the method presented above can be applied without major conceptual difficulties.

2.6 Numerical Results

The Markovian approach has been implemented by using the commercial solver CPLEX 12.4 [2] and run on a PC laptop with an Intel Core(TM) i7-2820QM 2.30GHz CPU and 8GB memory. The deterministic formulation is a special case of the Markovian formulation with only one state at each time instant. The stochastic programming approach with a small number of scenarios has also been directly implemented as a linear mixed-integer programming problem by using CPLEX for comparison purposes.

Two examples are provided. In Example 1, a simple two-unit three-hour problem is used to demonstrate the differences between the Markovian approach and the stochastic programming approach in terms of optimization costs, simulation costs, and impacts from different numbers of ramp rate constraints. In Example 2, a problem with 309 units over 24 hours of ISO-New England is tested to demonstrate the computational efficiency, the robustness with respect to the number of states, the impact of the number of nonzero elements in the state transition matrix, the effectiveness to accommodate different levels of wind penetration, and the ability of capturing low-probability high-impact events of the Markovian approach.

2.6.1 Example 1

Consider a two-unit three-hour problem without minimum up/down time for simplicity. The parameters of the two units are provided in Table 2.3.

Table 2.3. Unit Parameters for Example 1

Unit	p_{imin} (MW)	p_{imax} (MW)	Ramp rate	c_i (\$/MWh)	S_i (\$)	Initial
1	0	80	10	65	50	On/40
2	0	80	160	30	8000	Off

Assume that the three possible net demand levels are 70, 100 and 130 for all the three hours with the following state transition matrix for both optimization and simulation:

$$\pi = \begin{bmatrix} \pi_{11} & \pi_{12} & \pi_{13} \\ \pi_{21} & \pi_{22} & \pi_{23} \\ \pi_{31} & \pi_{32} & \pi_{33} \end{bmatrix} = \begin{bmatrix} 80\% & 20\% & 0 \\ 10\% & 80\% & 10\% \\ 0 & 20\% & 80\% \end{bmatrix}. \quad (2.15)$$

The probabilities of net system demand at 70, 100 and 130 at Hour 1 are given as 0.1, 0.8, and 0.1, respectively. The probabilities of demand levels at Hours 2 and 3 can be calculated from (2). The stopping criterion is the relative mixed integer programming (MIP) gap 0.01%.

The results of the new approach are summarized in Table 2.4. The optimization cost is \$21,200. Both units are online, since a single unit's capacity alone is not sufficient for demand levels 100 and 130. One thousand Monte Carlo simulation runs are conducted. The simulation cost is \$19,892, which is less than the optimization cost. This is because the simulation process is simplified as discussed in subsection 2.5.2.

The stochastic programming approach considers all 17 possible scenarios (= 33 minus 10 scenarios with zero probability). Even though the commitment decisions obtained by using the stochastic programming approach turn out to be the same as those obtained by using the Markovian approach, cheaper dispatch decisions are obtained under several scenarios, e.g., Scenario 10 as shown in Table 2.5, with less ramp rate constraints binding than the Markovian approach. Consequently, the optimization cost, \$19,943, is smaller than that of the Markovian approach as discussed in the third paragraph of subsection 2.5.4. The simulation cost turns out to be the same as that of the Markovian approach.

Table 2.4. Results for Example 1 by Using the Markovian Approach

Optimization cost		$21,200		CPU time		0.52s	
Net demand		u_1	u_2	x_1	x_2	p_1	p_2
Hour 1	70	0	1	1	1	30	40
	100					40	60
	130					50	80
Hour 2	70	0	0	1	1	30	40
	100					40	60
	130					50	80
Hour 3	70	0	0	1	1	30	40
	100					40	60
	130					50	80

Table 2.5. Dispatch Decisions in Scenario 10 for Example 1 by Using Stochastic Programming

Scenario		Net demand	p_1	p_2
10	Hour 1	100	30	70
	Hour 2	100	20	80
	Hour 3	100	20	80

2.6.2 Example 2

Consider ISO-New England's 24-hour problem with 309 units. The bid information of units and forecasted system demand values over 24 hours are taken from a summer day of ISO-NE's day-ahead energy market. All wind farms in New England are lumped together into one aggregated wind farm, and the total wind capacity is scaled to the corresponding values from [31] for different levels of wind penetration. Three cases are tested. The nominal case uses the 10-state transition matrix of Table 2.1 with the initial wind generation at State 5 (0.4 to 0.5 of the wind capacity) for optimization, and a detailed 50-state transition matrix based

on the same data set with the initial wind generation at State 25 (0.48 to 0.50 of the wind capacity) for simulation. It also considers 5% wind penetration with wind generation capacity 2.3 GW without rare events. For all the cases, if net system demand cannot be satisfied, penalties will be incurred for load shedding and over generation based on convex piecewise linear penalty functions as shown in Table 2.6 without considering wind curtailment for simplicity. The stopping criterion in optimization is the relative MIP gap 0.01% for Cases 1 and 3, and 0.2% for Case 2.

Table 2.6. Penalty Curves for Load Shedding and Over Generation for Example 2

Load shedding	0~1,000MWh	After 1,000MWh	
Penalty	$1,000/MWh	$85,000/MWh	
Over generation	0~100MWh	100~1,100MWh	After 1,100MWh
Penalty	$0/MWh	$1,000/MWh	$85,000/MWh

Case 1. The robustness with respect to the number of discretized states and the impact of the number of nonzero elements in the state transition matrix on the computational efficiency are tested. To demonstrate the robustness with respect to the number of discretized states in our approach, 10 states and 20 states are tested. In simulation, 1,000 Monte Carlo runs are conducted based on the 50-state detailed transition matrix.

The results are summarized in Table 2.7. It can be seen that the CPU time for solving the 20-state problem is longer than that of 10-state problem. Welch's t-test verifies the hypothesis that simulation costs of using 10 and 20 states are the same at the 0.05 level of significance, and F-test verifies that standard deviations are the same at the 0.05 level of significance. Thus 10 states are used in Cases 2 and 3.

To test the impact of the number of nonzero elements in the state transition matrix on the computational efficiency, one hypothetical case with a 10-state transition matrix where each element equals to 0.1 is tested. The state probabilities are calculated based on the hypothetical state transition matrix. The CPU time turns out to be 7 minutes and 18 seconds and is longer than the corresponding CPU time in Table

7 by using the block diagonal matrix. The main reason is that more ramp rate constraints are considered with more nonzero elements in the transition matrix.

Table 2.7. Results for Case 1

		10 states	20 states
Optimization	CPU time	1min4s	6min2s
	Cost (k$)	11,838	11,854
Simulation	Cost (k$)	11,803	11,802
	STD (k$)	513	520

Case 2. Different levels of wind penetration, 9%-24% from [31], are tested beyond the nominal 5%. The same transition matrix is used for different penetration for simplicity. The system demand is increased from that of Case 1 to avoid negative net demand and is the same for all penetration levels.

The results are summarized in Table 2.8. When the wind penetration level increases, the CPU time increases, since more ramp rate constraints (2.9) and (2.10) become (2.7), making the convex hull more difficult to obtain, as explained below. For the tested dataset, ramp constraints of units with small dispatch range ($p_{i\max} - p_{i\min}$) are mostly eliminated during preprocessing before optimization, since the dispatch range is even smaller than the ramp rate (Δ_i). Oppositely, ramp constraints of units with large dispatch range are often included in optimization. After eliminating obviously redundant ramp constraints, the number of possible ramp constraints (2.9) and (2.10) considered in optimization is the same 34,608 among different penetration levels, since the same transition matrix is used. When penetration level increases, units with ramp constraints considered are committed for more hours, so more ramp constraints (2.9) and (2.10) become (2.7), as shown in the fifth row of Table 2.8. Since constraints (2.7) are time-coupling and couple different states in two consecutive hours, more constraints (2.7) will make the convex hull more difficult to obtain. According to CPLEX log files, the stopping criterion is reached immediately after cuts are added

for 5%, 9% and 14% penetrations. However, for 20% and 24% penetrations, branching is needed after adding cuts.

Table 2.8. Results for Case 2

Penetration		5%	9%	14%	20%	24%
Wind Capacity (GW)		2.3	4.17	6.6	9	11
Optimization	CPU	1min02s	1min11s	2min41s	7min30s	38min19s
	Total (k$)	15,251	13,923	12,690	12,918	16,397
	Constraints (7)	14,066	14,066	14,140	16,918	23,212
Simulation	Total (k$)	15,188	13,803	12,473	12,276	15,909
	STD	729	1,006	1,308	2,050	11,759
	UCED	15,182	13,803	12,458	12,185	14,496
	Penalty	6	0	15	91	1,413

The simulation cost and the standard deviation of costs are also shown in Table 2.8, including the breakdown into the expected unit commitment and economic dispatch (UCED) cost and the expected penalty costs (all in $\$10^3$). It can be seen that the Markovian approach is effective to accommodate up to 20% penetration of wind generation efficiently, since UCED costs decrease and penalty costs do not increase much. However, UCED costs and penalty costs increase drastically from 20% to 24% of penetration with more expensive UCED decisions and more load shedding or over generation. Also, with increasing wind penetration, the standard deviations of total costs increase.

Case 3. The Markovian approach is compared with the stochastic programming approach and the deterministic approach in terms of cost efficiency. Special attention is paid to the ability of capturing low-probability high-impact events, resembling the sudden wind drop in Texas in February 2008. For the Markovian approach, the initial wind state is State 9 (0.8 to 0.9 of the wind capacity) to make sudden wind drops more likely to happen in the experiment. For the stochastic programming approach, wind generation

at each hour is assumed to follow a normal distribution with mean and standard deviation established based on the corresponding detailed 50-state transition matrix. Three thousand scenarios are produced. Scenario reduction is performed by using GAMS/SCENRED [18], [19]. The problem is solved with the reduced 10 scenarios as well as with 20 scenarios. For the deterministic approach, the net system demand uses the average demand plus 10% at each hour to secure more online generation capacity.

Results without considering rare events are summarized in Table 2.9. It can be seen from the CPU time that the Markovian approach is more computationally efficient than the stochastic programming approach with 20 scenarios. The optimization cost of our approach is higher than those of the stochastic programming approach with 10 and 20 scenarios as explained before. However, the simulation cost as well as the number of simulated scenarios with penalties of our approach is smaller than those of the stochastic programming approach. This demonstrates that 10 states can capture more information of wind generation than 10 or 20 scenarios. The simulation cost of the deterministic approach is much higher than others, indicating that the additional 10% online generation capacity is not as useful as stochastic models.

Table 2.9. Results for Case 3 without Rate Events

		Markovian	SP		Deterministic
			10 scenarios	20 scenarios	
Optimization	CPU time	2min29s	1min57s	6min1s	4s
	Total (k$)	10,856	10,475	10,504	13,206
Simulation	Penalty Scenarios	3	178	175	997
	Total (k$)	10,593	10,795	10,795	12,659
	STD (k$)	354	1,813	1,928	459

Considering rare events. Rare events can be captured in the transition matrix. Consider a hypothetical case where the transition probability from State 50 to State 1 of the detailed transition matrix is adjusted from 0 to 0.00001. The transition probability from State 50 to State 50 is correspondingly reduced by 0.00001. In

optimization, the transition probability from State 10 to State 1 in Table 2.1 is adjusted to 0.00001. In simulation, importance sampling is used as discussed in subsection 2.5.3.

The results are summarized in Table 2.10. The simulation cost, the standard deviation, and the number of simulated scenarios with penalties of the Markovian approach are smaller than those of other approaches, demonstrating that the solutions of the Markovian approach are more robust than those of other approaches. The reason is that for the stochastic programming approach, the scenarios with high-impact rare events are likely to be eliminated during the scenario reduction procedure. Also, it is difficult to specifically include such high-impact scenarios since which scenarios will cause harmful impacts cannot be identified before unit commitment decisions are made. In contrast, for the Markovian approach, multiple rare events can be captured in the state transition matrix with only one nonzero element in an off-diagonal position, and the adjusted transition matrix can be directly used in the unit commitment process.

Table 2.10. Results for Case 3 with Rate Events

		Markovian	SP		Deterministic
			10 scenarios	20 scenarios	
Optimization	CPU	1min57s	1min57s	6min1s	4s
	Total (k$)	10,857	10,475	10,504	13,206
Simulation	Penalty Scenarios	80	253	250	997
	Total (k$)	10,474	10,676	10,676	12,523
	STD (k$)	477	6,449	5,080	491

2.7 Conclusion

In this chapter, the aggregated wind generation is modeled as discrete Markov processes with state transition matrices established based on historical data. A stochastic unit commitment problem is formulated based on states instead of scenarios. With state transition probabilities given, state probabilities

calculated before optimization, and the objective function and constraints formulated in a linear manner, the linearly formulated problem can be effectively solved by using the branch-and-cut method. Numerical results demonstrate that the Markovian approach is computationally efficient, effective under 20% of wind penetration, and is able to capture low-probability high-impact events. The approach thus represents a new and effective way to address stochastic problems without scenario analysis.

References

[1] E. Ela and B. Kirby, "ERCOT Event on February 26, 2008: Lessons Learned," NREL, CO, Tech. Rep. NREL/TP-500-43373, July 2008. [Online]. Available: http://www.nrel.gov/docs/fy08osti/43373.pdf

[2] IBM ILOG, "Introducing IBM ILOG CPLEX Optimization Studio V12.4," 2012. [Online]. Available: http://pic.dhe.ibm.com/infocenter/cosinfoc/v12r4/index.jsp?topic=%2Filog.odms.studio.help%2FOptimization_Studio%2Ftopics%2FCOS_home.html

[3] Gurobi Optimization, Inc., "GUROBI Optimizer Reference Manual, Version 5.0," 2012. [Online]. Available: http://www.gurobi.com/documentation/5.0/reference-manual

[4] Y. Bar-Shalom, X. R. Li, and T. Kirubarajan, *Estimation with Applications to Tracking and Navigation: Theory Algorithms and Software*, J. Wiley and Sons, 2001.

[5] B. Zhang, P. B. Luh, E. Litvinov, T. Zheng, F. Zhao, J. Zhao and C. Wang, "Electricity Auctions with Intermittent Wind Generation," in *Proceedings of the IEEE Power and Energy Society 2011 General Meeting*, Detroit, Michigan, July 2011.

[6] X. Guan, P. B. Luh, H. Yan, and J. A. Amalfi, "An optimization-based method for unit commitment," *International Journal of Electrical Power & Energy Systems*, Vol. 14, No. 1, pp. 9-17, 1992.

[7] S. J. Wang, S. M. Shahidehpour, D. S. Kirschen, S. Mokhtari, and G. D. Irisarri, "Short-term generation scheduling with transmission and environmental constraints using an augmented Lagrangian relaxation," *IEEE Trans. on Power Systems*, Vol.10, No.3, pp.1294-1301, 1995.

[8] M. Carrión and J. M. Arroyo, "A Computationally Efficient Mixed-Integer Linear Formulation for the Thermal Unit Commitment Problem," *IEEE Transactions on Power System*, Vol. 21, No. 3, pp. 1371-1378, Aug. 2006.

[9] G. Morales-España, J. M. Latorre, and A. Ramos, "Tight and compact MILP formulation of Start-Up and Shut-Down ramping in unit commitment," *IEEE Transactions on Power Systems*, Vol. 28, No. 2, pp. 1288-1296, May 2013.

[10] D. Rajan and S. Takriti, "Minimum up/down polytopes of the unit commitment problem with start-up costs," IBM Res. Rep., 2005. [Online]. Available: http://www.research.ibm.com/people/d/dpkrjn/DeepakTR.pdf

[11] F. Bouffard and F. D. Galiana, "Stochastic Security for Operations Planning with Significant Wind Power Generation," *IEEE Transactions on Power Systems*, Vol. 23, No. 2, pp. 306-316, 2008.

[12] J. Wang, M. Shahidehpour, and Z. Li, "Security-constrained Unit Commitment with Volatile Wind Power Generation," *IEEE Trans. on Power Systems*, Vol. 23, No. 3, pp. 1319-1327, Aug. 2008.

[13] V. S. Pappala, I. Erlich, K. Rohrig, and J. Dobschinski, "A Stochastic Model for the Optimal Operation of a Wind-Thermal Power System," *IEEE Trans. on Power Systems*, Vol. 24, No. 2, pp. 940–950, May 2009.

[14] P. Ruiz, P. C. Philbrick, E. Zak, K. W. Cheung, and P. Sauer, "Uncertainty Management in the Unit Commitment Problem," *IEEE Trans. on Power Systems*, Vol. 24, No. 2, pp. 642–651, May 2009.

[15] A. Papavasiliou, S. Oren, and R. P. O'Neill, "Reserve Requirements for Wind Power Integration: A Scenario-Based Stochastic Programming Framework," *IEEE Transactions on Power Systems*, Vol. 26, No. 4, pp. 2197-2206, Nov. 2011.

[16] C. Weber, P. Meibom, R. Barth, and H. Brand, "WILMAR: A Stochastic Programming Tool to Analyze the Large-scale Integration of Wind Energy," *Optimization in the Energy Industry*, Ch. 19, pp. 437–458, Berlin, Germany, Springer, 2009.

[17] L. Wu, M. Shahidehpour, and Z. Li, "Comparison of Scenario-Based and Interval Optimization Approaches to Stochastic SCUC," *IEEE Transactions on Power Systems*, Vol. 27, No. 2, pp. 913-921, May 2012.

[18] J. Dupačová, N. Gröwe-Kuska, and W. Römisch, "Scenario Reduction in Stochastic Programming: An approach using probability metrics," *Mathematical programming*, Vol. 95, No. 3, pp. 493-511, 2003.

[19] H. Heitsch and W. Römisch, "Scenario Reduction Algorithms in Stochastic Programming," *Computational Optimization and Applications*, No. 24, pp. 187-206, 2003.

[20] N. Growe-Kuska, H. Heitsch, and W. Romisch, "Scenario Reduction and Scenario Tree Construction for Power Management Problems," in *Proc. of Power Tech Conference*, 2003 IEEE Bologna, June 2003.

[21] M. R. Garey and D. S. Johnson, *Computers and Intractability: A Guide to the Theory of NP-Completeness*, New York: W. H. Freeman, 1979.

[22] A. Ben-Tal and A. Nemirovski, "Robust Optimization – Methodology and Applications," *Mathematical Programming*, Vol. 92, No. 3, pp. 453-480, 2002.

[23] D. Bertsimas and S. Melvyn, "The Price of Robustness," *Operations Research*, Vol. 52, No. 1, pp. 35-53, 2004.

[24] M. Zhang and Y. Guan, "Two-stage Robust Unit Commitment Problem," Tech. Rep., Arizona State University, Tempe, AZ, 2009.

[25] R. Jiang, M. Zhang, G. Li, and Y. Guan, "Two-stage Robust Power Grid Optimization Problem," Tech. Rep., University of Florida, Gainesville, FL, USA, 2010.

[26] L. Zhao and B. Zeng, "Robust unit commitment problem with demand response and wind energy," University of South Florida, Tech. Rep., Oct. 2010, [Online]. Available: http://www.optimization-online.org/DB_FILE/2010/11/2784.pdf

[27] D. Bertsimas, E. Litvinov, X. A. Sun, J. Zhao, T. Zheng, "Adaptive Robust Optimization for the Security Constrained Unit Commitment Problem," *IEEE Transactions on Power Systems*, Vol. 28, No. 1, pp. 52-63, Feb. 2013.

[28] R. Jiang, J. Wang, Y. Guan, "Robust Unit Commitment with Wind Power and Pumped Storage Hydro," *IEEE Transactions on Power Systems*, Vol.27, No.2, pp.800-810, May 2012.

[29] D. Brooks, E. Lo, R. Zavadil, S. Santoso, and J. Smith, "Characterizing the Impacts of Significant Wind Generation Facilities on Bulk Power System Operations Planning," Xcel Energy – North Case Study Final Report, prepared for Utility Wind Integration Group, Arlington, VA, May 2003, [Online]. Available: http://www.uwig.org/UWIGOpImpactsFinal7-15-03.pdf

[30] J. Mur-Amada, Á. A. Bayod-Rújula, "Wind Power Variability Model," in *Proceedings of 9th International Conference Electrical Power Quality and Utilisation*, Barcelona, Oct. 2007.

[31] "Final Report: New England Wind Integration Study, Prepared for ISO New England," Dec. 5, 2010. [Online]. Available: http://www.iso-ne.com/committees/comm_wkgrps/prtcpnts_comm/pac/reports/2010/newis_report.pdf

[32] The National Renewable Energy Laboratory, Eastern Wind Dataset, 2010, [Online]. Available: http://www.nrel.gov/electricity/transmission/eastern_wind_methodology.html

[33] U. Focken, M. Lange, K. Mönnich, H. Waldl, H. G. Beyer, and A. Luig, "Short-term prediction of the aggregated power output of wind farms—a statistical analysis of the reduction of the prediction error by spatial smoothing effects," *Journal of Wind Engineering and Industrial Aerodynamics*, Vol. 90, No. 3, pp. 231-246, Mar. 2002.

[34] "'The Grid Scale Battery Storage Market to be Worth $1.2bn in 2013' Says Visiongain Report," 2013, [Online]. Available: http://www.visiongain.com/Press_Release/381/'The-grid-scale-battery-storage-market-to-be-worth-1-2bn-in-2013'-says-visiongain-report

[35] "The energy storage breakthrough we've been waiting for?" Smart Grid News.com, 2013, [Online]. Available: http://www.smartgridnews.com/artman/publish/Technologies_Storage/The-energy-storage-breakthrough-we-ve-been-waiting-for-5654.html#.UWRK4jBceNo

[36] M. Denny, "Introduction to Importance Sampling in Rare-event Simulations," *European J. of Physics*, Vol. 22, No 4, pp. 403–411, 2001.

[37] P. W. Glynn and D. L. Iglehart, "Importance Sampling for Stochastic Simulation," *Management Science*, Vol. 35, No. 11, pp. 1367-1392, Nov. 1989.

Chapter 3

Grid Integration of Distributed Wind Generation: Hybrid Markovian and Interval Unit Commitment

Grid integration of wind generation is challenging in view of wind uncertainties and possible transmission congestions. Without considering transmission, a stochastic unit commitment problem was solved in our previous work by modeling aggregated wind as a Markov chain instead of scenarios for reduced complexity. With congestion, wind generation at different locations cannot be aggregated and is modeled as a Markov chain per wind node, and the resulting global states are a large number of combinations of nodal states. To avoid explicitly considering all such global states, interval optimization is synergistically integrated with the Markovian approach in this chapter. The key is to divide the generation level of a conventional unit into a Markovian component that depends on the local state, and an interval component that manages extreme non-local states. With appropriate transformations, the problem is converted to a linear form and is solved by using branch-and-cut. Numerical results demonstrate that the over-conservativeness of pure interval optimization is much alleviated, and the new approach is effective in terms of computational efficiency, simulation cost, and solution feasibility. In addition, solar generation shares a similar uncertain nature as wind generation, and can thus be modeled and solved similarly.

3.1 Introduction

Wind energy can help reduce the dependence on fossil fuels and greenhouse gas emissions, and the global wind industry has been growing rapidly. In 2012, nearly 45 GW of wind capacity was brought online, and the global wind capacity was increased by 19% to almost 283 GW [2]. The U.S. Department of Energy sets the target to increase wind energy's contribution to 20% of electricity by 2030 [3]. Wind integration involves wind turbine technologies, power electronics, power systems, and market design issues. Related fundamentals of power systems include long-term planning, improved forecasting, operational processes and tools, and smart grid technologies [4].

A critical operational process is day-ahead unit commitment (UC) in which the Independent System Operator (ISO) commits conventional units to meet the forecasted demand of the following day while satisfying individual unit and transmission constraints. UC with high levels of wind generation, however, is challenging in light of the fact that wind generation is uncertain by nature and transmission congestions are possible. A straight-forward way to address uncertainty in this process is the deterministic approach that meets the expected system demand and adjusts reserve levels based on hourly standard deviations of wind generation [5], [6]. Since wind uncertainties are not explicitly captured, solutions may be infeasible for certain wind generation realizations [7].

Besides the deterministic approach, several other approaches have been presented in the literature, including stochastic programming, robust optimization, and interval optimization. Stochastic programming optimizes the expected cost over the probability distribution of uncertainties, with wind uncertainties commonly modeled by representative scenarios [8]-[15]. A scenario contains a trajectory of realizations over all hours in the time horizon, and the number of scenarios increases exponentially with the number of hours. It is difficult to select an appropriate number of scenarios to balance modeling accuracy, solution feasibility, and computational efficiency. Robust optimization finds the optimal solution of the worst-case realization in a given uncertainty set to ensure solution feasibility against all possible realizations, and may

lead to conservative solutions [7], [16], [17]. In addition, the two-stage robust model in [7] is nonlinear and computationally challenging. Interval optimization is another approach for linear problems with uncertainties modeled by intervals [14], [18]. The approach captures bounds of uncertain wind generation in system demand and transmission capacity constraints. Other realizations within these bounds will be guaranteed to be feasible. The effective use of interval arithmetic makes this approach computationally efficient. However, its results remain conservative. The literature is reviewed in Section II.

To overcome the difficulties of existing approaches, a pure Markovian approach was developed in our previous work to solve the day-ahead stochastic UC problem without transmission constraints [19]. Wind generation from all wind farms was aggregated and modeled as a Markov chain with state transition matrices established based on historical data. The UC problem was then formulated as a stochastic optimization problem based on states instead of scenarios. A state represents the wind generation value at a particular hour and captures past information probabilistically. Because the number of states increases linearly with the number of hours, the complexity of the problem is significantly reduced when compared to scenario-based formulations. With state transitions linearly formulated, the problem was effectively solved by using the branch-and-cut method [20], [21].

In this chapter, the pure Markovian approach in [19] is extended to consider transmission constraints. Since possible congestions imply that wind generation at different locations needs to be treated separately, wind generation is modeled as a Markov chain for each wind node[1]. There are multiple Markov chains in a transmission network. These chains are assumed independent for simplicity. The resulting global states are a large number of combinations of local/nodal states. Dispatch decisions of pure Markov-based optimization [19] should explicitly depend on the global states. To reduce this complexity, an approach that

[1] The Markovian model was validated in [22] for day-ahead and real-time wind generation series.

synergistically incorporates both Markov-based optimization and interval optimization is developed. The new hybrid Markovian and interval approach has the following three main contributions:

1. To make use of information from local states without considering all possible global states, the generation level (dispatch decision) of a conventional unit is divided into two components: the Markovian component that depends on the local state and the interval component that manages extreme non-local states.

2. Constraints are innovatively formulated to guarantee solution feasibility for all possible realizations without much complexity. Especially, the effective use of local wind states alleviates the over-conservativeness of interval optimization in transmission capacity and ramp rate constraints.

3. By analyzing the monotonicity of Markovian nodal injections, the problem is transformed into a linear form and is efficiently solved by using branch-and-cut.

Section 3.3 models distributed wind generation, presents pure Markov-based optimization, formulates the new hybrid Markovian and interval approach, and discusses two methods to reduce the wind uncertainty by considering wind power forecasts or incorporating spatial correlations of wind farms. Section 3.4 develops the solution methodology, and compares the complexity and conservativeness of the new approach with those of pure Markov-based optimization and pure interval optimization. Section 3.5 tests a simple problem, the IEEE 30-bus system, and the IEEE 118-bus system. Numerical results demonstrate that our approach alleviates the over-conservativeness of interval optimization and is effective in terms of computational efficiency, simulation cost, and solution feasibility.

Although the problem solved in this chapter is day-ahead UC, the new formulation is general and can model real-time UC as well. In addition, solar generation can be modeled and solved in ways similar to those for wind generation. The reason is that even though wind and solar have different diurnal patterns –

peak wind generation usually occurs in the morning and evening while that of solar usually occurs in the middle of a day [23], they share the similar uncertain nature.

3.2 Literature Review

This section reviews stochastic programming, robust optimization, pure interval optimization, and hybrid approaches.

Stochastic programming optimizes the expected cost over the probability distribution of uncertainties, with wind uncertainties commonly modeled by using representative scenarios [8]-[15]. A single set of UC decisions are determined to satisfy all the selected scenarios, together with multiple sets of dispatch decisions, one for each scenario. The objective is to minimize the commitment cost and the expected dispatch cost. Decomposition methods, such as Benders' decomposition [9], [14] or Lagrangian relaxation [13], [15], are used to solve stochastic UC problems.

Typically, wind generation or wind speed at each hour is assumed to follow a distribution to generate scenarios. Each scenario represents a sequence of realizations of uncertainties over the optimization horizon (e.g., 24 hours). As a result, the number of scenarios can be extremely large even when dealing with discrete probability distributions. Therefore, scenario reduction techniques are commonly used to eliminate very low-probability scenarios, to aggregate "close" scenarios [24], [25], or to measure the impact of each scenario on the objective function [26]. The reduced number of scenarios are then considered in the stochastic UC problem. In general, it is difficult to select an appropriate number of scenarios to balance modeling accuracy, solution feasibility, and computational efficiency. To refine the number of scenarios while retaining high-impact rare events, eleven criteria (e.g., the minimum possible wind output throughout the day) are discussed to select scenarios [13]. These criteria, however, are heuristic in nature based on daily patterns of wind, so important rare events of abnormal days may not be captured. Additionally, it is not clear how to extend this method to networks with multi-area wind production and transmission

constraints [15]. The alternative selection method presented in [15] ignores rare events with questionable validity.

Robust optimization seeks an optimal solution feasible for all possible realizations within a pre-determined uncertainty set. With uncertainties modeled by the uncertainty set without probabilistic information, it optimizes against the worst-case realization to ensure feasibility of all possible realizations [7], [16], [17]. The worst-case design avoids the combinatorial complexity caused by nodal uncertainties when all possible realizations are considered. The robust UC model in [7] has two stages. The first stage is to determine the optimal UC decisions feasible for all possible realizations by using Benders decomposition; and the second is to select ED decisions against the worst-case realization given UC decisions of the first stage by using outer approximation. Numerical experiments demonstrate that this approach is insensitive to different underlying probability distributions of wind generation. However, optimization of the worst-case realization leads to a conservative solution, which is a common concern of the robust optimization approach. In addition, the two-stage robust model in [7] is nonlinear and computationally challenging.

Pure interval optimization is another approach for linear problems with uncertainties modeled by closed intervals [14], [18]. Interval arithmetic captures bounds of uncertain wind generation in system demand and transmission capacity constraints, and a set of UC decisions are required to be feasible for all these bounds [18].

Wind generation for node *i* at hour *t* is denoted as $\tilde{p}_i^W(t)$ (MW), and is assumed to be within an interval $\left[\underline{p}_i^W(t), \overline{p}_i^W(t)\right]$. System demand constraints require that total wind generation plus total conventional generation equal system demand for each hour. Based on [18, Eq. (20)], the lower bound of total wind generation happens at the minimum realization *m* (when the outputs of all wind farms are at their lower limits), while the upper bound occurs at the maximum realization *M*. UC decisions of conventional units are required to meet these bounds in system demand constraints, so that any other realizations within these

bounds will be satisfied. For example, two wind farms are in a transmission network. Wind farm 1 can generate from 10 to 40 MW, wind farm 2 can generate from 20 to 50 MW, and system demand is 200 MW. The total wind generation is from 30 to 90 MW, and the resulting net system demand (= system demand – wind generation) is from 110 to 170 MW. If a set of UC decisions can meet the minimum net system demand at 110 MW and the maximum net system demand at 170 MW, then it will be able to meet any net system demand within them. Such minimum and maximum system demand constraints are:

$$\sum_i \sum_k p_{i,k,m}(t) = \sum_i p_i^L(t) - \sum_i \underline{p}_i^W(t), \forall t\,. \tag{3.1}$$

$$\sum_i \sum_k p_{i,k,M}(t) = \sum_i p_i^L(t) - \sum_i \overline{p}_i^W(t), \forall t\,. \tag{3.2}$$

where $p_{i,k,m}(t)$ is the dispatch decision of conventional unit k at node i (or unit$_{i,k}$) at time t under the minimum wind realization, $p_{i,k,M}(t)$ under the maximum wind realization, and $p_i^L(t)$ is the demand at node i at time t.

Transmission capacity constraints imply that the power flow through line l at time t, denoted as $f_l(t)$, cannot exceed its transmission capacity $f_l^{\max}$, i.e.,

$$-f_l^{\max} \le f_l(t) \le f_l^{\max}, \forall l, \forall t\,. \tag{3.3}$$

In DC power flow, a line flow is a linear combination of nodal injections weighted by generation shift factors (GSFs). When the dispatch decision of unit$_{i,k}$ is $p_{i,k}(t)$, the power flow is:

$$f_l(t) = \sum_i a_l^i \left(\sum_k p_{i,k}(t) + \tilde{p}_i^W(t) - p_i^L(t) \right), \forall l, \forall t, \tag{3.4}$$

where a_l^i is the GSF representing the sensitivity of $f_l(t)$ with respect to the nodal injection (= nodal generation – nodal demand) from node i. Similar to system demand constraints (3.1) and (3.2), the bounds of wind uncertainties through each line are captured based on [18, Eq. (16) and (19)]:

$$\sum_i \left(a_l^i \sum_k p_{i,k}(t) \right) \geq -f_l^{\max} - \min\left[\sum_i a_l^i \left(\tilde{p}_i^W(t) - p_i^L(t) \right) \right], \forall l, \forall t, \tag{3.5}$$

$$\sum_i \left(a_l^i \sum_k p_{i,k}(t) \right) \leq f_l^{\max} - \max\left[\sum_i a_l^i \left(\tilde{p}_i^W(t) - p_i^L(t) \right) \right], \forall l, \forall t. \tag{3.6}$$

A difference is that GSFs can be positive or negative. Nevertheless, since only inputs are contained on the right-hand-sides of (3.5) and (3.6), interval arithmetic can be used to compute these bounds before optimization. As long as one feasible solution can be found within bounds, all transmission capacity constraints through line *l* at time *t* will be feasible. Since system demand constraints have to be satisfied at the same time, two sets of dispatch decisions $\{p_{i,k,m}(t)\}$ and $\{p_{i,k,M}(t)\}$ are considered in (3.5) and (3.6).

Ramp rate constraints imply the change of generation level cannot exceed the unit's ramp rate between two consecutive hours. These constraints [18, Eq. (21) and (22)] are required to be feasible for the transitions of wind outputs between any pairs among the minimum, maximum and the expected realization that is considered in the objective function. The objective function in [27] uses the cost of the worst-case realization as that considered in robust optimization. The resulting optimization solutions may be conservative. Alternatively, the expected cost of all realizations could be considered. Due to the lack of probabilistic information, the cost of the expected realization is considered for simplicity as the objective function in [18, Eq. (1)]. In this case, the impacts of extreme realizations are not explicitly captured. The effective use of interval arithmetic makes this approach computationally efficient. However, results are still conservative. For the rest of this chapter, pure interval optimization refers to that in [18].

In addition to the approaches reviewed above, there are also hybrid stochastic and robust/interval approaches. A hybrid stochastic and robust approach [28] considers dispatch decisions and constraints from both stochastic programming and robust optimization at the same time, and the objective function is a weighted sum of the costs from both approaches. This approach provides more robust UC decisions than stochastic programming and a lower simulation cost than robust optimization. Its robust optimization part

remains nonlinear. A hybrid stochastic/interval approach [29] considers decision variables, constraints and the cost from stochastic programming at the first few hours, and then switch to pure interval optimization at the remaining hours. This approach provides a lower simulation cost than stochastic programming or pure interval optimization. Its pure interval optimization part remains conservative.

3.3 Problem Formulation

Subsection 3.3.1 models distributed wind generation as a Markov chain per wind node, and describes the UC problem. Subsection 3.3.2 presents pure Markov-based optimization with a few main formulas, and discusses its complexity. To reduce this complexity, subsection 3.3.3 formulates the new hybrid Markovian and interval approach. Subsection 3.3.4 discusses two methods to reduce the wind uncertainty by considering wind power forecasts or by incorporating spatial correlations of wind farms.

3.3.1 Wind Model and the UC Problem

1) Markovian model of nodal wind generation and global state

When transmission constraints are considered, wind generation at different locations cannot be aggregated and must be treated separately. For simplicity, wind generation at different network nodes is assumed to be modeled as independent Markov chains. Let i denote a node in the network with I being the total number of nodes. Based on [19], wind generation at node i is discretized into N_i states. These states are arranged in the ascending order of wind generation values. The transition probability from state n_i' to state n_i is based on historical data:

$$\pi_{n_i' n_i} = \frac{observed\ transitions\ from\ state\ n_i'\ to\ n_i}{occurrences\ of\ state\ n_i'}. \tag{3.7}$$

Denote wind generation of state n_i at time t as $p_{i,n_i}^{W}(t)$ (MW). Its probability, denoted as $\varphi_{n_i}(t)$, can be computed by using probabilities of previous states and transition probabilities,

$$\varphi_{n_i}(t) = \sum_{n_i'=1}^{N_i} \pi_{n_i' n_i} \varphi_{n_i'}(t-1) . \quad (3.8)$$

A global state at time *t*, denoted as *g*, is a combination of wind generation states at all nodes, i.e.,

$$g \equiv [n_1, n_2, \ldots, n_I]^T . \quad (3.9)$$

Its probability at time *t* is denoted as $\varphi_g(t)$ and can be computed as the product of probabilities of all nodal states. Given that each node has up to *N* possible states at time *t*, the number of possible global states can be N^I, which is extremely large for practical problems.

2) The UC problem setup

Building on [19] and [30], let K_i units at node *i* be indexed by (i, k) $(1 \le k \le K_i)$ and *L* transmission lines be indexed by *l* $(1 \le l \le L)$ in a day-ahead energy market over 24 (*T*) hours indexed by *t* $(1 \le t \le T)$. Unit *k* at node *i* has an increasing convex piecewise linear generation cost function $C_{i,k}(p_{i,k}(t))$ ($) for multiple generation blocks, a start-up cost $S_{i,k}$ ($/Start), a no-load cost $S_{i,k}^{NL}$ ($), minimum and maximum generation levels $p_{i,k}^{\min}$ (MW) and $p_{i,k}^{\max}$ (MW), respectively, a ramp rate $R_{i,k}$ (MW/hour), and minimum up and down times (hour). The demand is assumed to be given and is denoted by $p_i^L(t)$ (MW) for node *i* at hour *t*. Line *l* has a transmission capacity f_l^{max} (MW). The stochastic UC problem is to minimize the total cost by selecting a single set of UC decisions and multiple sets of dispatch decisions of conventional generators over a 24-hour horizon. For the conventional unit$_{i,k}$, the UC decision at time *t* is denoted by the binary variable $x_{i,k}(t)$, with "1" representing online and "0" offline. The start-up decision is denoted by the binary decision variable $u_{i,k}(t)$, with "1" representing start-up and "0" otherwise. Different sets of dispatch decisions will be made in pure Markov-based optimization to be presented in subsection 3.3.2 and in the hybrid Markovian and interval approach in subsection 3.3.3.

3.3.2 Pure Markov-based Optimization and Its Complexity

Dispatch decisions of the pure Markovian approach [19], denoted as $p_{i,k,g}(t)$ for unit$_{i,k}$ at time t at global state g, explicitly depend on the global states. The objective is to minimize the commitment cost plus the expected dispatch cost, i.e.,

$$\min \sum_{t=1}^{T} \sum_{i=1}^{I} \sum_{k=1}^{K_i} \left\{ \sum_{g=m}^{M} \left[\varphi_g(t) C_{i,k}\left(p_{i,k,g}(t)\right) \right] + u_{i,k}(t) S_{i,k} + x_{i,k}(t) S_{i,k}^{NL} \right\}. \tag{3.10}$$

where m represents the minimum global state where all wind farms are at their minimum possible state, and M the maximum global state. System demand constraints (3.11) and transmission capacity constraints (3.12) are satisfied for all possible global states.

$$\sum_i \sum_k p_{i,k,g}(t) + \sum_i p_{i,g}^{W}(t) = \sum_i p_{i,g}^{L}(t), \forall t, \forall g\,. \tag{3.11}$$

$$-f_l^{\max} \le f_{l,g}(t) \le f_l^{\max}, \forall l, \forall t, \forall g\,. \tag{3.12}$$

In the above equation, $f_{l,g}(t)$ denotes the power flow though line l at time t at global state g and is represented based on GSFs as in (3.13),

$$f_{l,g}(t) = \sum_i \left[a_l^i \cdot \left(\sum_k p_{i,k,g}(t) + p_{i,g}^{W}(t) - p_{i,g}^{L}(t) \right) \right], \forall l, \forall t, \forall g. \tag{3.13}$$

Individual unit constraints related to dispatch decisions include generator capacity constraints and ramp rate constraints. Generator capacity constraints are satisfied for possible global states. Ramp rate constraints are satisfied for possible state transitions from hour t-1 to hour t, i.e.,

$$p_{i,k,g'}(t-1) - R_{i,k} \le p_{i,k,g}(t) \le p_{i,k,g'}(t-1) + R_{i,k}, \forall (g', g) \in \{(g', g) \mid \varphi_{g'}(t) > 0, \pi_{g'g} > 0\}, \tag{3.14}$$

where g' denotes the global state at hour t-1. Since its dispatch decisions explicitly depend on a large number of possible global states, the pure Markov-based approach is very complex and thus not practical.

3.3.3 Hybrid Markovian and Interval UC Formulation

To reduce the dimension of the pure Markov-based stochastic UC problem, a synergistic combination of Markov-based optimization and interval optimization is developed.

1) Local and non-local states, and dispatch decisions

To avoid making dispatch decisions explicitly dependent on all possible realizations, our key idea is to divide the generation level (dispatch decision) of conventional unit$_{i,k}$ at time t into two components: $p^{M}_{i,k,n_i}(t)$ denotes the Markovian generation depending on local wind state n_i, and $p^{I}_{i,k,\bar{n}_i}(t)$ denotes the interval generation depending on extreme non-local states $\bar{n}_i$. For node i, its local state is the nodal wind state n_i. Its minimum possible local state is represented as $\min n_i$, and its maximum as $\max n_i$. Note that $\min n_i$ may not be 1 at time t, since state 1 at node i may have zero probability. Its extreme non-local states $\bar{n}_i$ are the minimum non-local state m_i and the maximum non-local state M_i, i.e., $\bar{n}_i \in \{m_i, M_i\}$. The minimum non-local state is a combination of possible minimum states of other nodes, i.e.,

$$m_i \equiv \left[\min\ n_1, \ldots, \min\ n_{i-1}, \min\ n_{i+1} \ldots, \min\ n_I\right]^T. \tag{3.15}$$

The maximum non-local state M_i is a combination of maximum possible states of other nodes, i.e.,

$$M_i \equiv \left[\max n_1, \ldots, \max n_{i-1}, \max n_{i+1} \ldots, \max n_I\right]^T. \tag{3.16}$$

In simulation where only one global state is realized at an hour in each scenario, one level of conventional generation will be obtained. This generation level will be within the ranges delineated by sums of corresponding Markovian generation and interval generation levels.

In addition, the dispatch decisions corresponding to the expected realization E (where all wind farms are at their expected outputs), denoted as $p_{i,k,E}(t)$, will also be considered in the objective function to be discussed later. The constraints for the expected realization can be easily included as one set of deterministic constraints with the same set of commitment decisions $\{x_{i,k}(t)\}$ and one set of dispatch decisions $\{p_{i,k,E}(t)\}$.

These constraints are not presented for conciseness. Constraints corresponding to the Markovian and interval dispatch decisions are formulated as follows.

2) Nodal level analysis

As a result of dividing the generation level, each nodal or unit-level constraint considers these two components. In particular, we have

Generator capacity constraints. If the unit is committed, its generation level is within the minimum and maximum values; otherwise, its generation level should be zero.

$$x_{i,k}(t)\,p_{i,k}^{\min} \le p_{i,k,n_i}^{M}(t) + p_{i,k,\bar{n}_i}^{I}(t) \le x_{i,k}(t)\,p_{i,k}^{\max}, \forall i, \forall k, \forall t, \forall n_i \in \Omega_i(t), \forall \bar{n}_i \,. \qquad (3.17)$$

where $\Omega_i(t)$ is the set of possible wind states at node *i* at hour *t* ($\Omega_i(t) \equiv \{n_i | \varphi_{n_i}(t) > 0\}$). For the rest of the chapter, the expression, $n_i \in \Omega_i(t)$, is omitted.

Nodal injections. The nodal injection at node *i* is wind generation plus conventional generation minus demand, i.e.,

$$P_{i,n_i,\bar{n}_i}(t) = p_{i,n_i}^{W}(t) + \sum_k \left(p_{i,k,n_i}^{M}(t) + p_{i,k,\bar{n}_i}^{I}(t)\right) - p_i^{L}(t), \forall i, \forall t, \forall n_i, \forall \bar{n}_i \,. \qquad (3.18)$$

3) System demand constraints.

Based on (3.1) and (3.2) [18, Eq. (20)] as reviewed in the **pure interval optimization** part of Section 3.2, as long as the minimum and maximum global states are satisfied, all other realizations will satisfy system demand at time t. In the minimum global state *m*, we have

$$\sum_i \sum_k p_{i,k,m_i}^{I}(t) = \sum_i \left(p_i^{L}(t) - p_{i,\min n_i}^{W} - \sum_k p_{i,k,\min n_i}^{M}(t) \right), \forall t \,. \qquad (3.19)$$

Similarly, system demand constraints at the maximum global state *M* are:

$$\sum_i \sum_k p^I_{i,M_i}(t) = \sum_i \left(p^L_i(t) - p^W_{i,\max n_i} - \sum_k p^M_{i,k,\max n_i}(t) \right), \forall t \,. \tag{3.20}$$

4) Transmission capacity constraints

DC power flow is used since it is sufficient for the UC purpose, and a line flow is a linear combination of nodal injections weighted by GSFs. Since GSFs can be positive or negative, the selection of extreme flow levels is more complicated than system demand. Therefore, the terms in the nodal injection in **Error! Reference source not found.**(3.18) are regrouped to a Markovian nodal injection consisting of those related to local states:

$$P^M_{i,n_i}(t) \equiv p^W_{i,n_i}(t) + \sum_k p^M_{i,k,n_i}(t) - p^L_i(t), \forall i, \forall t, \forall n_i, \tag{3.21}$$

and an *interval nodal injection* related to non-local states:

$$P^I_{i,\bar{n}_i}(t) \equiv \sum_k p^I_{i,k,\bar{n}_i}(t), \forall i, \forall t, \forall \bar{n}_i \,. \tag{3.22}$$

For line *l* at time *t*, the flow has two parts corresponding to the two components of nodal injections from (3.21) and (3.22).

Wind uncertainties are contained in Markovian nodal injections, and bounds of Markovian flow levels are selected based on signs of GSFs and corresponding extreme Markovian nodal injections, i.e.,

$$\begin{aligned} &\sum_{i:a^i_l>0} [a^i_l \cdot \min_{n_i} P^M_{i,n_i}(t)] + \sum_{i:a^i_l<0} [a^i_l \cdot \max_{n_i} P^M_{i,n_i}(t)] \le f^M_{l,n_1,\cdots,n_I}(t) = \sum_i [a^i_l \cdot P^M_{i,n_i}(t)] \\ &\le \sum_{i:a^i_l>0} [a^i_l \cdot \max_{n_i} P^M_{i,n_i}(t)] + \sum_{i:a^i_l<0} [a^i_l \cdot \min_{n_i} P^M_{i,n_i}(t)], \forall l, \forall t \,. \end{aligned} \tag{3.23}$$

The min/max operations to select extreme Markovian nodal injections are nonlinear and will be transformed to linear forms in subsection 3.4.1.

The two sets of interval nodal injections from (3.19) and (3.20) can be directly translated to two interval flow levels, i.e.,

$$f_{l,m}^{I}(t) = \sum_{i}[a_l^i \cdot P_{i,m_i}^{I}(t)], \forall l, \forall t\,. \tag{3.24}$$

$$f_{l,M}^{I}(t) = \sum_{i}[a_l^i \cdot P_{i,M_i}^{I}(t)], \forall l, \forall t\,. \tag{3.25}$$

These two interval flow levels are required to satisfy the two bounds of Markovian flow levels in transmission capacity constraints as formulated in (3.26) and (3.37), so that other realizations will satisfy transmission capacity constraints.

$$f_{l,g}^{I}(t) \geq -f_l^{\max}(t) - \sum_{i:a_l^i>0}[a_l^i \cdot \min_{n_i} P_{i,n_i}^{M}(t)] - \sum_{i:a_l^i<0}[a_l^i \cdot \max_{n_i} P_{i,n_i}^{M}(t)], \forall l, \forall t, \forall g \in \{m, M\}, \tag{3.26}$$

$$f_{l,g}^{I}(t) \leq f_l^{\max}(t) - \sum_{i:a_l^i>0}[a_l^i \cdot \max_{n_i} P_{i,n_i}^{M}(t)] - \sum_{i:a_l^i<0}[a_l^i \cdot \min_{n_i} P_{i,n_i}^{M}(t)], \forall l, \forall t, \forall g \in \{m, M\}\,. \tag{3.27}$$

Constraints (3.26) and (3.27) are different from those in pure interval optimization (3.5) and (3.6) [18, Eq. (16) and (19)]. Pure interval optimization selects extreme combinations of wind generation (uncertain parameters), while Eq. (3.23) selects extreme combinations of Markovian nodal injections, which involve wind generation, the Markovian generation (decision variables) and nodal demand.

It is interesting to note that the bounds of Markovian flows in (3.23) are correlated with bounds of system demand, since nodal wind generation appears in both types of bounds. Thus, not all bounds will happen at the same realization, and interval generation feasible for all bounds are conservative. Nevertheless, Markovian generation in (3.21) can accommodate local uncertainties that appear in flows in (3.23), and Example 1 in Section 3.5 will illustrate that the conservativeness in transmission of pure interval optimization is much alleviated.

An issue that also exists in pure interval optimization is that results are sensitive to the selection of the slack bus, and the reason will be explained in Appendix 3.A. To alleviate this sensitivity, the distributed slack bus [31], which distributes the impacts of the slack bus into multiple buses, is adopted.

5) *Ramp rate constraints.*

If unit$_{i,k}$ is online at hours *t*-1 and *t*, then for all possible state transitions and the two extreme non-local states, the change of generation level cannot exceed the unit's ramp rate, i.e.,

$$p^{M}_{i,k,n_i'}(t-1)+p^{I}_{i,k,\bar{n}_i'}(t-1)-R_{i,k}\le p^{M}_{i,k,n_i}(t)+p^{I}_{i,k,\bar{n}_i}(t)\le p^{M}_{i,k,n_i'}(t-1)+p^{I}_{i,k,\bar{n}_i'}(t-1)+R_{i,k},\forall i,\forall k,\forall t,$$
$$\forall(n_i',n_i)\in\{(n_i',n_i)\mid\varphi_{n_i'}(t)>0,\pi_{n_i'n_i}>0\},\forall\bar{n}_i\in\{m_i,M_i\},\forall\bar{n}_i'\in\{m_i,M_i\}, \quad (3.28)$$

where $\bar{n}_i'$ denotes the non-local state of node *i* at hour *t*-1. The changes in wind generation at possible state transitions (except for transitions between extreme states) are smaller than those between the min and max realizations in pure interval optimization. Thus, the conservativeness in ramp rate constraints of pure interval optimization is also alleviated. In addition, generation limits at start-up and shut-down hours [32, Eq. (11)] are also considered and merged with (3.28), based on [19, Eq. (9) and (10)].

6) Commitment constraints of individual units

Start-up constraints. The start-up decision is coupled with commitment decisions:

$$u_{i,k}(t)\ge x_{i,k}(t)-x_{i,k}(t-1),\forall i,\forall k,\forall t\,. \quad (3.29)$$

Minimum up/down Time. The unit must remain online or offline for its minimum up or down time, respectively. The convex hull formulas in [33, Eq. (3) and (5)] are employed.

7) *The objective function.*

The goal of the optimization problem is to minimize the commitment cost plus the expected dispatch cost of all possible realizations rather than that of the worst-case realization to reduce conservativeness. Since

the generation cost function $C_{i,k}(p^{M}_{i,k,n_i}(t) + p^{I}_{i,k,\bar{n}_i}(t))$ is piecewise linear, the cost cannot be separated into a Markovian generation cost and an interval generation cost. Given that only two extreme realizations are considered in interval generation, their costs may not reflect the costs of other possible realizations. To approximate the expected cost without much complexity, the cost of the expected realization *E* is included in addition to the costs of the few extreme realizations. The resulting objective function is to minimize the total weighted generation cost, plus the commitment cost, i.e.,

$$\min \sum_{t=1}^{T}\sum_{i=1}^{I}\sum_{k=1}^{K_i}\Bigg\{\sum_{n_i=1}^{N_i}\Big[w_{n_i,m_i}(t)C_{i,k}\left(p^{M}_{i,k,n_i}(t)+p^{I}_{i,k,m_i}(t)\right)+w_{n_i,M_i}(t)C_{i,k}\left(p^{M}_{i,k,n_i}(t)+p^{I}_{i,k,M_i}(t)\right)\Big]$$

$$+ w_{E}(t)C_{i,k}\left(p_{i,k,E}(t)\right)+u_{i,k}(t)S_{i,k}+x_{i,k}(t)S^{NL}_{i,k}\Bigg\}. \qquad (3.30)$$

where $w_{n_i,m_i}(t)$ is the weight of the conventional generation when local state is at n_i and non-local at m_i at time *t*, $w_{n_i,M_i}(t)$ when non-local at M_i, and $w_E(t)$ the expected realization. The weights among realizations are not directly selected based on corresponding probabilities. The reason is that the expected realization corresponds to no particular state and probability. Since the cost of the expected realization represents the expected cost of the vast majority of realizations, its weight should be larger than those of others. The weights $w_{n_i,m_i}(t)$ and $w_{n_i,M_i}(t)$ can further consider local probabilities. The sum of all weights at time *t* equals one.

The above stochastic UC problem (3.17)-(3.22), (3.24)-(3.30), and minimum up/down time constraints is a nonlinear mixed-integer optimization problem with binary decision variables $\{u_{i,k}(t)\}$ and $\{x_{i,k}(t)\}$, and continuous variables $\{p^{M}_{i,k,n_i}(t)\}$, $\{p^{I}_{i,k,\bar{n}_i}(t)\}$ and $\{p_{i,k,E}(t)\}$. The nonlinearity lies in the min/max operations of selecting extreme Markovian nodal injections in (3.26) and (3.27).

3.3.4 Discussion on Reducing the Wind Uncertainty

Two methods to reduce the wind uncertainty by considering wind power forecasts or by incorporating spatial correlations of wind farms are discussed. Testing them, however, is out of the scope of this thesis.

Considering wind power forecasts. With historical data only, solutions may be conservative due to the large uncertainty of day-ahead wind generation. Wind power forecasts consider weather conditions, terrain characteristics, and historical forecast errors to reduce the uncertainty [34]. Our previous work [35] converted wind power forecasts into state probabilities, instead of only using historical data based on (3.8), to fit in the Markovian approach. Considering wind power forecasts is expected to reduce the conservativeness of solutions.

Incorporating spatial correlations of wind farms. The outputs of nearby wind farms are likely to be correlated. Although the outputs of the wind farms are assumed to be independent for simplicity in subsection 3.3.1, incorporating the spatial correlations can help reduce the uncertainty and thus reduce the conservativeness of solutions. A method is to aggregate the generation of nearby wind farms through aggregating buses that are connected by transmission lines with sufficient capacities. In this way, their correlations are contained in the aggregated wind generation to smooth out the uncertainty of each wind farm. An issue is to identify if transmission lines have sufficient capacities in the presence of wind uncertainty. For deterministic transmission-constrained UC problems, necessary and sufficient conditions for a transmission capacity constraint to be redundant were derived by solving an MILP problem that maximizes or minimizes the flow through that line [36]. To significantly simplify the process, an analytical sufficient condition was obtained from an LP problem after dropping transmission constraints of other lines and integrality constraints associated with UC decisions, and was able to quickly identify most of the redundant constraints [36]. This identification method can be extended to UC with uncertain wind generation by using interval models. Buses connected by lines with sufficient capacities can then be aggregated through network reduction based on GSF matrix reduction [37], and corresponding wind

generation can be aggregated. Transmission capacities of lines in the reduced network can be calculated based on QR-factorization of the reduced GSF matrix [38]. States of the aggregated wind generation will be considered with corresponding state probabilities and state transition matrices. Local and extreme non-local states will be based on states of aggregated wind generation at different areas.

3.4 Solution Methodology

The above problem is transformed into a linear form and is solved by using branch-and-cut in Section 3.4.1. Its complexity and conservativeness are analyzed, and are compared with those of pure Markov-based optimization and pure interval optimization in Section 3.4.2.

3.4.1 Transformation of the Min/Max Operations

To transform the min/max operations in (3.23), (3.26) and (3.27) into linear forms, the conjecture below describes the monotonicity of Markovian nodal injections with respect to nodal wind states. Based on this monotonicity, extreme Markovian nodal injections are selected based on indices of nodal wind states without optimization. Consider two possible local states at node i time t: state n_i, and state $n_i - 1$ which has less wind generation than state n_i.

The Monotonicity Conjecture: The local state with lower wind generation provides less or equal Markovian nodal injection at the optimum, i.e.,

$$P^M_{i,n_i-1}(t) \le P^M_{i,n_i}(t), \forall i, \forall t, \forall n_i, \forall (n_i - 1) \in \{n_i - 1 \mid \varphi_{n_i-1}(t) > 0\}. \tag{3.31}$$

Generalized monotonicity analysis [39] will be used to support this conjecture in Appendix 3.B. Based on the above conjecture, the minimum (maximum) Markovian nodal injection happens at the minimum (maximum) local wind generation state at the optimum, i.e.,

$$\min_{n_i} P^M_{i,n_i}(t) = P^M_{i,\min n_i}(t), \forall i, \forall t\ , \tag{3.32}$$

$$\max_{n_i} P^M_{i,n_i}(t) = P^M_{i,\max n_i}(t), \forall i, \forall t\,. \tag{3.33}$$

The overall problem is thus linear after including (3.31) as constraints and substituting the min/max operations with corresponding states of nodal injections as (3.32) and (3.33). Moreover, with state transition matrices given and state probabilities pre-computed as discussed in [19], the linearized problem can be effectively solved by using branch-and-cut.

3.4.2 Comparison of Approaches

Complexity. The complexity of the new approach is compared with those of pure Markov-based optimization and pure interval optimization in terms of the number of dispatch decisions and flow levels, because the same number of UC decisions are made. Considering *I* wind farms located at different buses and *N* states for each wind farm at each hour, Table 3.1 summarizes the comparison.

Table 3.1. Comparison of the Complexity of the Three Approaches

	No. of dispatch decisions per unit per hour	No. of flow levels per line per hour
Pure Markov-based	N^I	N^I
Pure Interval	2+1	2+1
Markovian and Interval	N+2+1	2+2+1

The pure Markov-based formulation is very complicated as discussed in subsection 3.3.2. The pure interval formulation is much simpler, since each unit/line at each hour has only three dispatch/flow levels corresponding to the two extreme realizations and the expected realization. Although the Markovian and interval formulation has *N* more dispatch decisions and two more flow levels than the pure interval formulation, the complexity is significantly reduced when compared to the pure Markov-based formulation. Furthermore, the complexity of the new formulation does not increase as the number of distributed wind farms increases.

Conservativeness. Pure Markov-based optimization makes use of information provided by global states and state transitions. Its UC formulation is not conservative. Pure interval optimization pre-computes bounds of wind uncertainty in transmission constraints without making use of local flexibility, and considers all extreme state transitions in ramp rate constraints. As a result, pure interval optimization is over-conservative.

In the hybrid Markovian and interval approach, the Markovian generation makes use of information provided by local states and their transitions. The interval generation does not depend on all possible non-local states but extreme ones. This makes our approach more conservative than pure Markov-based optimization in transmission capacity and ramp rate constraints, and leads to more conservative UC decisions. This set of UC decisions will result in a higher simulation cost. However, our approach is still less conservative than pure interval optimization.

3.5 Numerical Results

Testing is conducted using CPLEX 12.5.1.0 [21] on a PC laptop with an Intel Core(TM) i7-2820QM 2.30GHz CPU and 8GB memory. Three examples of different-size problems are provided. In Example 1, a simple problem is used to demonstrate that our approach is less conservative than pure interval optimization, and to illustrate dispatch decisions of our approach. In Example 2, the IEEE 30-bus system is tested to demonstrate modeling accuracy and solution feasibility of our approach at different levels of wind penetration by comparing with the deterministic approach and pure interval optimization [18]. In Example 3, the IEEE 118-bus system is tested to demonstrate the computational efficiency of our approach. In Examples 2 and 3 where infeasibility is possible, wind curtailment and load shedding are considered. Wind curtailment is assumed to depend on local wind states for simplicity and to incur no cost. Load shedding is modeled in a manner similar to conventional generation with Markovian and interval components with a penalty of $5,000/MWh. The stopping criterion for all approaches in Examples 2 and 3 is a relative mixed-integer programming gap tolerance of 0.1%.

3.5.1 Example 1

Consider a 3-bus 1-hour problem with two wind farms as shown in Fig. 3.1. This figure also shows the values and probabilities of the wind generation states, and the capacity and reactance values of the transmission lines. Table 3.2 provides the parameters of the two conventional units. For the single hour problem, time-coupling constraints such as ramp rate and minimum up/down time constraints are ignored, and the time index *t* is dropped.

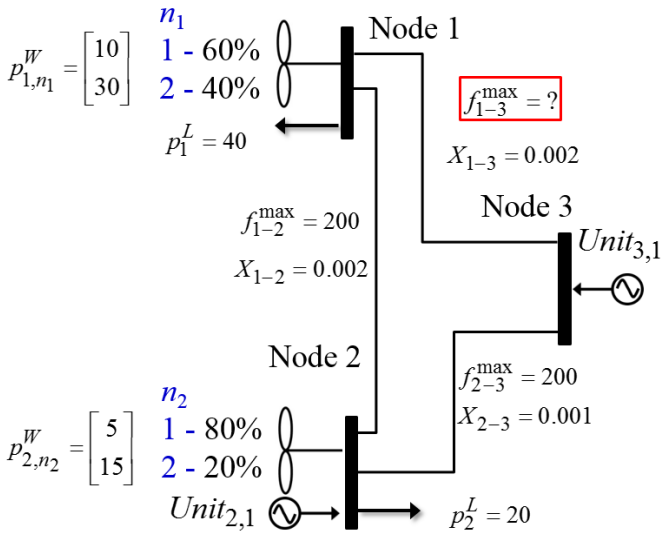

Fig. 3.1. The three-bus transmission network for Example 1

Table 3.2. Unit Parameters for Example 1

Unit	$p_{i,k}^{min}$ (MW)	$p_{i,k}^{max}$ (MW)	$c_{i,k}$ ($/MWh)
$Unit_{2,1}$	10	35	30
$Unit_{3,1}$	5	10	65

To compare the conservativeness in transmission of the different approaches, we use the minimum transmission capacity required on the line connecting Nodes 1 and 3, $f_{1\text{-}3}^{max}$, to provide feasible solutions as the criterion for illustrative purposes. For pure interval optimization, the required transmission capacity

is 16.667 MW. For our approach, the required transmission capacity is 14 MW. Thus, our approach is less conservative in transmission.

For Wind Farm 1, its output p^{W}_{1,n_1} has two nodal states: 10 MW when $n_1 = 1$, and 30 MW when $n_1 = 2$. With another two possible nodal states at Wind Farm 2, there are four possible global states $[n_1, n_2]^T$: $[1, 1]^T$, $[1, 2]^T$, $[2, 1]^T$, and $[2, 2]^T$. To illustrate the Markovian generation and interval generation of conventional units, results of our approach when $f_{1\text{-}2}^{\max} = 14$ MW are provided in Tables 3.3. Since $\text{Unit}_{2,1}$ is located at the same node as Wind Farm 2, its Markovian generation depends on the local state n_2. $\text{Unit}_{3,1}$ is not located with any local wind farm, so it does not have Markovian generation (or it equals 0). The non-local state of $\text{Unit}_{2,1}$ and that of $\text{Unit}_{3,1}$ are the same n_1 in this small system.

Table 3.3. Optimization Results for Example 1 Using the Markovian and Interval approach

Optimization cost		\$1,230.5		CPU time		0.05s
Unit	$p_{i,k,1}^{M}$	$p_{i,k,2}^{M}$	$p_{i,k,mi}^{I}$	$p_{i,k,Mi}^{I}$	$p_{i,k}^{E}$	$x_{i,k}$
$\text{Unit}_{2,1}$	20	10	15	0	30	1
$\text{Unit}_{3,1}$	\	\	10	5	5	1

To illustrate how conventional generation realizes, simulation is conducted by fixing UC decisions at the optimal solution and solving the deterministic dispatch problem for each global state. Results are summarized in Table 3.4. Each unit's generation level under each global state turns out to be within the ranges delineated by sums of corresponding Markovian generation and interval generation levels.

Table 3.4. Simulation Results for Example 1

$g = [n_1, n_2]^T$		$p_{2,1,g}$		$p_{3,1,g}$	
$(1, 1)^T$	$(1, 2)^T$	35	30	10	5
$(2, 1)^T$	$(2, 2)^T$	20	10	5	5

3.5.2 Example 2

The IEEE 30-bus system is tested over a 24-hour horizon with parameters adjusted as in [1]. There is a wind farm located at Node 1 with a capacity of 42.5 MW. An additional wind farm with a capacity of 28.3 MW is added to Node 2. Two different levels of wind penetration are tested.

In each case, our approach is compared with the deterministic approach and pure interval optimization. For our approach, 10 states are used for each wind farm based on [19], and the expected realization is calculated based on 50-state transition matrices. Based on the discussion after (3.30), the weights in the objective function, $w^E(t)$, $w_{n_i,m_i}(t)$, and $w_{n_i,M_i}(t)$, are set to be 0.8, $0.1\varphi_{n_i}(t)$, and $0.1\varphi_{n_i}(t)$, respectively. For pure interval optimization [18], extreme states from 10-state matrices and the expected realization from 50-state matrices are used for fair comparison. For the same purpose, the costs of the minimum and maximum realizations are also considered in the objective function, both with the same weight 0.1. The deterministic approach sets the spinning reserve levels at 3.5 standard deviations of hourly wind generation based on [5]. To evaluate the UC decisions obtained by different approaches, 10,000 Monte Carlo simulation runs are performed with scenarios sampled based on the 50-state transition matrices. In the simulations, UC decisions are fixed at the optimal solution, and the deterministic dispatch problem is solved repeatedly for the sampled scenarios following [7], [11]. The simulation cost is the average cost of all sampled scenarios. Modeling accuracy of each approach is measured by the absolute percentage error (APE):

$$APE \equiv \frac{\left|optimization\ \mathrm{cost} - simulation\ \mathrm{cost}\right|}{simulation\ \mathrm{cost}} \times 100\%. \tag{3.34}$$

The standard deviation (STD) of costs of sampled scenarios reflects the variation of costs.

Case 1. State transition matrices of the two wind farms are established based on measured hourly generation data of two wind sites from April to September in 2006 (the non-winter season) from National

Renewable Energy Laboratory's Eastern Wind Dataset [40], one site per wind farm. The wind penetration level, calculated as the total expected wind generation divided by the total demand without considering wind curtailment and load shedding, is 13.9%.

Results are summarized in Table 3.5. It takes more time for our approach to reach the stopping criterion than the other two approaches. Optimization costs of the three approaches are very similar. However, the deterministic approach has the highest simulation cost and incurs the highest penalty cost of load shedding. This indicates that even with reserve, the deterministic approach cannot guarantee solution feasibility against all possible realizations. Both pure interval optimization and our approach are accurate in sense of their small APEs.

Table 3.5. Results for Case 1 of Example 2

Approach		Deter.	Interval	Ours
Optimization	CPU time	2s	5s	1min4s
	Cost (k$)	326.416	326.963	323.409
	Penalty (k$)	0	0	0.553
UC cost (k$)		87.642	72.616	72.201
Simulation	Cost (k$)	360.733	325.103	323.689
	APE	9.513%	0.572%	0.087%
	STD (k$)	56.669	15.082	14.998
	Penalty (k$)	30.621	0	0.010

Case 2. To create 40% wind penetration, capacities of the two wind farms are scaled with demand unchanged. The results are summarized in Table 3.6. Our approach only spends about twice as much time as pure interval optimization. Our approach has a simulation cost 5.23% lower than that of pure interval optimization without incurring much penalty, indicating that our approach is less conservative. In addition, our approach is the most accurate, as it has the smallest APE.

Table 3.6. Results for Case 2 of Example 2

Approach		Deter.	Interval	Ours
Optimization	CPU time	2s	53s	1min53s
	Cost (k$)	248.659	280.672	253.403
	Penalty (k$)	0	0.466	0.008
UC cost (k$)		89.461	67.715	65.216
Simulation	Cost (k$)	314.889	263.264	250.172
	APE	21.033%	6.612%	1.292%
	STD (k$)	74.456	33.771	35.126
	Penalty (k$)	40.823	0	0.003

3.5.3 Example 3

The IEEE 118-bus system [41] is tested. There are three wind farms, 54 conventional generators, 186 transmission lines, and 91 load centers with peak system demand 3733.07 MW. The wind farms use the capacities in [41], and their state transition matrices are based on measured hourly data of three wind sites from April to September in 2006 from [40]. The hourly system demand values in percent of peak system demand are calculated based on corresponding factors for summer weekdays of IEEE Reliability Test System [42]. The wind penetration level is 7.2%. The quadratic cost curves of conventional generators are approximated by piecewise linear cost curves with three blocks.

The results of our approach are summarized in Table 3.7. The CPU time is 49 seconds, demonstrating that our approach is computational efficient. Based on the statistics provided by CPLEX, there are 150,308 constraints, 2,592 binary variables, and 52,489 continuous variables (including additional decision variables for the three-block piecewise linear costs) in optimization. The main reason why the CPU time of solving this system by using the Markovian and interval approach is even less than those in Example 2 may

be that the wind penetration level is lower. With relatively smaller ranges of uncertainty, it is easier to find feasible solutions.

The APE of our approach is 0.253%, demonstrating its modeling accuracy. Under this relatively low level of wind penetration, no load is shed and no wind is curtailed in any of the 10,000 simulation runs.

Table 3.7. Results for Example 3

Optimization	CPU time	49s
	Cost (k$)	909.860
	Penalty load shedding (k$)	0.036
	Curtailed wind (MWh)	0
UC cost (k$)		12.690
Simulation	Cost (k$)	907.567
	APE	0.253%
	STD (k$)	24.188
	Penalty load shedding (k$)	0
	Curtailed wind (MWh)	0

3.6 Conclusion

This chapter develops a synergistic combination of Markov-based optimization and interval optimization to solve the transmission-constrained UC problem with uncertain wind generation. Ideas from interval optimization are used to capture bounds of constraints to ensure solution feasibility, while Markov-based optimization uses information of local states for reduced conservativeness. Numerical results demonstrate that the new approach is effective in terms of computational efficiency, simulation cost, and solution feasibility. This work opens a new and effective way to address stochastic problems without scenario analysis and to avoid over-conservativeness. In addition, solar generation shares a similar uncertain nature as wind generation, and can thus be modeled and solved similarly.

Appendix 3.A

This appendix discusses the sensitivity of results with respect to the selection of the slack bus. DC power flows can be represented by using voltage phase angles with nodal power balance constraints (that require the nodal injection to equal the sum of out flows from this node) or by using GSFs with system demand constraints (that require system-level power balance) [30]. In the deterministic approach, there is no difference between them. The reason is that when computing GSFs, one row and one column corresponding to the slack bus are taken out, assuming that system demand is satisfied. In this case, although GSF values change when the slack bus changes, power flow levels do not change. However, if the system-level power balance assumption for GSFs is not strictly satisfied as in pure interval optimization, power flow levels will change when the slack bus changes.

In pure interval optimization, on the one hand, power flow equations based on voltage phase angles cannot be used because of the following complexity. These power flow equations go hand-in-hand with nodal power balance constraints. Each nodal power balance constraint is an interval equality and will result in two constraints based on [27], similar to system demand constraints (3.1) and (3.2). When there are I nodes in a network, there will be 2^I possible combinations of these constraints to be considered at each hour. On the other hand, power flow equations with GSFs can be used to bypass this complexity, since power flows (from uncertain wind generation) can be directly substituted by a weighted sum of nodal injections. In this case, GSFs have to be computed. However, the system-level power balance assumption for GSFs is not strictly satisfied since only bounds of system demand are considered. Consequently, when slack bus changes, GSF values change, and power flow levels change. Results are therefore sensitive to the selection of the slack bus. Results of the Markovian and interval approach have the same sensitivity issue.

Appendix 3.B

This appendix is to support the *Monotonicity Conjecture* (3.31). Since the monotonicity is on nodal injections or dispatch decisions, we focus on the corresponding dispatch problem with UC decisions fixed. The deterministic dispatch problem, which considers a special case where the probability distribution at each hour is a singleton, will first be analyzed based on *generalized monotonicity analysis* [39]. When wind generation decreases, the corresponding nodal injection will decrease or remain the same. The result will then be extended to the Markovian and interval dispatch problem.

For the deterministic dispatch problem, the procedure is similar to Example 4.1.2 in [39]. Lagrangian relaxation is first used to relax all constraints, namely system demand, transmission capacity, generator capacity, and ramp rate constraints. The KKT conditions [43] are used to establish a set of equalities among variables and parameters at the optimum. By taking total derivatives on both sides of the KKT conditions based on [39, Eq. (2)], the directional derivative of the nodal injection will be contained in another set of equations. After solving all the above equations together, an explicit form of the directional derivative can be obtained. With the change direction of parameters imposed along the direction of wind generation, the monotonicity of the nodal injection can be observed.

Solving for this directional derivative is difficult and requires symbolic solvers. Symbolic solvers, such as Maple [44] and Symbolic Math Toolbox in MATLAB [45], do not support a general form of equations with an arbitrary size. Therefore, problems with known sizes have to be solved case by case. Moreover, the memory requirement and CPU time increase drastically as the problem size increases. Nevertheless, we solve a small case with two buses, two lines, two hours, and linear generation cost functions by using Symbolic Math Toolbox [45] in MATLAB R2013b. Due to computational limits, we first impose the change direction of parameters, v, along the direction of wind generation at Node 1 at Hour 2, i.e., the element in v corresponding to this wind generation, $v_{p_1^W(2)}$, is considered and other elements are

set to zero. Then we solve for the directional derivative of the corresponding nodal injection, $w_{P_1(2)}$, and the result is that

$$w_{P_1(2)} = v_{p_1^w(2)} \text{ or } 0 . \tag{3.35}$$

This result demonstrates that the nodal injection will decrease or remain the same when wind generation decreases. The result of this small case is believed to hold in general, since all types of constraints are considered.

The above result is then extended to the Markovian and interval dispatch problem. The monotonicity can be easily applied to two deterministic cases, where the only difference is that wind generation at node *i* at hour *t* in Case 1 is less than that in Case 2. Obviously, the corresponding nodal injection in Case 1 will be less than or equal to that in Case 2. For the pure Markov-based dispatch problem, wind generation values at states $n_i - 1$ and n_i fit into the situation of these two deterministic cases. Therefore, the nodal injection at state $n_i - 1$ will be less than or equal to that at state n_i. As for the Markovian and interval dispatch problem, since the interval nodal injection depends on extreme non-local states, it will not be changed by local states. Therefore, the Markovian nodal injection at state $n_i - 1$ will be less than or equal to that at state n_i.

References

[1] Y. Yu, P. B. Luh, E. Litvinov, T. Zheng, F. Zhao, and J. Zhao, "Unit commitment with intermittent wind generation via Markovian analysis with transmission capacity constraints," in *Proc. of the 2012 IEEE Power and Energy Soc. Gen. Meet.*, San Diego, California, July 2012.

[2] Global Wind Energy Council, "Global wind report – Annual market update 2012," Brussels, Belgium, April 2013 [Online]. Available: http://www.gwec.net/wp-content/uploads/2012/06/Annual_report_2012_LowRes.pdf

[3] U.S. Department of Energy, "20% wind energy by 2030: Increasing wind energy's contribution to U.S. electricity supply", DOE/GO-102008-2567, July 2008 [Online]. Available: http://www.nrel.gov/docs/fy08osti/41869.pdf

[4] M. Holloway, "Challenges and solutions for wind integration in ERCOT," panel presentation in *2014 IEEE PES Innovative Smart Grid Technologies Conference*, Washington, D.C., March 2014, [Online]. Available: http://sites.ieee.org/isgt2014/files/2014/03/Day1_Panel1A_Holloway.pdf

[5] M. Black and G. Strbac, "Value of bulk energy storage for managing wind power fluctuations," *IEEE Transactions on Energy Conversion*, vol.22, no.1, pp.197-205, March 2007.

[6] M. A. Ortega-Vazquez and D. S. Kirschen, "Estimating the spinning reserve requirements in systems with significant wind power generation penetration," *IEEE Transactions on Power Systems*, vol.24, no.1, pp. 114-124, Feb. 2009.

[7] D. Bertsimas, E. Litvinov, X. A. Sun, J. Zhao, and T. Zheng, "Adaptive robust optimization for the security constrained unit commitment problem," *IEEE Trans. Power Syst.*, vol. 28, no. 1, pp. 52-63, Feb. 2013.

[8] F. Bouffard and F. D. Galiana, "Stochastic security for operations planning with significant wind power generation," *IEEE Transactions on Power Systems*, vol. 23, no. 2, pp. 306-316, 2008.

[9] J. Wang, M. Shahidehpour, and Z. Li, "Security-constrained unit commitment with volatile wind power generation," *IEEE Transactions on Power Systems*, vol. 23, no. 3, Aug. 2008.

[10] V. S. Pappala, I. Erlich, K. Rohrig, and J. Dobschinski, "A stochastic model for the optimal operation of a wind-thermal power system," *IEEE Trans. Power Syst.*, vol. 24, no. 2, pp. 940–950, May 2009.

[11] P. Ruiz, P. C. Philbrick, E. Zak, K. W. Cheung, and P. Sauer, "Uncertainty management in the unit commitment problem," *IEEE Transactions on Power Systems*, vol. 24, no. 2, pp. 642–651, May 2009.

[12] C. Weber, P. Meibom, R. Barth, and H. Brand, "WILMAR: A stochastic programming tool to analyze the large-scale integration of wind energy," *Optimization in the Energy Industry*, Chapter 19, pp. 437–458, Berlin, Germany, Springer, 2009.

[13] A. Papavasiliou, S. Oren, and R. P. O'Neill, "Reserve requirements for wind power integration: A scenario-based stochastic programming framework," *IEEE Transactions on Power Systems*, vol. 26, no. 4, pp. 2197-2206, Nov. 2011.

[14] L. Wu, M. Shahidehpour, and Z. Li, "Comparison of scenario-based and interval optimization approaches to stochastic SCUC," *IEEE Transactions on Power Systems*, vol. 27, no. 2, pp. 913-921, May 2012.

[15] A. Papavasiliou and S. Oren, "Multiarea stochastic unit commitment for high wind penetration in a transmission constrained network," *Operations Research*, vol. 61, no. 3, pp. 578-592, May-June 2013.

[16] L. Zhao and B. Zeng, "Robust unit commitment problem with demand response and wind energy," in *Proc. of the 2012 IEEE Power and Energy Soc. Gen. Meet.*, San Diego, California, July 2012.

[17] R. Jiang, J. Wang, Y. Guan, "Robust unit commitment with wind power and pumped storage hydro," *IEEE Transactions on Power Systems*, vol. 27, no. 2, pp.800-810, May 2012.

[18] Y. Wang, Q. Xia, and C. Kang, "Unit commitment with volatile node injections by using interval optimization," *IEEE Transactions on Power Systems*, vol. 26, no. 3, pp. 1705-1713, 2011.

[19] P. B. Luh, Y. Yu, B. Zhang, E. Litvinov, T. Zheng, F. Zhao, J. Zhao, and C. Wang, "Grid integration of intermittent wind generation: a Markovian approach," *IEEE Transactions on Smart Grid*, vol. 5, no. 2, pp. 732-741, March 2014.

[20] R. E. Bixby, M. Fenelon, Z. Gu, E. Rothberg, and R. Wunderling, "MIP: Theory and practice – closing the gap." *System Modelling and Optimization*, pp. 19-49, 2000.

[21] IBM ILOG, "IBM ILOG CPLEX Optimization Studio Information Center," 2013. [Online]. Available: http://pic.dhe.ibm.com/infocenter/cosinfoc/v12r5/index.jsp

[22] D. Brooks, E. Lo, R. Zavadil, S. Santoso, and J. Smith, "Characterizing the impacts of significant wind generation facilities on bulk power system operations planning," Xcel Energy, Arlington, VA, USA, North Case Study Final Rep., May 2003.

[23] NERC, "Special report: Accommodating high levels of variable generation," April, 2009, [Online]. Available: http://www.nerc.com/files/IVGTF_Report_041609.pdf

[24] J. Dupačová, N. Gröwe-Kuska, and W. Römisch, "Scenario reduction in stochastic programming." *Mathematical Programming*, vol. 95, no. 3, pp. 493-511, 2003.

[25] N. Growe-Kuska, H. Heitsch, and W. Romisch, "Scenario reduction and scenario tree construction for power management problems," in *Proc. of Power Tech Conf. 2013 IEEE Bologna*, June 2003.

[26] J. M. Morales, S. Pineda, A. J. Conejo, and M. Carrion, "Scenario reduction for futures market trading in electricity markets," *IEEE Transactions on Power Systems*, vol. 24, no. 2, pp. 878-888, May 2009.

[27] J. W. Chinneck and K. Ramadan, "Linear programming with interval coefficients," *J. Oper. Res. Soc.*, vol. 51, no. 2, pp. 209-220, 2000.

[28] C. Zhao and Y. Guan, "Unified stochastic and robust unit commitment," *IEEE Trans. Power Syst*., vol. 28, no. 3, pp. 3353–3361, Aug. 2013.

[29] Y. Dvorkin, H. Pandzic, M. A. Ortega-Vazquez, and D. S. Kirschen, "A hybrid stochastic/interval approach to transmission-constrained unit commitment," *IEEE Trans. Power Syst*., vol. 30, no. 2, pp. 621–631, Mar. 2015.

[30] M. Ilic, F. Galiana, and L. Fink, *Power Systems Restructuring: Engineering and Economics*, Boston/Dordrecht/London: Kluwer, 1998.

[31] E. Litvinov, T. Zheng, G. Rosenwald, and P. Shamsollahi, "Marginal loss modeling in LMP calculation," *IEEE Transactions on Power Systems*, vol.19, no.2, pp. 880-888, May 2004.

[32] X. Guan, P. B. Luh, H. Yan, and J. A. Amalfi, "An optimization-based method for unit commitment," *International Journal of Electrical Power & Energy Systems*, vol. 14, no. 1, pp. 9-17, 1992.

[33] D. Rajan and S. Takriti. "Minimum up/down polytopes of the unit commitment problem with start-up costs," IBM Research Report, 2005.

[34] C. Monteiro, R. Bessa, V. Miranda, A. Botterud, J. Wang, and G. Conzelmann, "Wind Power Forecasting: State-of-the-Art 2009," Report ANL/DIS-10-1, Argonne National Laboratory, Nov. 2009. [Online]. Available: http://www.dis.anl.gov/projects/windpowerforecasting.html.

[35] Y. Yu, P. B. Luh, E. Litvinov, T. Zheng, F. Zhao, and J. Zhao, "Markov-based stochastic unit commitment considering wind power forecasts," in *Proc. of the 2013 IEEE Power and Energy Soc. Gen. Meet.*, Vancouver, British Columbia, Canada, July 2013.

[36] Q. Zhai, X. Guan, J. Cheng, and H. Wu, "Fast identification of inactive security constraints in SCUC problems," *IEEE Trans. Power Syst.*, vol. 25, no. 4, pp. 1946-1954, 2010.

[37] H. Oh, "A new network reduction methodology for power system planning studies," *IEEE Transactions on Power Systems*, vol. 25, no. 2, pp. 677-684, 2010.

[38] H. Oh, "Aggregation of buses for a network reduction," *IEEE Transactions on Power Systems*, vol. 27, no. 2, pp. 705-712, 2012.

[39] B. H. Strulovici and T. A. Weber, "Generalized monotonicity analysis," *Economic Theory*, vol. 43, no. 3, pp. 377-406, 2010.

[40] The National Renewable Energy Laboratory, Eastern Wind Dataset, 2010, [Online]. Available: http://www.nrel.gov/electricity/transmission/eastern_wind_methodology.html

[41] IEEE 118-bus system. [Online]. Available: http://motor.ece.iit.edu/data/.

[42] C. Grigg, P. Wong, P. Albrecht, R. Allan, M. Bhavaraju, R. Billinton, Q. Chen, C. Fong, S. Haddad, S. Kuruganty, W. Li, R. Mukerji, D. Patton, N. Rau, D. Reppen, A. Schneider, M. Shahidehpour, and C. Singh, "The IEEE Reliability Test System-1996," *IEEE Trans. on Power Syst.*, vol. 14, no. 3, pp. 1010-1020, Aug 1999.

[43] D. P. Bertsekas, *Nonlinear Programming* (2nd ed.), Athena Scientific, 1999.

[44] Maple 18. [Online]. Available: www.maplesoft.com/products/Maple

[45] Symbolic Math Toolbox. [Online]. http://www.mathworks.com/products/symbolic/index.html

Chapter 4

Transmission Contingency-Constrained Unit Commitment with High Penetration of Renewables via Interval Optimization

Reliability is an overriding concern for power systems that involve different types of uncertainty including contingencies and intermittent renewables. Contingency-constrained unit commitment (CCUC) satisfying the "N – 1 rule" is extremely complex, and the complexity is now compounded by the drastic increase in renewables. This chapter develops a novel interval optimization approach for CCUC with N – 1 transmission contingencies and renewable generation. A large number of transmission contingencies are innovatively described by treating corresponding generation shift factors (GSFs) as uncertain parameters varying within intervals. To ensure solution robustness, bounds of GSFs and renewables in different types of constraints are captured based on interval optimization. The resulting model is a mixed-integer linear programming (MILP) problem. To alleviate its conservativeness and to further reduce the problem size, ranges of GSFs are shrunk through identifying and removing redundant transmission constraints. To solve large-scale problems, Surrogate Lagrangian Relaxation (SLR) and branch-and-cut (B&C) are used to simultaneously exploit separability and linearity. Numerical results demonstrate that the new approach is effective in terms of computational efficiency, solution robustness, and simulation costs.

4.1 Nomenclature

Indices and sets

c	Index of transmission contingencies, $0 \le c \le L$. $c = 0$, if the system is under the base case where no line is tripped; $c = l \ne 0$, if line l is tripped
i	Index of nodes, $1 \le i \le I$
(i, k)	Index of conventional units at node i, $1 \le k \le K_i$
l or l'	Index of transmission lines, $1 \le l \le L$, $1 \le l' \le L$
r or r'	Index of the maximal (M), minimal (m), and expected (E) net demand realizations
t or t'	Index of time periods (hours), $1 \le t \le T$ (24), $1 \le t' \le T$ (24)
Φ_p, Φ_n	Sets of remaining interval transmission constraints in positive and negative directions, respectively

Parameters, variables, and functions

$a_{l,c}^{i}$	Generation shift factor (GSF) of line l from node i under contingency c
$\left[\underline{a}_l^i, \overline{a}_l^i\right]$	Interval of GSFs of line l from node i
$C_{i,k}(p_{i,k}(t))$	Increasing convex piecewise linear generation cost function ($)
$D_i(t)$	Nodal demand at node i at time t (MW)
$\widetilde{D}_i(t)$	Net nodal demand (≡ nodal demand – wind generation) at node i at time t (MW)
$\widehat{D}_i(t)$	Expected value of the net nodal demand at node i at time t (MW)
$\left[\underline{D}_i(t), \overline{D}_i(t)\right]$	Interval of the net nodal demand at node i at time t (MW)
$f_l^{\max}$	Transmission capacity of line l (MW)
$\overline{f}_l^E(t), \underline{f}_l^E(t)$	Revised transmission capacities of line l considering the expected net demand realization at time t for positive and negative directions, respectively (MW)
$\overline{f}_l(t), \underline{f}_l(t)$	Revised transmission capacities of line l considering uncertain net demand at time t for positive and negative directions, respectively (MW)
$p_{i,k}(t)$	Generation level of unit (i, k) at time t (MW)
$p_{i,k}^r(t)$	Generation level of unit (i, k) at time t under net demand realization r (MW)
$p_{i,k}^{min}$, $p_{i,k}^{max}$	Minimum and maximum generation limits of unit (i, k), respectively (MW)
$q_{i,k}(t)$	Spinning reserve of unit (i, k) at time t (MW)
$S_{i,k}$	Start-up cost of unit (i, k) ($/Start),

$S_{i,k}^{NL}$	No-load cost of unit (i, k) ($/hour)
$T_{i,k}^{U}, T_{i,k}^{D}$	Minimum up and down times of unit (i, k), respectively (hours)
$u_{i,k}(t)$	Binary start-up decision for unit (i, k) at time t
$\widetilde{W}_i(t)$	Wind generation at node i at time t (MW)
$\widehat{W}_i(t)$	Expected value of wind generation at node i at time t (MW)
$[\underline{W_i}(t), \overline{W}_i(t)]$	Interval of wind generation at node i at time t (MW)
$x_{i,k}(t)$	Binary UC decision for unit (i, k) at time t
$\alpha^r(t)$	Weight of net demand realization r at time t
$\Delta_{i,k}$	Ramp rate of unit (i, k) (MW/hour)
$\lambda^r(t)$	Lagrangian multiplier of the system demand constraint at time t under net demand realization r ($/MWh)
$\mu_l^r(t)$, $v_l^r(t)$	Lagrangian multipliers of interval transmission constraints for positive and negative directions, respectively, at time t under net demand realization r ($/MWh)
$\sigma_i(t)$	Standard deviation of wind generation at node i at time t (MW)

4.2 Introduction

Reliability is an overriding concern for power systems, and power engineers have been striving hard to keep the lights on under different kinds of uncertainty. One major source of uncertainty is contingencies, which are unpredicted outages of components (generators or transmission lines). To avoid cascading failures and even blackouts, the North American Electric Reliability Corporation established, among other reliability rules, the "$N-1$ rule": for a system with N components, no single outage will cause violations on other components [2]. This rule has been embedded in unit commitment (UC), a critical operational process that determines the most economic set of online/offline decisions for all units one day ahead or hours ahead, resulting in "contingency-constrained unit commitment" (CCUC). Under the current practice, generator contingencies are typically managed by pre-defined reserve requirements [3]. Transmission contingencies are managed by preventive economic dispatch (ED), where ED decisions are made before contingencies are realized [3], [4]. One set of such ED decisions is guarded against the base case (under

which no contingency happens) and transmission contingencies by corresponding transmission constraints in the deterministic $N-1$ model. To avoid the complexity of directly including transmission constraints under all transmission contingencies, the "Simultaneous Feasibility Test" (SFT) is usually used [4]. The SFT determines whether a violation occurs in each post-contingency state at each hour and adds a constraint for each such violation to the next CCUC iteration. Iterations continue between CCUC and 24 SFTs (for 24 hours) until a solution with no violation is reached. Depending on the number of contingencies, this iterative process can be computationally burdensome. As a result, current practice terminates the process after a specified number of iterations and may lead to suboptimal solutions.[2]

Aside from contingencies, power systems now face new challenges associated with the uncertainty of intermittent renewables such as wind and solar [8]. Since contingencies and unexpected renewable output can occur simultaneously and cause constraint violations, a joint consideration of both factors is important. However, the resulting combinatorial complexity has limited research in this area to [9], [10] and [11]. In [9], "$N-k$" generator contingencies and wind uncertainty were jointly considered in UC via chance-constrained optimization. Unfortunately, transmission constraints and transmission contingencies were ignored. Authors in [10] considered transmission contingencies, generator contingencies, and wind uncertainty through stochastic programming, which minimizes the expected cost over the probability distribution of uncertainty represented by scenarios. A scenario was a combination of a contingency and a trajectory of wind realizations over 24 hours. As a result, the number of scenarios equals the product of the number of wind trajectories and the number of contingencies. After ignoring low-probability events, remaining scenarios were selected based on likelihoods proportional to their impacts on the expected cost. However, it is difficult to ensure computational efficiency while capturing low-probability but high-impact

[2] Another model to manage transmission contingencies (and can be used for generator contingencies) in CCUC is corrective ED. It is out of the scope of this paper, and interested readers can refer to [5]-[7].

events. In [11], "$N-1$" transmission and generator contingencies and spatially correlated nodal demand uncertainty were jointly considered for a single period through robust optimization. Although the problem was solved by using Benders decomposition and a binary expansion approach, the extension to a multi-period model would increase the computational burden significantly. Though the deterministic $N-1$ model with the SFT is used as the current practice to manage $N-1$ transmission contingencies, there is no publication using it for the joint consideration of contingencies and renewables to the best of our knowledge.[3]

To overcome the aforementioned complexity difficulties, this chapter develops a novel interval optimization approach for the CCUC problem with preventive ED considering "$N-1$" transmission contingencies and renewables. Section 4.3 formulates the interval CCUC problem. Instead of being analyzed one at a time, a large number of transmission contingencies are innovatively described by treating corresponding GSFs as uncertain parameters varying within intervals. In particular, under each transmission contingency, the line flow is the sum of net nodal injections weighted by corresponding GSFs. The ranges of GSFs varying among contingencies are then covered by intervals.[4] In this way, for each transmission line, we can use one single interval-based transmission constraint to represent the set of transmission constraints under all contingencies. Renewable generation is modeled by intervals and is jointly considered in the interval CCUC model in a consistent framework. To ensure solution robustness (i.e., solution feasibility under contingencies and renewable realizations), bounds of GSFs and renewable generation in different types of constraints are captured based on interval optimization [13], [14]. Since the boundary conditions of transmission contingencies and renewables are considered, there are only a few combinations.

[3] Readers interested in papers focusing on uncertain renewables without contingencies in UC can refer to the Literature Review section of [12].

[4] Although computing a large number of GSFs under transmission contingencies can be time-consuming for real-world systems, this can be implemented offline with results stored.

The interval model is reformulated as a mixed-integer linear programming (MILP) problem. Its conservativeness is reduced through improved interval computation.

To further reduce conservativeness and the problem size, Section 4.4 shrinks ranges of GSFs by a pre-processing step that identifies and removes redundant transmission constraints, prior to the interval model of transmission contingencies. Such an identification method for deterministic transmission-constrained UC [15] is extended to consider uncertain renewables via interval modeling. To efficiently solve large-scale MILP problems, Section 4.5 develops a solution methodology using Surrogate Lagrangian Relaxation (SLR) [16] and branch-and-cut (B&C) [17].

Section 4.6 tests the new approach using a simple six-bus problem, a modified IEEE Reliability Test System, and a modified IEEE 118-bus system. Optimization and simulation results demonstrate that our approach is computationally efficient and robust against transmission contingencies and renewable realizations. It also has a lower simulation cost (i.e., the expected total cost from simulation runs) than the deterministic approach.

Our approach differs from those in [12], [14], and [18]-[21] where interval optimization [13] was used to consider uncertain renewable generation or demand in UC without contingencies. While uncertain renewable generation varying within continuous ranges can be directly modeled by intervals, contingencies are often viewed as discrete events and therefore have not been looked at from an interval perspective before.

In the rest of this chapter, wind generation will be used as a representative renewable resource. Although solar generation has a different diurnal pattern from wind generation, both can be modeled as intervals.

4.3 Interval CCUC Formulation

Subsection 4.3.1 describes the CCUC problem and its deterministic model, subsection 4.3.2 formulates the interval optimization model considering transmission contingencies and the expected net demand, Section 4.3.3 incorporates uncertain net demand in the model, and Section 4.3.4 reduces its conservativeness through improved interval computation.

4.3.1 The CCUC Problem and the Deterministic Model

The CCUC problem is to minimize the total production cost by selecting one set of UC decisions for conventional units over the 24-hour horizon. For easy understanding of the derivation of the interval CCUC model and the redundant constraint identification method to be presented in Section 4.4, we start with a deterministic model, and reserves are not included in the formulation without loss of generality. The deterministic model manages transmission contingencies by multiple sets of transmission constraints and represents wind generation at each node (and the resulting net nodal demand) by its expected value. Based on [2], [22] and [23], this model can be formulated as:

$$\min \sum_{t=1}^{T}\sum_{i=1}^{I}\sum_{k=1}^{K_i}\left[u_{i,k}(t)S_{i,k} + x_{i,k}(t)S_{i,k}^{NL} + C_{i,k}(p_{i,k}^{E}(t))\right], \tag{4.1}$$

s.t. $$\sum_i \sum_k p_{i,k}^{E}(t) = \sum_i \hat{D}_i(t), \forall t, \tag{4.2}$$

$$-f_l^{\max} \le \sum_i a_{l,c}^{i}\left(\sum_k p_{i,k}^{E}(t) - \hat{D}_i(t)\right) \le f_l^{\max}, \forall l, \forall c \ne l, \forall t, \tag{4.3}$$

$$x_{i,k}(t)\,p_{i,k}^{\min} \le p_{i,k}^{E}(t) \le x_{i,k}(t)\,p_{i,k}^{\max}, \forall i, \forall k, \forall t, \tag{4.4}$$

$$-\Delta_{i,k} \le p_{i,k}^{E}(t) - p_{i,k}^{E}(t-1) \le \Delta_{i,k}, \forall i, \forall k, \forall t, \tag{4.5}$$

$$u_{i,k}(t) \ge x_{i,k}(t) - x_{i,k}(t-1), \forall i, \forall k, \forall t, \tag{4.6}$$

$$\sum_{t'=t-T_{i,k}^{U}+1}^{t} u_{i,k}(t') \le x_{i,k}(t), \forall i, \forall k, \forall t \in [T_{i,k}^{U}, T], \tag{4.7}$$

$$\sum_{t'=t-T_{i,k}^{D}+1}^{t} u_{i,k}(t') \le 1 - x_{i,k}(t - T_{i,k}^{D}), \forall i, \forall k, \forall t \in [T_{i,k}^{D}, T]. \tag{4.8}$$

The objective function (4.1) minimizes the total UC and ED cost. System demand constraints - total conventional generation equals total *expected* net demand - are represented by (4.2). Transmission constraints under the base case and all "*N* – 1" transmission contingencies are represented by (4.3). Generator capacity and ramp rate constraints are given by (4.4) and (4.5), respectively. Commitment-related constraints include start-up constraints (4.6), minimum up time constraints (4.7), and minimum down time constraints (4.8) (deviations of (4.7) and (4.8) are in [23]).

4.3.2 Interval CCUC Formulation with Expected Net Demand

Interval optimization uses closed intervals to model uncertainties. When these intervals are captured in the constraint set, the resulting solution will be feasible for every possible uncertainty realization within them (see [13], [14]). For the CCUC problem studied here, uncertainties are present in transmission contingencies and renewable generation.

We first analyze transmission contingencies without considering wind generation uncertainties. In (4.3), transmission contingencies are reflected by multiple sets of GSFs (i.e., contingency-specific $a_{l,c}^{i}$). As each contingency is treated as a discrete event, there are *L* cases for line *l* at hour *t*. The total number of constraints for each direction in (4.3) is $T \times L^2$.

To reduce the complexity, our novel idea is to treat GSFs as uncertain parameters varying within intervals as in Fig. 4.1.

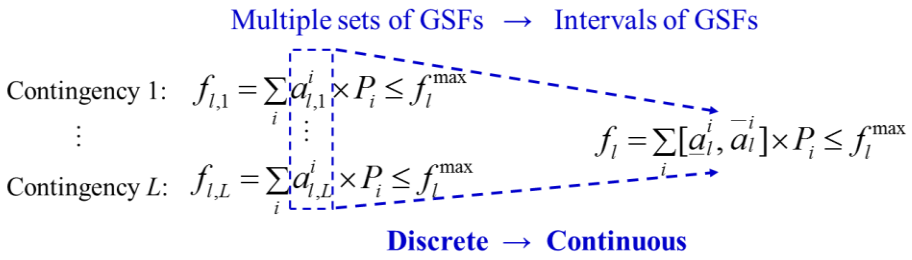

Fig. 4.1. Illustration of the interval contingency model. Time index t is ignored, and P_i is the net nodal injection from node i.

The intervals of GSFs that capture all $N-1$ transmission contingencies are determined as follows. GSFs are precalculated for all the contingencies. Then, for line l node i, the lower and upper bounds of GSFs are selected across all contingencies in (4.9) and (4.10), respectively:

$$\underline{a}_l^i = \min_{c \neq l} \{a_{l,c}^i\}, \forall l, \forall i, \tag{4.9}$$

$$\bar{a}_l^i = \max_{c \neq l} \{a_{l,c}^i\}, \forall l, \forall i. \tag{4.10}$$

These bounds establish an interval $\left[\underline{a}_l^i, \bar{a}_l^i\right]$.

The positive direction (right inequality) of (4.3) becomes:

$$\sum_i [\underline{a}_l^i, \bar{a}_l^i] \times \left(\sum_k p_{i,k}^E(t) \right) \le f_l^{\max} + \sum_i [\underline{a}_l^i, \bar{a}_l^i] \times \hat{D}_i(t), \forall l, \forall t. \tag{4.11}$$

Compared to (4.3), the major advantage of (4.11) is that only one constraint is needed to capture transmission contingencies for line l at hour t. The total number of (4.11) is only $T \times L$, and the reduced number of constraints is $T \times (L^2 - L)$.

To convert (4.11) into linear constraints, interval optimization is applied. Based on interval inequality [13], as long as the upper bound of the left-hand side (LHS) of (4.11) is less than or equal to the lower bound of the right-hand side (RHS), the transmission capacity will be satisfied under all contingencies.

These bounds can be obtained based on interval arithmetic [24]. The bounds of the LHS are obtained as in (4.12), because $p_{i,k}^{E}(t)$ is non-negative.

$$\sum_i [\underline{a}_l^i, \overline{a}_l^i] \times \left(\sum_k p_{i,k}^{E}(t) \right) = \sum_i \left[\underline{a}_l^i \left(\sum_k p_{i,k}^{E}(t) \right), \overline{a}_l^i \left(\sum_k p_{i,k}^{E}(t) \right) \right] = \left[\sum_i \underline{a}_l^i \left(\sum_k p_{i,k}^{E}(t) \right), \sum_i \overline{a}_l^i \left(\sum_k p_{i,k}^{E}(t) \right) \right], \forall l, \forall t. \tag{4.12}$$

As for the RHS, although the expected net nodal demand for each node *i* at each time *t* can be positive or negative, it is constant and is treated as the coefficient of the GSF intervals. The resulting interval can be obtained based on the sign of the expected net nodal demand to select corresponding bounds of GSFs, i.e.,

$$[\underline{a}_l^i, \overline{a}_l^i] \times \hat{D}_i(t) = \begin{cases} \left[\underline{a}_l^i \hat{D}_i(t), \overline{a}_l^i \hat{D}_i(t) \right], & when\, \hat{D}_i(t) \geq 0; \\ \left[\overline{a}_l^i \hat{D}_i(t), \underline{a}_l^i \hat{D}_i(t) \right], & when\, \hat{D}_i(t) < 0. \end{cases} \tag{4.13}$$

The lower bound of the RHS can thus be obtained:

$$f_l^{\max} + \sum_i [\underline{a}_l^i, \overline{a}_l^i] \times \hat{D}_i(t) \geq f_l^{\max} + \sum_i \min \left\{ \underline{a}_l^i \hat{D}_i(t), \overline{a}_l^i \hat{D}_i(t) \right\} = f_l^{\max} + \sum_{i:\hat{D}_i(t) \geq 0} \underline{a}_l^i \hat{D}_i(t) + \sum_{i:\hat{D}_i(t) < 0} \overline{a}_l^i \hat{D}_i(t), \forall l, \forall t. \tag{4.14}$$

Thus, (4.11) is reformulated as linear constraints:

$$\sum_i \overline{a}_l^i \left(\sum_k p_{i,k}^{E}(t) \right) \leq f_l^{\max} + \sum_{i:\hat{D}_i(t) \geq 0} \underline{a}_l^i \hat{D}_i(t) + \sum_{i:\hat{D}_i(t) < 0} \overline{a}_l^i \hat{D}_i(t), \forall l, \forall t. \tag{4.15}$$

In the same way, we have for the negative direction:

$$\sum_i \underline{a}_l^i \left(\sum_k p_{i,k}^{E}(t) \right) \geq -f_l^{\max} + \sum_{i:\hat{D}_i(t) \geq 0} \overline{a}_l^i \hat{D}_i(t) + \sum_{i:\hat{D}_i(t) < 0} \underline{a}_l^i \hat{D}_i(t), \forall l, \forall t. \tag{4.16}$$

Other constraints (4.2) and (4.4)-(4.8) and the objective function (4.1) are not affected by transmission contingencies, and are thus unchanged. The new interval optimization model, including (4.1), (4.2), (4.4)-(4.8), (4.15), and (4.16), significantly reduces the problem size and still guarantees that all "*N* – 1"

contingencies are feasible. The new model can be conservative because it ignores the dependency of GSFs on contingency (i.e., the upper or lower bounds of GSFs selected by interval arithmetic may not happen under the same contingency). This conservativeness will be reduced in subsection 4.3.4 and Section 4.4.

Note that the above interval optimization model relies on power flow equations based on GSFs to convert transmission contingencies into continuous intervals of GSFs. Other types of power flow equations, including the ones based on voltage phase angles, do not provide such intervals and therefore cannot be used to model transmission contingencies via interval optimization.

4.3.3 Interval CCUC Formulation with Uncertain Net Demand

This section presents how to incorporate uncertain renewables in the interval CCUC framework. Renewable generation is continuous and can thus be modeled by intervals in a consistent framework. To ensure solution robustness without much complexity, the boundary conditions of transmission contingencies and renewables are considered. The resulting conservativeness will be reduced in subsection 4.3.4.

Within the interval optimization framework, nodal wind generation is assumed to be within an interval. Wind generation at different nodes is further assumed independent of each other for simplicity [4.14]. The resulting net nodal demand, denoted as $\widetilde{D}_i(t)$ (MW), is thus within an interval $\left[\underline{D_i}(t), \overline{D}_i(t)\right]$ with an expected value $\widehat{D}_i(t)$.

1) Transmission constraints.

Substitute the expected net nodal demand with the uncertain net nodal demand in (4.3) and rearrange the positive direction (right inequality):

$$\sum_i a_{l,c}^i \left(\sum_k p_{i,k}(t) \right) \leq f_l^{\max} + \sum_i a_{l,c}^i \widetilde{D}_i(t), \forall l, \forall c \neq l, \forall t. \tag{4.17}$$

Similar to (4.11), the interval representation of (4.17) is:

$$\sum_i [\underline{a}_l^i, \overline{a}_l^i] \left(\sum_k p_{i,k}(t) \right) \le f_l^{\max} + \sum_i [\underline{a}_l^i, \overline{a}_l^i] \times [\underline{D}_i(t), \overline{D}_i(t)], \forall l, \forall t. \quad (4.18)$$

Its LHS is similar to that in (4.11), while its RHS involves the multiplication of two intervals. The lower bound of the RHS can be obtained based on traditional interval arithmetic [24]:

$$f_l^{\max} + \sum_i [\underline{a}_l^i, \overline{a}_l^i] \times [\underline{D}_i(t), \overline{D}_i(t)] \ge f_l^{\max} + \sum_i \min\{\underline{a}_l^i \underline{D}_i(t), \underline{a}_l^i \overline{D}_i(t), \overline{a}_l^i \underline{D}_i(t), \overline{a}_l^i \overline{D}_i(t)\}, \forall l, \forall t. \quad (4.19)$$

The corresponding boundary condition of (4.18) can also be expressed as linear constraints:

$$\sum_i \overline{a}_l^i \left(\sum_k p_{i,k}(t) \right) \le f_l^{\max} + \sum_i \min\{\underline{a}_l^i \underline{D}_i(t), \underline{a}_l^i \overline{D}_i(t), \overline{a}_l^i \underline{D}_i(t), \overline{a}_l^i \overline{D}_i(t)\}, \forall l, \forall t. \quad (4.20)$$

The impacts of both transmission contingencies and uncertain net nodal demands on power flows are captured in (4.20) simultaneously without the combinatorial complexity. Constraints (4.20) are linear with respect to decision variables $\{p_{i,k}(t)\}$ because the bounds of GSFs and net nodal demands are input parameters, and the minimization operation can be conducted before the optimization. However, the computation of the lower bound of the RHS involves two levels of interval operations: interval multiplication (between GSF and renewable intervals) and interval addition, and may cause conservativeness through unwanted expansion of the resulting intervals. Likewise, the constraints for the negative direction are:

$$\sum_i \underline{a}_l^i \left(\sum_k p_{i,k}(t) \right) \ge -f_l^{\max} + \sum_i \max\{\underline{a}_l^i \underline{D}_i(t), \underline{a}_l^i \overline{D}_i(t), \overline{a}_l^i \underline{D}_i(t), \overline{a}_l^i \overline{D}_i(t)\}, \forall l, \forall t. \quad (4.21)$$

2) System demand constraints.

Transmission contingencies do not affect system demand, so system demand constraints [14, Eq. (20)] can be directly adopted. Since net demands at different nodes are assumed independent, we have:

$$\sum_i \sum_k p_{i,k}(t) = \sum_i [\underline{D}_i(t), \overline{D}_i(t)] = \left[\sum_i \underline{D}_i(t), \sum_i \overline{D}_i(t) \right], \forall t. \quad (4.22)$$

The above equation demonstrates that the boundary conditions of net system demand happen at the minimum realization *m* where all net nodal demands are at their minima, and at the maximum realization *M* where all net nodal demands at their maxima. To guarantee that generation and demand are met for any possible net nodal demand realizations, these boundary conditions are required to be satisfied:

$$\sum_i \sum_k p_{i,k}^m(t) = \sum_i \underline{D}_i(t), \forall t, \quad (4.23)$$

$$\sum_i \sum_k p_{i,k}^M(t) = \sum_i \overline{D}_i(t), \forall t. \quad (4.24)$$

Constraints (4.23) and (4.24) imply that, under the optimal UC solution, there exist two sets of ED decisions $\{p_{i,k}^m(t)\}$ and $\{p_{i,k}^M(t)\}$ that can meet *m* and *M*, respectively.

Because both system demand and transmission constraints have to be satisfied at the same time in the CCUC problem, these two sets of ED decisions $\{p_{i,k}^m(t)\}$ and $\{p_{i,k}^M(t)\}$ are also considered in LHSs of (4.20) and (4.21) based on [14].

For the same reason, generator capacity constraints (4.4) become:

$$x_{i,k}(t) p_{i,k}^{\min} \le p_{i,k}^r(t) \le x_{i,k}(t) p_{i,k}^{\max}, \forall i, \forall k, \forall t, r = m, M. \quad (4.25)$$

3) Ramp rate constraints.

The ramp rate of each unit is required to be satisfied for any self- or cross-transition between minimum (*m*) and maximum (*M*) net demand realizations in two consecutive hours, i.e.,

$$-\Delta_{i,k} \le p_{i,k}^r(t) - p_{i,k}^{r'}(t-1) \le \Delta_{i,k}, \forall i, \forall k, \forall t, r = m, M, r' = m, M. \quad (4.26)$$

As pointed out in [12] and [21], (4.26) may be conservative since the cross-transitions between *m* and *M* realizations may not happen. This conservativeness can be reduced by improved ramp requirements based on the maximum possible inter-hour net demand increase and decrease [21]. In that way, the temporal correlation of the net demand (or renewable generation) can be somehow incorporated. Nevertheless, this extension is out of the scope of this chapter, and (4.26) is still used here. In addition, the start-up and shut-down generation limits [22, eq. (11)] are considered and merged with (4.26) linearly.

4) The objective function.

The goal of the optimization problem is to minimize the UC cost plus the expected ED cost of all possible wind realizations. However, the above interval constraints only contain ED decisions corresponding to the minimal and maximal realizations to reduce complexity [14]. Costs of these two extreme realizations may not reflect the costs of other possible ones. Based on [12], a weighted ED cost of minimal (*m*), maximal (*M*), and expected (*E*) realizations is used to approximate the expected ED cost with the resulting objective function:

$$\min \sum_{t=1}^{T}\sum_{i=1}^{I}\sum_{k=1}^{K_i}\left[u_{i,k}(t)S_{i,k} + x_{i,k}(t)S_{i,k}^{NL} + \alpha^{E}(t)C_{i,k}(p_{i,k}^{E}(t)) + \alpha^{m}(t)C_{i,k}(p_{i,k}^{m}(t)) + \alpha^{M}(t)C_{i,k}(p_{i,k}^{M}(t))\right] \tag{4.27}$$

The constraints for the expected realization can be easily included as in subsection 4.3.2. Weights $\alpha^{E}(t)$, $\alpha^{m}(t)$, and $\alpha^{M}(t)$ sum up to one at each hour. They affect the optimization cost (the total cost of (4.27) at the optimal solution) and the simulation cost but do not affect solution robustness to uncertainty. These weights can be selected based on the system operator's preference similar to [25] since they reflect the emphases on the minimal, maximal, or expected net demand realizations. Because the majority of net nodal demand realizations are likely to happen near *E*, a guideline is that $\alpha^{E}(t)$ should be larger than the other weights. It is interesting to note that our objective function is a generalization of those in interval UC papers that minimize the cost of the expected realization [14], [18], [21].

The complete interval CCUC model is (4.2), (4.4)-(4.8), (4.15), (4.16), (4.20), (4.21), and (4.23)-(4.27) with one set of binary variables $\{x_{i,k}(t)\}$ and $\{u_{i,k}(t)\}$, and three sets of continuous variables $\{p_{i,k}^{m}(t)\}$, $\{p_{i,k}^{M}(t)\}$, and $\{p_{i,k}^{E}(t)\}$. The above interval CCUC model is an MILP problem. Note that generator contingencies can be managed by pre-defined reserve requirements based on the current practice [3] through extending our model in a straightforward way.

4.3.4 Improved Interval Computation

To reduce the conservativeness of the interval CCUC model, this section focuses on improving the computing of RHS intervals in (4.15), (4.16), (4.20), and (4.21). Section 4.4 will further alleviate the overall conservatives through shrinking the input intervals of GSFs.

Given that there are a finite number of transmission contingencies and GSF values are constant under each contingency, our idea is to pre-compute the RHS over net nodal demands under each contingency, and then select their minimum over all contingencies. For the expected realization without wind uncertainty, instead of using (4.14), the lower bound of the RHS of (4.11) is computed as:

$$f_l^{\max} + \sum_i [\underline{a}_l^i, \overline{a}_l^i] \times \hat{D}_i(t) \geq f_l^{\max} + \min_{c \neq l} \left(\sum_i a_{l,c}^i \hat{D}_i(t) \right) \equiv \bar{f}_l^E(t). \tag{4.28}$$

In the above, $\overline{f}_l^E(t)$ is the tightest lower bound of the RHS, and can be understood as a revised transmission capacity (for the positive direction) considering transmission contingencies and expected net demand. This lower bound can still be pre-computed before optimization. Thus, (4.15) is substituted by *interval transmission constraints*:

$$\sum_i \overline{a}_l^i \left(\sum_k p_{i,k}^E(t) \right) \leq \bar{f}_l^E(t), \forall l, \forall t. \tag{4.29}$$

In the same way, (4.16) is substituted by

$$\sum_i \underline{a}_l^i \left(\sum_k p_{i,k}^E(t) \right) \geq -f_l^{\max} + \max_{c \neq l} \left(\sum_i a_{l,c}^i \hat{D}_i(t) \right) \equiv \underline{f}_l^E(t), \forall l, \forall t. \quad (4.3016)$$

When uncertain wind generation is considered, as net nodal demands are assumed independent, interval addition [24] is applied to compute the lower bound of the RHS of (4.17) (less a constant transmission capacity $f_l^{\max}$) under each contingency,

$$\min_{\tilde{D}_i(t)} \left(\sum_i a_{l,c}^i \tilde{D}_i(t) \right) = \sum_{i:a_{l,c}^i \geq 0} a_{l,c}^i \underline{D}_i(t) + \sum_{i:a_{l,c}^i < 0} a_{l,c}^i \overline{D}_i(t), \quad (4.31)$$

The minimum among all contingencies is then selected,

$$f_l^{\max} + \min_{c \neq l, \tilde{D}_i(t)} \left(\sum_i a_{l,c}^i \tilde{D}_i(t) \right) = f_l^{\max} + \min_{c \neq l} \left[\min_{\tilde{D}_i(t)} \left(\sum_i a_{l,c}^i \tilde{D}_i(t) \right) \right] \equiv \bar{f}_l(t), \forall l, \forall t. \quad (4.32)$$

In the above, $\overline{f}_l(t)$ is the tightest lower bound of the RHS, and can be understood as a revised transmission capacity (for the positive direction) considering transmission contingencies and uncertain net demand. Constraints (4.20) (with ED decisions $\{p_{i,k}^m(t)\}$ and $\{p_{i,k}^M(t)\}$ on the LHS) are substituted by

$$\sum_i \overline{a}_l^i \left(\sum_k p_{i,k}^r(t) \right) \leq \bar{f}_l(t), \forall l, \forall t, r = m, M. \quad (4.33)$$

Likewise, Constraints (4.18) are substituted by

$$\sum_i \underline{a}_l^i \left(\sum_k p_{i,k}^r(t) \right) \geq \underline{f}_l(t), \forall l, \forall t, r = m, M, \quad (4.34)$$

where $\underline{f}_l(t)$ can be pre-computed similar to (4.31) and (4.32). With (4.33) and (4.34), interval multiplication between GSF and renewable intervals is avoided, and the conservativeness of considering both contingencies and renewable at the same time is reduced.

Note that UC solutions and the resulting simulation cost are sensitive to the selection of the slack bus. Because GSFs depend on the choice of the slack bus, when the slack bus changes, GSFs change, and the

derived intervals may also change. Consequently, the UC solutions and the simulation cost may also change. In this chapter, a distributed slack bus is used to "average out" this dependence [26].

With improved interval computation, the interval CCUC formulation becomes (4.2), (4.4)-(4.8), (4.23)-(4.27), (4.29), (4.30), (4.33), and (4.34). There is still conservativeness at the LHSs of interval transmission constraints (4.29), (4.30), (4.33), and (4.34), and when considering them of different transmission lines together, because of the dependency issue of GSFs.

4.4 Alleviation of Conservativeness

To further alleviate the conservativeness and to further reduce the problem size, this section first identifies and removes redundant transmission constraints in the original CCUC model (4.1)-(4.8) but with uncertain renewables considered. The results of this pre-processing are then used to shrink GSF intervals considered in (4.29), (4.30), (4.33), and (4.34).

A redundant constraint identification method was developed for deterministic UC problems in [15]. An analytical estimate of the worst-case power flow along each line was obtained. If it was within the transmission capacity, the corresponding transmission constraint would be redundant, meaning that it could be removed without affecting the optimal solution.

In this section, this identification method is extended to account for uncertain wind generation. In this process, uncertain wind generation $\widetilde{W}_i(t)$ cannot be treated as part of net demand. The reason is that the worst-case power flow along a line may be caused by the minimum or maximum wind realization, or other realizations within them, depending on signs of GSFs. Because the redundant constraint identification method is to find the worst-case power flow, wind generation can be modeled as intervals and be treated as conventional generation. The worst-case flow from generation in the positive direction can be estimated by solving the following MILP problem (the negative direction is similar):

$$f_{l,c}^{*}(t) = \max_{x_{i,k}(t),\, p_{i,k}(t),\, \tilde{W}_i(t)} \left[\sum_i a_{l,c}^{i} \left(\sum_k p_{i,k}(t) \right) + \sum_i a_{l,c}^{i} \tilde{W}_i(t) \right], \tag{4.35}$$

s.t. $$\sum_i \sum_k p_{i,k}(t) + \sum_i \tilde{W}_i(t) = \sum_i D_i(t), \tag{4.36}$$

$$-f_{l'}^{\max} \le \sum_i a_{l',c}^{i} \left(\sum_k p_{i,k}^{E}(t) + \tilde{W}_i(t) - D_i(t) \right) \le f_{l'}^{\max}, \forall l' \ne l, \forall c \ne l', \tag{4.37}$$

$$x_{i,k}(t)\, p_{i,k}^{\min} \le p_{i,k}(t) \le x_{i,k}(t)\, p_{i,k}^{\max}, \forall i, \forall k, \tag{4.38}$$

$$\underline{W}_i(t) \le \tilde{W}_i(t) \le \overline{W}_i(t), \forall i. \tag{4.39}$$

The objective function (4.35) is to maximize (minimize for the negative direction) the flow of line l under contingency c at time t. Since time-coupling ramp rate and commitment-related constraints are ignored, the optimal objective value $f_{l,c}^{*}(t)$ is an upper bound of the actual worst-case flow.

A sufficient condition for its corresponding transmission constraint to be redundant in the CCUC problem (4.1)-(4.8) (with uncertain renewables considered) is for the maximum power flow to be less than or equal to its capacity:

$$f_{l,c}^{*}(t) - \sum_i a_{l,c}^{i} D_i(t) \le f_l^{\max}. \tag{4.40}$$

To avoid the computational burden of solving these MILP problems for each line, each hour, and each contingency, an analytical sufficient condition is obtained after dropping other transmission constraints (4.37) and integrality constraints associated with UC decisions in (4.38), following the development of [15, Theorem 5]. Since these conditions are independent for different lines, hours, and transmission contingencies, they can be checked in parallel.

After the identification, removing redundant transmission constraints (4.3) does not affect results of the original CCUC model (4.1)-(4.8). However, the remaining interval transmission constraints become

less conservative. More specifically, the GSF intervals $\left[\underline{a}_l^i, \overline{a}_l^i\right]$ shrink because fewer contingencies are considered. As a result, the feasibility region of decisions is larger than that of the interval CCUC problem with all of the transmission contingencies considered. The removal of redundant transmission constraints can therefore lead to a less conservative interval CCUC problem. In addition, this conservativeness alleviation technique is a pre-processing step that only shrinks GSF intervals but does not change the interval CCUC formulation as summarized at the end of subsection 4.3.4.

Another possible way to further reduce the conservativeness is to somehow consider the spatial correlation of renewable generation through affine arithmetic [27], [28] in our approach. In affine arithmetic, the interval of renewable generation at each node will be decomposed into sub-intervals associated with different sources of uncertainties based on correlations. Interval addition in (4.31) will then be carried out based on these sub-intervals, thereby avoiding unnecessary expansion of the resulting intervals. Affine arithmetic has been shown to provide better bounds than the standard interval arithmetic [27]. The testing with spatial correlation, however, is out of the scope of this dissertation.

4.5 Solution Methodology

The computational process used to solve the interval CCUC problem consists of the following three steps:

1. Remove redundant transmission constraints from the original CCUC problem using the technique described in Section 4.4.

2. Formulate the interval CCUC problem (4.2), (4.4)-(4.8), (4.23)-(4.27), (4.29), (4.30), (4.33), and (4.34) as in Section 4.3 with the remaining contingencies.

3. Apply SLR [16] and B&C methods to solve the interval CCUC problem as an MILP problem.

This section focuses on Step 3.

The interval CCUC problem is formulated as an MILP problem, which is generally non-deterministic polynomial-time hard (NP-hard). Although the B&C method [17] exploits linearity, it ignores potentially beneficial problem separability so computational challenges may still arise when problems are large in scale. The purpose of our solution methodology is to find a high-quality feasible solution in a short amount of time. Therefore, the problem is decomposed into multiple unit-level subproblems that are solved by B&C. Subproblem solutions are coordinated by applying SLR [16], which has provable convergence without requiring the relaxed problem to be fully optimized and without requiring knowledge of the optimal dual value. Moreover, after solving the dual problem, feasible solutions for the original problem can be recovered using heuristics which is the best that can be expected for even the state-of-the-art branch-and-cut method in CPLEX or Gurobi. This section only includes a few necessary equations to clarify the solution methodology as an application of SLR, but does not claim SLR itself as an original contribution of this chapter.

In the above interval CCUC formulation (the primal problem), units are coupled by system demand and interval transmission constraints. After relaxing these constraints, the problem becomes (constraints for the expected realization E are not included for conciseness of presentation):

$$\begin{aligned}
&\min \sum_{t=1}^{T}\left\{\sum_{i=1}^{I}\sum_{k=1}^{K_i}[u_{i,k}(t)S_{i,k}+x_{i,k}(t)S_{i,k}^{NL}+\sum_{r}\alpha^{r}(t)C_{i,k}(p_{i,k}^{r}(t))]\right\}+\lambda^{m}(t)[\sum_{i}\underline{D}_{i}(t)-\sum_{i}\sum_{k}p_{i,k}^{m}(t)]\\
&+\lambda^{M}(t)[\sum_{i}\overline{D}_{i}(t)-\sum_{i}\sum_{k}p_{i,k}^{M}(t)]+\sum_{(l,t)\in\Phi^{p}}\sum_{r\in\{m,M\}}\mu_{l}^{r}(t)[\sum_{i}\overline{a}_{l}^{i}(t)(\sum_{k}p_{i,k}^{r}(t))-\overline{f}_{l}(t)]\\
&+\sum_{(l,t)\in\Phi^{n}}\sum_{r\in\{m,M\}}\nu_{l}^{r}(t)[\underline{f}_{l}(t)-\sum_{i}\underline{a}_{l}^{i}(t)(\sum_{k}p_{i,k}^{r}(t))], \qquad (4.41)
\end{aligned}$$

s.t. Unit-level constraints: (4.6)-(4.8), (4.25), and (4.26).

This relaxed problem can be decomposed into unit-level subproblems. For unit k, its subproblem is

$$\min L_k=\min\left\{\sum_{t=1}^{T}\left[u_{i,k}(t)S_{i,k}+x_{i,k}(t)S_{i,k}^{NL}+\sum_{r}\alpha^{r}(t)C_{i,k}(p_{i,k}^{r}(t))-\lambda^{m}(t)p_{i,k}^{m}(t)-\lambda^{M}(t)p_{i,k}^{M}(t)\right]\right.$$

$$+\sum_{(l,t)\in\Phi^p}\sum_{r\in\{m,M\}}\mu_l^r(t)\overline{a}_l^i(t)p_{i,k}^r(t)-\sum_{(l,t)\in\Phi^n}\sum_{r\in\{m,M\}}\nu_l^r(t)\underline{a}_l^i(t)p_{i,k}^r(t)\Bigg\}, \tag{4.42}$$

s.t. Unit-level constraints: (4.6)-(4.8), (4.25), and (4.26) for unit *k*.

These subproblems are MILP problems that can be proven not NP-hard, and can be efficiently solved by using B&C. The optimal Lagrangian of subproblem *k*, for given dual variables, is denoted by $L_k^*(\lambda^r(t), \mu_l^r(t), \nu_l^r(t))$.

To coordinate subproblem solutions, the Lagrangian is maximized in an upper-level dual problem:

$$\max_{\lambda^r(t),\mu_l^r(t),\nu_l^r(t)}\Bigg\{\sum_{i=1}^{I}\sum_{k=1}^{K_i}L_k^*(\lambda^r(t),\mu_l^r(t),\nu_l^r(t))+\sum_{t=1}^{T}\Bigg[\lambda^m(t)(\sum_i\underline{D}_i(t))+\lambda^M(t)(\sum_i\overline{D}_i(t))\Bigg]$$
$$-\sum_{(l,t)\in\Phi^p}\sum_{r\in\{m,M\}}\mu_l^r(t)\overline{f}_l(t)+\sum_{(l,t)\in\Phi^n}\sum_{r\in\{m,M\}}\nu_l^r(t)\underline{f}_l(t)\Bigg\}. \tag{17}$$

To efficiently solve the dual problem, SLR is used to update multiplier values. Since SLR does not require solving all subproblems to update multipliers for separable problems, at each iteration, one group of subproblems is solved and the optimal multipliers are updated based on [16].

After solving the dual problem, feasible solutions for the primal problem can be recovered using heuristics. One possible way solves a smaller CCUC problem by fixing online UC decisions for relatively cheap units (based on full load average costs) and offline UC decisions for expensive ones.

The combined SLR and B&C method is illustrated in Fig. 4.2.

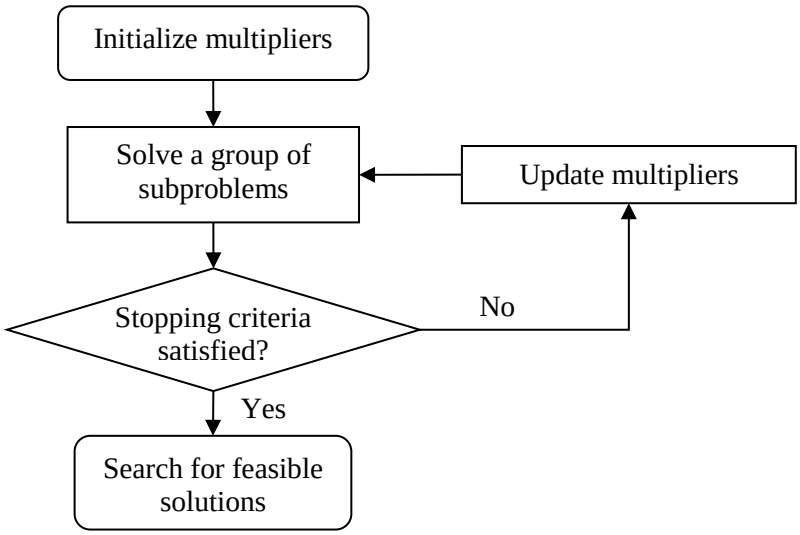

Fig. 4.2. Flowchart of the combined SLR and B&C method.

4.6 Numerical Results

Three problems are tested to demonstrate properties of the interval CCUC approach. In Example 1, a simple six-bus problem is tested to demonstrate solution robustness of the interval CCUC model against transmission contingencies and examine its conservativeness. In Example 2, a modified IEEE Reliability Test System with six wind farms is tested to compare the new approach with a deterministic approach. The benefits of redundant constraint removal are also exhibited. In Example 3, a modified IEEE 118-bus system with ten wind farms is tested to demonstrate the computational efficiency of SLR. Examples 1 and 2 are tested on a PC laptop with an Intel i7-2820QM 2.30GHz CPU (4 cores and 8 threads) and 8GB memory, while Example 3 on a PC laptop with an Intel i7-6920HQ 2.90GHz CPU (4 cores and 8 threads) and 32GB memory. Optimization and simulation of all examples are conducted using CPLEX 12.5.1.0 with OPL.[5]

[5]Testing data and results are available at http://www.engr.uconn.edu/msl/J1_IEEE.htm.

4.6.1 Example 1

The six-bus test problem from [7] is solved for a one-hour period. Uncertain renewable generation is not considered, and the quadratic cost function of each generator is approximated by a single bid block and a no-load cost.

Case 1. To illustrate the interval CCUC model, intervals of GSFs of Line 1 at six buses are plotted in Fig. 4.3.

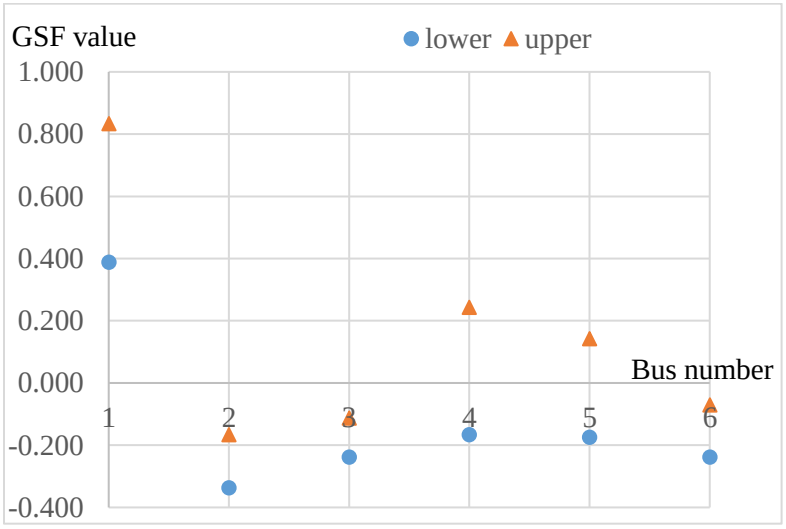

Fig. 4.3. GSF intervals of Line 1 at six buses of Case 1 in Example 1.

These GSF intervals, consisting of lower and upper bounds, are used to capture the base case and 8 contingency cases in transmission constraints in the interval CCUC model.

The interval CCUC model is solved using pure B&C without redundant constraint identification. Since the interval CCUC model is a simplified model, simulation is conducted to evaluate its UC solution. In simulation, the optimal UC solution is used as input and the $N-1$ contingency-constrained ED problem is solved. As a benchmark, the original CCUC model (4.1)-(4.8) is also tested. The original CCUC model does not need additional simulation, since $N-1$ contingency-constrained ED is included within the model, and its optimization and simulation costs are thus the same.

To examine the impact of transmission limits on costs, the problem is solved with f_3^{max} increasing from 18 MW to 90 MW in 2MW increments. Optimization and simulation costs are summarized in Fig. 4.4.

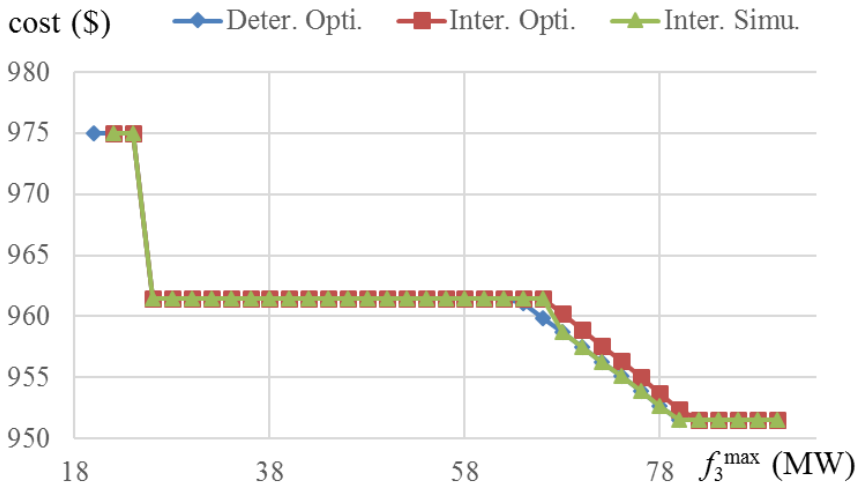

Fig. 4.4. Optimization and simulation results of Case 1 in Example 1.

Both models are infeasible when f_3^{max} is 18 MW. The original model becomes feasible when f_3^{max} is 20 MW, and the interval model does when f_3^{max} is 22 MW. When both models are feasible, the optimization cost of the interval model is higher than or equal to that of the original model, since the interval model can be more conservative. The largest percentage difference between these two costs is 0.17%.

The simulation process of the interval model is feasible as long as its optimization process is feasible, indicating that its solution is robust against contingencies. Moreover, its optimization cost is at least its corresponding simulation cost (i.e., the optimal UC cost plus the simulated ED cost), showing that the former can serve as the upper bound of the latter when only contingencies are considered. The simulation cost of the interval model equals that of the original model where their UC solutions turn out to be the same, except when f_3^{max} is 64 or 66 MW. This demonstrates that the conservativeness of the interval model is not high in this case.

Case 2. To demonstrate the sensitivity of our interval CCUC model to the selection of the slack bus, optimization is performed with different slack buses, and simulation is then conducted with UC solutions from optimization. Transmission capacity f_3^{max} is fixed at 60 MW. Results are summarized in Table 4.1 (the time index t is omitted since only one period is considered in this example).

Table 4.1. Optimization and Simulation Results of Case 2 in Example 1

Slack	Opti. ($)	$x_{1,1}$	$x_{3,1}$	$x_{5,1}$	Simu. ($)
1	968.28	1	1	0	963.50
2	969.66	1	1	0	963.50
3	961.50	1	0	0	961.50
4	967.15	1	1	0	963.50
5	961.50	1	0	0	961.50
6	961.50	1	0	0	961.50
7	961.50	1	0	0	961.50
8	961.50	1	0	0	961.50
Dist.	961.50	1	0	0	961.50

The optimization cost changes when the slack bus changes, and it appears that when the distributed slack bus is selected, the optimization cost is the lowest. The reason is that the power flow from demand, $\sum_i a_{l,c}^i \hat{D}_i(t)$, at the RHSs of (4.29) (obtained in (4.28)) and (4.30) is always zero with the distributed slack bus. The resulting interval of the power flow from demand, $\left[\min_{c\neq l}\left(\sum_i a_{l,c}^i \hat{D}_i(t)\right), \ \max_{c\neq l}\left(\sum_i a_{l,c}^i \hat{D}_i(t)\right)\right]$, is the narrowest as a point 0. This demonstrates that the distributed slack bus is the least conservative among different slack bus choices.

UC decisions and the resulting simulation cost also change when the slack bus changes, but are less sensitive to the selection of the slack bus than the optimization cost. The simulation cost is also the lowest when the distributed slack bus is selected, since this selection is the least conservative.

4.6.2 Example 2

Consider the IEEE RTS as modified in [1]. There are 38 transmission lines with reactance values, normal capacities, and long-term emergency (LTE) capacities for transmission contingencies [29]. To avoid islanding or infeasibility when the line from Bus 7 to Bus 8 is tripped, the line between those buses is replaced by two parallel lines, each with a reactance of 0.123 p.u., a normal capacity of 175 MW, and an LTE capacity of 208 MW. There are 24 conventional units, two must-run nuclear units, and six base-load hydroelectric units.

Six 110MW wind farms are added to the model. Wind generation of each wind farm in each hour (normalized by capacity) is assumed to follow a normal distribution truncated at two standard deviations and the physical limits [0, 1]. Its expected values for 24 hours are based on the day-ahead forecasts of a wind site on August 1, 2006 from [30]. Its standard deviation, denoted as $\sigma_i(t)$ for node i at hour t, is assumed to depend on the corresponding expected value [31]:

$$\sigma_i(t) = 0.02 + 0.2\hat{W}_i(t), \forall i, \forall t. \tag{4.44}$$

Case 1. Our approach is compared with the deterministic approach. Demand data from Tuesday of Week 28, a Summer Weekday, is used [29]. The wind penetration (≡ total expected wind generation / total demand × 100%) is 18.9%.

The analytical sufficient condition is checked in serial using MATLAB R2014a and uses the CPU time of 2.25 seconds. The original number of transmission constraints is 219,024 [= $39^2 \times 24 \times 2$ (positive and negative directions) × 3 (m, M, and E realizations)]. The number of interval transmission constraints

after the removal of the redundant constraints is 705, demonstrating a significant reduction of the model size.

The interval CCUC model is solved using pure B&C with and without the redundant constraint identification. In optimization, the weights in (4.27) are $\alpha^E(t) = 0.8$ and $\alpha^m(t) = \alpha^M(t) = 0.1$.

For benchmarking, the deterministic approach (4.1)-(4.8) is also tested. To provide a fair comparison with our interval optimization approach, uncertain wind generation is managed by spinning reserves [32]. The system spinning reserve requirements are set as the sum of two standard deviations over all wind farms, i.e.,

$$\sum_i \sum_k q_{i,k}(t) \geq \sum_i 2\sigma_i(t), \forall t. \tag{4.45}$$

The spinning reserve of each unit plus its generation level should be within its capacity, i.e.,

$$x_{i,k}(t)\, p_{i,k}^{\min} \leq p_{i,k}^{E}(t) + q_{i,k}(t) \leq x_{i,k}(t)\, p_{i,k}^{\max}, \forall i, \forall k, \forall t. \tag{4.46}$$

The optimization for each approach is terminated at a relative MIP gap 0.01%.

To evaluate the solution of each approach, 1,000 Monte Carlo simulation runs are conducted. 1,000 wind scenarios are sampled from truncated normal distributions, i.e., one scenario for each run. In each run, UC decisions are fixed at the solution obtained from optimization, and a 24-hour deterministic $N - 1$ contingency-constrained ED problem is solved. Each such ED problem considers all possible $N - 1$ transmission contingencies in transmission constraints similar to (4.3) based on the "$N - 1$ rule." To address possible infeasibility issues, wind generation can be curtailed at a penalty cost of \$150/MWh,[6] while load

[6] This penalty cost provides priority for wind generation to be dispatched. The bid floor of wind generation at the California ISO is -\$150/MWh [33], i.e., 1MWh of wind generation is can at most reduce \$150 from the total cost. Correspondingly, 1MWh of wind curtailment is penalized at \$150.

can be shed at a penalty cost of $5,000/MWh. Note that wind curtailment or load shedding is not allowed for all approaches in optimization to demonstrate the solution robustness of our approach (i.e., as long as there is one feasible UC solution obtained from optimization, it will be feasible against all $N - 1$ transmission contingencies and possible wind realizations). If the problem becomes infeasible in other systems, load shedding and wind curtailment can be considered similar to conventional generation (wind curtailment as negative generation) as decision variables in our interval optimization approach with penalty costs.

Table 4.2. Optimization and Simulation Results of Example 2

Approach	Deter.	Inter. w/o iden.	Inter. w/ iden.	
Optimization	Total cost (k$)	236.03	298.18	246.87
	CPU time (s)	5.88	21.98	4.01
Simulation	E(Total cost) (k$)	254.26	275.36	245.84
	STD(Total cost) (k$)	1.91	1.38	1.47
	99.7% confidence interval of E(Total cost) (k$)	[254.08, 254.44]	[275.23, 275.49]	[245.70, 245.98]
	E(Load shed penalty) (k$)	0.20	0	0
	E(Wind curtailed penalty) (k$)	0	0	0
	# of runs incurring penalties	32	0	0

Results are summarized in Table 4.2. With the redundant constraint identification, the optimization cost of the interval CCUC model decreases from $298.18k to $246.87k, and the simulation cost decreases by 12.01% from $275.36k to $245.84k. This demonstrates that the model and the resulting UC solution are less conservative, after redundant constraints are removed.

Although our approach with the identification still has a higher optimization cost than the $236.03k from the deterministic approach, our approach has a 3.42% lower simulation cost. The interval approach avoids wind curtailment and load shedding in all simulation runs, demonstrating its solution robustness.

The deterministic approach, on the other hand, requires load shedding in 32 out of 1,000 scenarios. This indicates that the deterministic approach, even with spinning reserves, cannot guarantee solution robust against all possible wind realizations.

Case 2. Different choices of weights in the objective function (4.22) of the interval CCUC model are tested with the redundant constraint identification. Demand data from Tuesday of Week 31, a Summer Weekday, are used [29]. The wind penetration is 21.4%.

The weight $\alpha^E(t)$ is changed from 0 to 1 at a step of 0.1. Since the truncated normal distributions assumed for wind generation are symmetric, $\alpha^m(t)$ and $\alpha^M(t)$ are chosen to be the same for simplicity. For example, when $\alpha^E(t) = 0.8$, $\alpha^m(t) = \alpha^M(t) = 0.1$. Optimization and simulation results are summarized in Fig. 4.5.

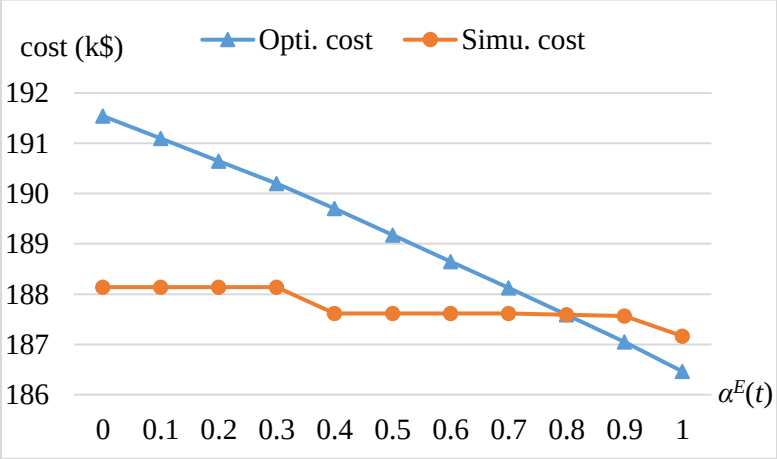

Fig. 4.5. Sensitivity of optimization and simulation costs with respect to $\alpha^E(t)$.

The optimization cost decreases as $\alpha^E(t)$ increases, indicating that the larger $\alpha^E(t)$ moves the optimization cost closer to *E* realization, and *M* realization (more expensive with higher net demand) affects the cost more than *m*. The simulation cost also decreases but more slowly, and does not change when $\alpha^E(t)$ is from 0 to 0.3, or from 0.4 to 0.7. This is because the UC solutions do not change in these ranges, although the optimal cost changes due to the weight variations in the objective function. This demonstrates that UC

solutions are not very sensitive to these weights. To reflect the modeling accuracy, the absolute percentage error (APE) between optimization and simulation costs is calculated. The highest APE is 1.81% when $\alpha^E(t) = 0$, while the lowest APE turns out to be 0.00% when $\alpha^E(t) = 0.8$. The APE is below 1% when $\alpha^E(t)$ is from 0.5 to 1.

In addition, two extreme cases are also tested. When $\alpha^m(t) = 1$ (and other weights are zero), the optimization cost is \$156.14k, the simulation cost \$189.27, and the APE 17.50%. When $\alpha^m(t) = 1$, the optimization cost is \$225.53k, the simulation cost \$189.57k, and the APE 18.97%. The above results demonstrate that considering *E* realization in the objective function (4.13) with a relatively high weight provides an accurate approximation of the expected cost of all wind realizations. Moreover, no matter how these weights change, UC solutions are always feasible against possible renewable realizations and contingencies, since the ranges of uncertainty are captured in constraints.

4.6.3 Example 3

The IEEE 118-bus system with ten additional wind farms is solved. In this model, there are 54 conventional units, 186 transmission lines, and 91 demand centers with a peak system demand of 3733.07 MW [34]. Each additional wind farm has a capacity of 100 MW, and the treatment of its generation is the same as in Example 2. The wind penetration is 17.0%. To avoid islanding or infeasibility, nine lines are added and capacities of four lines are increased, similar to [7]. The LTE capacity of each line is assumed to be 1.2 times its normal capacity.

Similar to Case 1 of Example 2, our interval CCUC model with the redundant constraint identification is compared with the deterministic model (4.1)-(4.8), (4.45) and (4.46). Both models are solved by using the pure B&C method, with a relative MIP gap 0.5% as the stopping criterion. 1,000 Monte Carlo simulation runs are then conducted to evaluate the solution of each model. The results are summarized in the first two columns of Table 4.3.

Table 4.3. Optimization and Simulation Results of Example 3[7]

Model		Deter.	Inter. w/ iden.	
Method		Pure B&C	Pure B&C	SLR+B&C
Optimization	Total cost (k$)	797.48	834.26	834.88
	CPU time	2min14s	58s	56s
	CPU time/iteration	-	-	2.80s
	CPU time/group	-	-	0.47s
Simulation	E(Total cost) (k$)	827.03	821.68	819.46
	STD(Total cost) (k$)	8.06	2.40	2.39
	99.7% confidence interval of E(Total cost) (k$)	[826.26, 827.79]	[821.45, 821.91]	[819.23, 819.69]
	E(Load shed penalty) (k$)	0	0	0
	E(Wind curtailed penalty) (k$)	13.49	0	0
	# of runs incurring penalties	974	0	0

The deterministic model takes 2 minutes and 14 seconds to solve by using pure B&C, while our interval CCUC model takes 58 seconds. This implies that the new model with redundant constraint identification is more computationally efficient than the deterministic model. Moreover, the deterministic approach incurs wind curtailment in 974 out of 1,000 scenarios. The interval model, in contrast, avoids wind curtailment and load shedding in all simulation runs. This further demonstrates the solution robustness of our interval model, in addition to results in Case 1 of Example 2.

[7] The time required for generating models and updating multipliers is much longer than the CPU time of solving subproblems for SLR+B&C. This issue can be addressed by using more advanced optimization languages such as Julia instead of OPL.

Furthermore, our model is also solved by using the combined SLR and B&C method. In the combined method, the 54 units are grouped into six 9-unit groups and each group of subproblems are solved together. Similar to traditional Lagrangian relaxation, we count an SLR iteration here as solving all subproblems (even though Lagrangian multipliers are updated six times). After termination, a near-optimal feasible UC solution is recovered. Results are summarized in the third column of Table 4.3.

SLR+B&C finishes 20 iterations for the dual problem with the CPU time of 56 seconds. The total cost of the obtained feasible solution from SLR+B&C is $834.88k, very close to $834.26k of pure B&C. The simulation costs of both methods are also very close.

Fig. 4.6 further illustrates the computational performance of both methods for solving the CCUC model with redundant constraint identification. The pure B&C method obtains its first feasible solution of $916.83k at a 9.3% MIP gap after 31 seconds. However, it takes 58 seconds to reach the solution within the 0.5% MIP gap as in Table 4.3, and takes 2 minutes and 18 seconds to obtain a solution of $833.72k at a 0.1% MIP gap. In contrast, the SLR+B&C method finishes 12 iterations for the dual problem after 34 seconds and obtains a feasible solution of $837.57k, only 0.46% higher than the $833.72k solution of B&C. This demonstrates that SLR+B&C is able to find a high-quality feasible solution in a shorter CPU time.

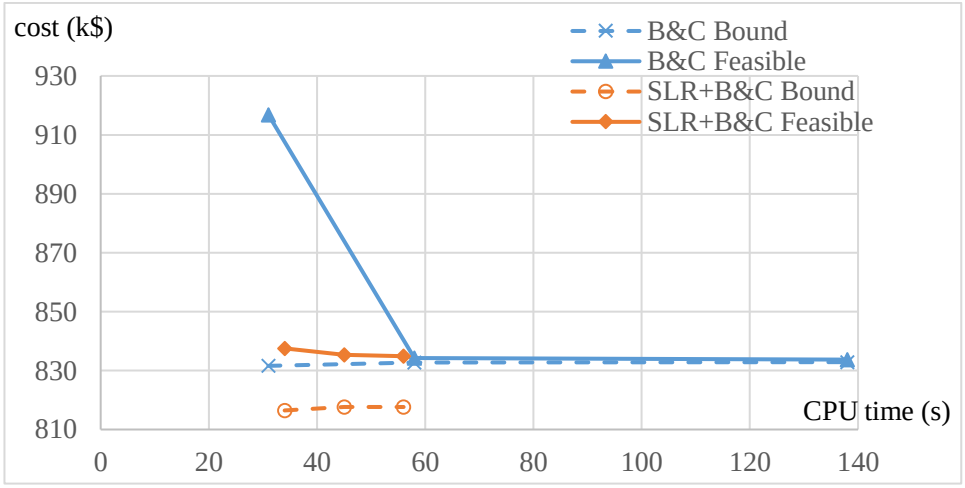

Fig. 4.6. Comparison between pure B&C and the SLR+B&C method for solving the interval CCUC model with the redundant constraint identification.

4.7 Conclusion

This chapter develops a novel interval optimization approach to manage both transmission contingencies and uncertain renewable generation in CCUC. Transmission contingencies are modeled by intervals for the first time, and its conservativeness is reduced. The resulting MILP problem is decomposed into unit-level subproblems so that SLR and B&C can be efficiently applied. The underlying idea of converting discrete events into continuous intervals can be used in other problems to capture multiple cases by one case.

References

[1] Y. Yu, P. B. Luh, E. Litvinov, T. Zheng, J. Zhao, and F. Zhao "Transmission contingency-constrained unit commitment with uncertain wind generation via interval optimization," in *Proc. of the 2015 IEEE Power and Energy Soc. Gen. Meet.*, Denver, CO, July 2015.

[2] A. J. Wood, B. F. Wollenberg, and G. B. Sheble, *Power Generation, Operation and Control* (3rd ed.), Wiley, 2013.

[3] ISO New England, "ISO New England operating procedure No. 8 operating reserve and regulation," May 2015, http://www.iso-ne.com/rules_proceds/operating/isone/op8/op8_rto_final.pdf

[4] J. Zhu, and K. Cheung, "Flexible simultaneous feasibility test in energy market," in *Proceedings of the 2010 IEEE Power and Energy Society General Meeting*, Redmond, WA, USA, 2010.

[5] J. Wang, M. Shahidehpour, and Z. Li, "Contingency-constrained reserve requirements in joint energy and ancillary services auction," *IEEE Trans. Power Syst.*, vol. 24, no. 3, pp. 1457-1468, 2009.

[6] A. Street, F. Oliveira, and J. M. Arroyo, "Contingency-constrained unit commitment with security criterion: A robust optimization approach," *IEEE Trans. Power Syst.*, vol. 26, no. 3, pp. 1581-1590, 2011.

[7] Q. Wang, J-P. Watson, and Y. Guan, "Two-stage robust optimization for *N* - *k* contingency-constrained unit commitment," *IEEE Trans. Power Syst.*, vol. 28, no. 3, pp. 2366-2375, 2013.

[8] REN 21, "Renewables 2014 global status report," 2014, http://www.ren21.net/Portals/0/documents/Resources/GSR/2014/GSR2014_full%20report_low%20res.pdf

[9] D. Pozo and J. Contreras, "A chance-constrained unit commitment with an *n* - *K* security criterion and significant wind generation," *IEEE Trans. Power Syst.*, vol. 28, no. 3, pp. 2842-2851, Aug. 2013.

[10] A. Papavasiliou and S. Oren, "Multiarea stochastic unit commitment for high wind penetration in a transmission constrained network," *Operations Research*, vol. 61, no. 3, pp. 578-592, May-June 2013.

[11] A. Moreira, A. Street, and J. M. Arroyo, "Energy and reserve scheduling under correlated nodal demand uncertainty: An adjustable robust optimization approach," *Electr. Power Energy Syst.*, vol. 72, pp. 91-98, Nov. 2015.

[12] Y. Yu, P. B. Luh, E. Litvinov, T. Zheng, J. Zhao, and F. Zhao, "Grid integration of distributed wind generation: Hybrid Markovian and interval unit commitment," *IEEE Transactions on Smart Grid*, vol. 6, no. 6, pp. 3061-3072, Nov. 2015.

[13] W. Chinneck and K. Ramadan, "Linear programming with interval coefficients," *J. Oper. Res. Soc.*, vol. 51, no. 2, pp. 209-220, 2000.

[14] Y. Wang, Q. Xia, and C. Kang, "Unit commitment with volatile node injections by using interval optimization," *IEEE Trans. Power Syst.*, vol. 26, no. 3, pp. 1705-1713, 2011.

[15] Q. Zhai, X. Guan, J. Cheng, and H. Wu, "Fast identification of inactive security constraints in SCUC problems," *IEEE Trans. Power Syst.*, vol. 25, no. 4, pp. 1946-1954, 2010.

[16] M. A. Bragin, P. B. Luh, J. H. Yan, N. Yu, and G. A. Stern, "Convergence of the surrogate Lagrangian relaxation method," *Journal of Optimization Theory and Applications*, vol. 164, pp. 173-201, 2015.

[17] R. E. Bixby, M. Fenelon, Z. Gu, E. Rothberg, and R. Wunderling, "MIP: Theory and practice – closing the gap," *System Modelling and Optimization*, pp. 19-49, 2000.

[18] X. Sun and C. Fang, "Interval mixed-integer programming for daily unit commitment and dispatch incorporating wind power," in *Proc. of 2010 International Conference on Power System Technology*, Hangzhou, China, Oct. 2010.

[19] L. Wu, M. Shahidehpour, and Z. Li, "Comparison of scenario-based and interval optimization approaches to stochastic SCUC," *IEEE Transactions on Power Systems*, vol. 27, no. 2, pp. 913-921, May 2012.

[20] Y. Dvorkin, H. Pandzic, M. A. Ortega-Vazquez, and D. S. Kirschen, "A hybrid stochastic/interval approach to transmission-constrained unit commitment," *IEEE Trans. Power Syst*., vol. 30, no. 2, pp. 621–631, Mar. 2015.

[21] H. Pandžić, Y. Dvorkin, T. Qiu, Y. Wang, and D. S. Kirschen, "Toward cost-efficient and reliable unit commitment under uncertainty," *IEEE Trans. Power Syst.*, vol. 31, no. 2, pp. 970-982, Mar. 2016.

[22] X. Guan, P. B. Luh, H. Yan, and J. A. Amalfi, "An optimization-based method for unit commitment," *International Journal of Electrical Power & Energy Systems*, vol. 14, no. 1, pp. 9-17, 1992.

[23] D. Rajan and S. Takriti. "Minimum up/down polytopes of the unit commitment problem with start-up costs," IBM Research Report, 2005.

[24] R. E. Moore, R. B. Kearfott and M. J. Cloud, *Introduction to Interval Analysis*, SIAM, Philadelphia, 2009.

[25] C. Zhao and Y. Guan, "Unified stochastic and robust unit commitment," *IEEE Trans. Power Syst.*, vol. 28, no. 3, pp. 3353–3361, Aug. 2013.

[26] E. Litvinov, T. Zheng, G. Rosenwald, and P. Shamsollahi, "Marginal loss modeling in LMP calculation," *IEEE Transactions on Power Systems*, vol. 19, no. 2, pp. 880-888, May 2004.

[27] A. Vaccaro, C. A. Canizares, and D. Villacci, "An affine arithmetic-based methodology for reliable power flow analysis in the presence of data uncertainty," *IEEE Trans. on Power Syst*., vol. 25, no. 2, pp. 624-632, May 2010.

[28] M. Pirnia, C. A. Cañizares, K. Bhattacharya, and A. Vaccaro, "A novel affine arithmetic method to solve optimal power flow problems with uncertainties," *IEEE Trans. on Power Syst.*, vol. 29, no. 6, pp. 2775-2783, Nov., 2014.

[29] IEEE RTS Task Force of APM Subcommittee, "The IEEE reliability test system-1996," *IEEE Trans. Power Syst.*, vol. 14, no. 3, pp. 1010-1020, Aug 1999.

[30] National Renewable Energy Laboratory, Eastern Wind Dataset, 2010, http://www.nrel.gov/electricity/transmission/eastern_wind_methodology.html

[31] F. Bouffard and F. D. Galiana, "Stochastic security for operations planning with significant wind power generation," *IEEE Trans. Power Syst.*, vol. 23, no. 2, pp. 306-316, 2008.

[32] M. A. Ortega-Vazquez and D. S. Kirschen, "Estimating the spinning reserve requirements in systems with significant wind power generation penetration," *IEEE Transactions on Power Systems*, vol. 24, no. 1, pp. 114-124, Feb. 2009.

[33] L. Bird, J. Cochran, and X. Wang, "Wind and solar energy curtailment: Experience and practices in the United States," NREL Tech. Rep., 2014.

[34] IEEE 118-bus system. [Online]. Available: http://motor.ece.iit.edu/data/

Chapter 5

Scalable Corrective Security-constrained Economic Dispatch Considering Conflicting Contingencies

Reliability is an overriding factor in power system operations. Corrective security-constrained economic dispatch (SCED) satisfying the "$N-1$" criterion is difficult because of a large number of contingencies and the strict time limit for real-time operations. The existence of conflicting contingencies further complicates the problem. To overcome these difficulties, this chapter develops a new iterative contingency filtering approach to manage "$N-1$" transmission and generator contingencies via decomposition and coordination. Instead of always removing conflicting contingencies as in existing papers, we offer system operators an important option to keep them for increased reliability, enabled by identifying multiple conflicting contingencies simultaneously. To satisfy the strict time requirements in real-time operations, the computational performance of our approach is significantly enhanced by novel warm-start of subproblem models and by parallel computing. Numerical results demonstrate that our new approach is computationally efficient and scalable, and increases the system reliability. In particular, the Polish 2383-bus system with all transmission contingencies is solved within two minutes.

5.1 Introduction

Reliability is an overriding factor in power system operations. Power engineers make great efforts to "keep the lights on" under normal operation conditions and contingencies. A contingency is an unexpected outage of a component (a transmission line or a generator). To protect power systems against cascading failures and even blackouts, the North American Electric Reliability Corporation (NERC) set, among other reliability standards, the "$N-1$" criterion: in a system that has N components, no single contingency will lead to violations of other components [1]. In real-time wholesale electricity markets, this criterion is considered in economic dispatch (ED), a central operational process. ED is conducted every five minutes to decide how much MW of power each online generator (or unit) should produce to minimize the total generation cost. The version of ED considering the "$N-1$" criterion is known as "security-constrained economic dispatch" (SCED).

5.1.1 Motivations of Corrective SCED

There are two categories of SCED models: preventive and corrective. Preventive SCED is currently practiced to manage transmission contingencies, and requires one set of ED decisions feasible against the base case (under which no contingency happens) and all "$N-1$" transmission contingencies [2]. Such a model restricts ED decisions to remain unchanged from the base-case values after a contingency occurs. This restriction brings three drawbacks. First, the mathematical models of preventive SCED are more conservative than those of corrective SCED. Second, preventive SCED does not have the capability to model the adjustment of post-contingency flows, which are required to be within corresponding Long-Time Emergency (LTE) ratings within 15 minutes after a contingency [3], [4]. Consequently, post-contingency flows currently rely on operators' manual adjustments [4]. Third, preventive SCED cannot model "$N-1$" generator contingencies since the output of the tripped generator needs to be picked up by corrective actions of others. Currently, generator contingencies are managed by pre-defined reserve requirements based on

capacities of certain generators [1]. Since these requirements do not explicitly consider each generator contingency, results can be infeasible for certain contingencies.

To make results less conservative and to explicitly model post-contingency flows and generator contingencies, the corrective SCED model was introduced by [5]. In corrective SCED, corrective actions can be taken after each contingency happens so post-contingency ED decisions can deviate from base-case ED decisions. The deviation for each unit should be within the maximal allowed variation. As a result, multiple sets of ED decisions are made, one set per contingency. The total cost of corrective ED will be lower than that of preventive ED since preventive ED is a special case of corrective ED where the maximal allowed variation is zero. Moreover, post-contingency flows and generator contingencies are explicitly modeled. However, corrective SCED involves large numbers of post-contingency ED decisions and constraints, and has traditionally been very hard to solve within the timeframe of the real-time market. Furthermore, different types of infeasible contingencies, especially conflicting ones, often exist in practical systems and further complicate the solution process [6], [7]. It is thus important to identify, differentiate, and manage them.

5.1.2 Literature Review

To solve the corrective SCED problem, there are three typical approaches: the direct approach, contingency filtering, and Benders decomposition. The direct approach considers all possible contingencies and solves the corrective SCED problem as a large linear programming (LP) problem or a large nonlinear programming problem depending on whether the DC or AC power flow model is assumed. Since there are large numbers of decision variables and constraints corresponding to contingencies, the direct approach can easily lead to computer memory problems and long solution times [8]. In addition, although a pre-screening step can be developed to identify some of the infeasible contingencies, that step can take considerable time and is blind to those contingencies that are conflicting with each other [7].

To reduce the problem size, contingency filtering methods (often considering AC power flow) started with solving the base-case model, and then iteratively added selected active contingencies to revise the solution [6], [9], [10]. The base-case and selected active contingencies were solved in a master problem, while candidate contingencies were checked or ranked in subproblems. Because most contingencies were not active at the optimum, candidate ones were selected by ranking all contingencies based on the severity index (the 2-norm of weighted constraint violations) [9], the rescheduling index (the minimum of the maximal controllable redispatch value) [6], or by using the non-dominated contingency technique (comparing constraint violations) [10]. Infeasible contingencies were first discussed in [6] where only transmission contingencies were considered. All islanding contingencies, identified in a primary contingency filtering step, were directly removed. Conflicting contingencies were identified and removed one at a time by relaxing the redispatch constraints with penalty terms. Removing conflicting contingencies and all islanding ones may decrease system reliability as will be discussed in subsection5.2.2. The authors of [6] also developed a decomposed parallel interior point method to accelerate the solution process, and tested parallel computing by using from 3 to 8 processes.

Alternatively, Benders decomposition was used to divide the corrective SCED problem into a base-case master problem and multiple contingency subproblems [5], [7], [11]. For a given ED solution, "violated cuts" were derived from subproblems and were added to the master problem to revise solutions. In [5] and [11], AC power flow was considered, and the generalized Benders decomposition was used. However, convergence was not guaranteed. In the recent work [7], DC power flow was considered, and multi-stage redispatch was modeled for transmission contingencies. All infeasible contingencies were removed. Performance enhancements in [7] included reducing the amount of subproblems in iterations, solving subproblems by using the barrier method without crossover, including difficult contingencies within the master problem, and using parallel computing. The overall approach was able to solve the Polish 2383-bus system with all transmission contingencies within 10 minutes, using GAMS on a server that had

two 3.46 G X5690 Xeon chips with 12 Cores, and 288 GB Memory. A faster approach is still desired to satisfy the strict time requirements in real-time operations.

5.1.3 Contributions and Organization of this Chapter

To overcome the above difficulties and to improve the system reliability, economic efficiency, and computational performance, this chapter develops a new contingency filtering approach for the real-time corrective SCED problem. There are three main contributions:

1) Our overall approach, consisting of the decomposition and coordination method, and enhancements by novel warm-start of subproblem models and by parallel computing, is scalable for corrective SCED problems.

2) Instead of always removing conflicting contingencies as in existing papers, we offer system operators an important option to keep them for increased reliability, enabled by identifying multiple conflicting contingencies simultaneously.

3) Our approach is able to solve the Polish 2383-bus system with all transmission contingencies within two minutes, demonstrating its computational efficiency for practical use in real-time operations.

Section 5.2 formulates the problem considering "N - 1" transmission and generator contingencies. DC power flow is used following [7], because it is very difficult to solve the corrective SCED problem with AC power flow for practical problems in real-time. There is a tradeoff between modeling corrective actions and considering AC power flow. The overall model is a large LP problem. Based on the formulation, infeasible contingencies are analyzed. Section 5.3 develops the new contingency filtering approach. The problem is decomposed into a master SCED problem and multiple contingency subproblems. In the solution process, infeasible contingencies, especially conflicting ones, are identified and managed. The method that identified and removed conflicting contingencies one at a time in [6] is improved to identify multiple conflicting ones simultaneously.

Section 5.4 significantly enhances the computational performance by novel warm-start of subproblem models and by parallel computing. Section 5.5 tests our new approach using the IEEE Reliability Test System (RTS) and a Polish 2383-bus system. Optimization and simulation results demonstrate that our approach is computationally efficient and scalable, and increases the system reliability.

5.2 Problem Formulation

Subsection 5.2.1 formulates the problem considering "$N - 1$" transmission and generator contingencies, and subsection 5.2.2 analyzes infeasible contingencies.

5.2.1 Real-time Corrective SCED Formulation

The problem is to minimize the total base-case ED cost by selecting one set of base-case ED decisions and multiple sets of post-contingency ED decisions for online units. A single time period is considered based on the current practice of the majority of ISOs (e.g., ISO New England [12] and PJM [13]).

Building on [5], consider a transmission network with L lines indexed by l ($1 \le l \le L$), I nodes indexed by i ($1 \le i \le I$), and K online units indexed by k ($1 \le k \le K$). Let $\Phi(i)$ be the set of units at node i. Let c be the index of contingencies. When $c = 0$, the system is under the base case; when $c = 1, \ldots, L$, the system is under a transmission contingency where line c is tripped; when $c = L + 1, \ldots, L + K$, the system is under a generator contingency where unit $(c - L)$ is tripped.

Unit k has an increasing continuous piecewise linear generation cost function $C_k(\cdot)$ (\$) with multiple generation blocks, minimum and maximum generation levels $p_k^{\min}$ (MW) and $p_k^{\max}$ (MW), respectively, a ramp rate R_i (MW/minute), and the maximal allowed variation under contingency c denoted by $\Delta_{k,c}$ (MW). Transmission line l has reactance X_l (Ω), and its line rating under contingency c is $f_{l,c}^{\max}$ (MW).

As for decision variables, the dispatch decision of unit k under contingency c is denoted by $p_{k,c}$ (MW). The voltage phase angle at node i under contingency c is denoted by $\theta_{i,c}$. Given that generator contingencies

are explicitly considered in our model, reserves are not included. Constraints and the objective function are presented as follows.

1) Transmission constraints:

The power flow along line l under contingency c, modeled by DC power flow with voltage phase angles, should be within the corresponding line rating for the positive and negative directions, i.e.,

$$-f_{l,c}^{\max} \le f_{l,c} = \frac{\theta_{\alpha(l),c} - \theta_{\beta(l),c}}{X_l} \le f_{l,c}^{\max}, \forall l, \forall c = 0, 1, \ldots, l-1, l+1, \ldots, L+K, \quad (5.1)$$

where $\alpha(l)$ and $\beta(l)$ are the from and to nodes of line l, respectively. Transmission capacity $f_{l,0}^{\max}$ is the normal rating under the base case ($c = 0$), and is the Long-Time Emergency rating under the contingency case ($c \neq 0$) [3], [4]. When l is tripped ($c = l$), its power flow is zero, i.e.,

$$f_{l,l} = 0, \forall l. \quad (5.2)$$

2) Generator capacity constraints:

The dispatch level of unit k under contingency c should be within its minimum and maximum generation limits, i.e.,

$$p_k^{\min} \le p_{k,c} \le p_k^{\max}, \forall k, \forall c = 0, 1, \ldots, L+k-1, L+k+1, \ldots, L+K, \quad (5.3)$$

When unit k is tripped ($c = L + k$), its dispatch level is zero:

$$p_{k,L+k} = 0, \forall k. \quad (5.4)$$

3) Nodal flow balance constraints:

The net nodal injection (i.e., generation minus demand) at node i equals the total outflow minus the total inflow. The base-case constraints are:

$$\sum_{k\in\Phi(i)} p_{k,0} - D_i = \sum_{l:\,\alpha(l)=i} f_{l,0} - \sum_{l:\,\beta(l)=i} f_{l,0},\ \forall i. \tag{5.5}$$

Under transmission contingency *c*, the power flow at line *c* is not included, i.e.,

$$\sum_{k\in\Phi(i)} p_{k,c} - D_i = \sum_{l:\,\alpha(l)=i,\ l\neq c} f_{l,c} - \sum_{l:\,\beta(l)=i,\ l\neq c} f_{l,c},\ \forall i, \forall c = 1, ..., L. \tag{5.6}$$

Similarly, under generator contingency *c*, the generation of unit ($c - L$) is not included, i.e.,

$$\sum_{k\in\Phi(i):\,k\neq c-L} p_{k,c} - D_i = \sum_{l:\,\alpha(l)=i} f_{l,c} - \sum_{l:\,\beta(l)=i} f_{l,c},\ \forall i, \forall c = L+1, ..., L+K. \tag{5.7}$$

4) Post-contingency redispatch constraints:

Under contingency *c*, the deviation between the post-contingency dispatch decision and the base-case one for each unit should be within the maximal allowed variation, i.e.,

$$p_{k,0} - \Delta_{k,c} \le p_{k,c} \le p_{k,0} + \Delta_{k,c},$$

$$\forall k, \forall c = 1, \ldots, L+k-1, L+k+1, \ldots, L+K, \tag{5.8}$$

where the maximal allowed variation is the ramp rate multiplied by the corresponding time allowed for corrective actions t_c (minute), i.e.,

$$\Delta_{k,c} = R_k t_c, \forall k, \forall c = 1, \ldots, L+k-1, L+k+1, ..., L+K. \tag{5.9}$$

Under a transmission contingency, t_c = 15 (minute) [3], [4]; under a generator contingency, t_c = 10 (minute) [14], [15][8].

[8] NERC requires the area control error to be recovered within 15 minutes after a generator contingency [14], and ISO New England uses 10-minute reserves to provide a buffer for this requirement [15].

5) Objective function:

The objective is to minimize the total base-case ED cost based on [5]-[11], i.e.,

$$\min \sum_k C_k(p_{k,0}). \tag{5.10}$$

The above corrective SCED model is a large LP problem that has a large number of contingency dispatch decisions with corresponding constraints. These decisions are loosely coupled with the base case through (5.8). Given that constraints (5.6) exclude the power flow at the tripped line, constraints (5.2) are redundant. Likewise, constraints (5.4) are redundant given (5.7). In addition, (5.9) can be computed before optimization. The SCED model only needs to include (5.1), (5.3), (5.5) - (5.8), and (5.10).

5.2.2 Infeasible Contingencies

In practical problems, there does not always exist a feasible solution that satisfies all contingencies. Some of them may incur infeasibility, and load shedding may be necessary. However, even under these infeasible cases, system operators still want to "keep the lights on" as much as possible. As a result, it is important to understand the causes of infeasible contingencies (in this section), and to identify and manage them in the solution process (in the next section).

Enlighted by [6] and [7], we categorize infeasible contingencies that are possible to exist in our SCED model into two types. A Type 1 contingency violates contingency-level constraints (5.1), (5.3), (5.6), or (5.7) at this contingency ($c \neq 0$), is thus "uncorrectable" from the base case. Type 1 contingencies should be removed from the problem [6], [7]. Furthermore, islanding contingencies are not necessarily infeasible. If the tripping of a transmission line islands a load bus, this contingency is Type 1 [7]. Under other islanding contingencies, it may still be possible to balance both the main grid and the island. This possibility should be considered.

A Type 2 contingency conflicts with either the base case or with other contingencies. There may be insufficient ramp rates to make enough adjustment between the base case and a contingency as modeled in (5.8). Multiple contingencies conflict with each other when each one of them is feasible with the base case, but there are not enough rate rates to adjust the base-case ED decisions to satisfy all of them at the same time. Existing methods [6], [7] remove Type 2 contingencies, which is questionable because system operators may still want to keep them, so that the base-case ED decisions are pre-positioned to an operating point where the total violation is minimized for increased reliability.

5.3 Solution Methodology

To solve the above problem, subsection 5.3.1 presents key points and the flow control of our new contingency filtering approach. Our approach decomposes the problem into a linear master SCED problem in subsection 5.3.2 and multiple linear contingency subproblems in subsection 5.3.3.

5.3.1 Key Points and the Flow Control of our Approach

Inspired by [6] and [10], our approach starts with the base-case model, and then solves subproblems to detect active contingencies to be added to the master problem to revise its solution iteratively. In the process, Type 1 contingences are identified and removed in subproblems, and feasible islanding contingencies are managed. As for Type 2 contingencies, instead of always removing them as in existing papers [6], [7], our approach is able to switch the mode on how to handle them based on the operator's option. They can be kept in the master problem for increased reliability; or can be removed for reduced base-case costs.[9] Moreover, the method in [6] is improved to identify simultaneously multiple Type 2 contingencies, which

[9] Quantification of the risk of each option will involve probabilities that are not modeled by the standard corrective SCED formulation [5], and is out of the scope of this paper.

is a necessary feature when keeping them. The reason is that if only one Type 2 contingency can be identified before another one is removed, the second one cannot be identified when the first one is kept.

The flowchart of our algorithm is provided in Fig. 5.1, where sets of contingencies are defined as:

S_C Set of candidate contingencies

S_A Set of (possibly) active contingencies

S_1 Set of Type 1 contingencies

S_2 Set of Type 2 contingencies

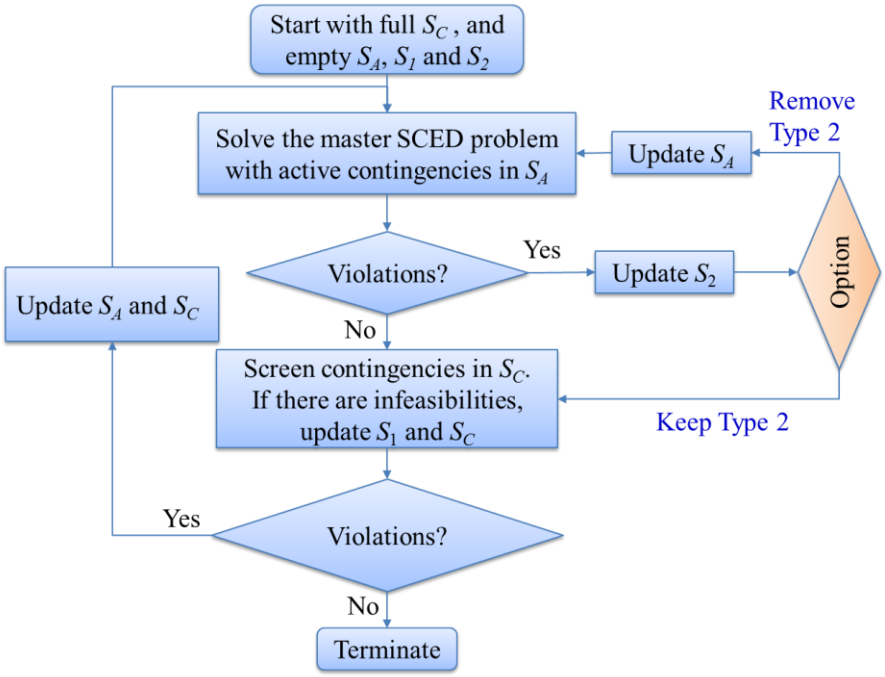

Fig. 5.1. Flowchart of our contingency filtering approach.

The main steps of the solution process are as follows:

1. Initialize a full S_C that contains all "$N-1$" contingencies, and empty S_A, S_1, and S_2.

2. Solve the master SCED problem with all active contingencies in S_A, including corresponding ED decisions and constraints. Obtain an operating point that is delineated by the set of base-case decisions at the n^{th} iteration $\{p_{k,0}{}^n\}$.

3. Check for violated contingencies in the master problem. Once detected, add such contingencies to S2. Otherwise, directly go to Step 5.

4. Proceed to Step 4a or 4b, depending on the option selected by the operator.

   4a: If keeping Type 2 contingencies, go to Step 5;

   4b: If removing Type 2 contingencies, remove them from S_A and go back to Step 2.

5. Screen all contingencies in S_C to minimize violations by solving contingency subproblems. If there are infeasibilities, add infeasible contingencies in S_1 and remove them from S_C.

6. Check for violations. If yes, add violated contingencies in S_A and remove them from S_C, and then go back to Step 2. Otherwise, terminate the algorithm as it converges.

5.3.2 The Master SCED Problem

In the decomposition, we want to formulate the master problem and subproblems linearly so that they can be solved by existing LP solvers. The master problem is formulated as:

$$\min\left[\sum_k C_k(p_{k,0}) + \sum_{c\in S_A} y_c\right], \tag{5.11}$$

where

$$y_c = M \sum_{k\neq c-L} \left(s^U_{k,c} + s^D_{k,c}\right). \tag{5.12}$$

s.t. $$p_{k,c} - s^U_{k,c} \le p^n_{k,0} + \Delta_{k,c}, \forall c \in S_A, \forall k \neq c-L, s^U_{k,c} \ge 0, \tag{5.13}$$

$$p_{k,0}^{n} - \Delta_{k,c} - s_{k,c}^{D} \le p_{k,c}, \forall c \in S_A, \forall k \ne c - L, s_{k,c}^{D} \ge 0, \tag{5.14}$$

Constraints (5.1), (5.3), and (5.5) – (5.7) for $c \in \{0\} \cup S_A$.

Constraints (5.13) are relaxed versions of right inequalities (ramp-up) of redispatch constraints (5.8), with non-negative slack variables $s_{k,c}^{U}$. Symmetrically, constraints (5.14) are relaxed versions of left inequalities (ramp-down) of (5.8), with non-negative slack variables $s_{k,c}^{D}$. These slack variables are penalized by a penalty factor M (as in (5.12)) in the objective function (5.11) to minimize the violation. The value of M should be large (e.g., \$5,000MWh); otherwise, feasible active contingencies may tend to "violate" the relaxed redispatch constraints (5.13) and (5.14), and will be thus misidentified as Type 2 contingencies.

Because penalty terms y_c have resolutions on each contingency (with index c), we are able to identify multiple Type 2 contingencies that appear in the master problem simultaneously. Among multiple contingencies conflicting with each other, those affect the objective value in (5.11) more than others will be identified through optimization.

Since the master problem is an LP problem with a few possibly active contingencies, we need to identify possibly active (and Type 1) ones in subproblems, without ranking contingencies and selecting top-ranked ones.

5.3.3 Contingency subproblems

Subproblems are formulated to check for violations in contingencies to identify possibly active ones. The subproblem of transmission contingency c given $\{p_{k,0}^{n}\}$ is:

$$v_c = \min \sum_k \left(s_{k,c}^{U} + s_{k,c}^{D} \right), \tag{5.15}$$

s.t. $$p_{k,c} - s_{k,c}^{U} \le p_{k,0}^{n} + \Delta_{k,c}, \forall k, s_{k,c}^{U} \ge 0, \tag{5.16}$$

$$p_{k,0}^{n} - \Delta_{k,c} - s_{k,c}^{D} \le p_{k,c}, \forall k, s_{k,c}^{D} \ge 0, \tag{5.17}$$

Constraints (5.1), (5.3), and (5.6) for contingency *c*.

A positive optimal objective value, v_c^*, indicates that contingency *c* is active. When $v_c^* = 0$, contingency *c* is feasible and inactive. If the subproblem is infeasible, contingency *c* is Type 1.

Similarly, the subproblem of generator contingency *c* is:

$$v_c = \min \sum_{k \ne c-L} \left(s_{k,c}^{U} + s_{k,c}^{D} \right), \tag{5.18}$$

s.t. $$p_{k,c} - s_{k,c}^{U} \le p_{k,0}^{n} + \Delta_{k,c}, \forall k \ne c - L, s_{k,c}^{U} \ge 0, \tag{5.19}$$

$$p_{k,0}^{n} - \Delta_{k,c} - s_{k,c}^{D} \le p_{k,c}, \forall k \ne c - L, s_{k,c}^{D} \ge 0, \tag{5.20}$$

Constraints (5.1), (5.3) and (5.7) for contingency *c*.

The coordination between the master problem and subproblems are through the iterative process as in Fig. 5.1. Only a minimum amount of information needs to be communicated. From the master problem to a subproblem, the base-case ED decisions are passed. From a subproblem to the master, the solution status and the objective value are passed.

It can be observed that feasibilities of subproblems do not depend on values of $p_{k,0}^{n}$, so all Type 1 contingencies can be identified and removed at the 1st iteration. Moreover, since all active contingencies identified in subproblems are included in S_A and the master problem, the algorithm converges fast (within 2 to 3 iterations for examples tested in Section 5.5).

5.4 Performance Enhancements

To enhance the performance of our approach, subsection 5.4.1 significantly reduces the overhead through our new warm-start of subproblem models, and subsection 5.4.2 discusses parallel computing implementations.

5.4.1 Warm-start of subproblem models

The overhead issue can be a "performance killer" when deploying optimization methods to practical use. For the corrective SCED problem, the overhead mainly occurs when creating models for all subproblems in software. There may be thousands of subproblems to be solved at each iteration. The overhead time of generating a new LP model for each subproblem may be comparable to or even more than the CPU time of solving it. However, this issue has not been discussed in existing papers related to the corrective SCED problem to the best of our knowledge.

To overcome this issue, we explore the flow control of our contingency filtering approach and structures of subproblem models, and develop new warm-start of subproblem models. This method creates, over all iterations, only two subproblem models (for the first transmission contingency and the first generator contingency), and then reuses created models and makes the fewest number of modifications from one subproblem to another.

The contingency screening procedure (in Step 5) of our approach in serial computing is detailed as in Fig. 5.2, and the parallel computing correspondence will be presented in subection IV-B. The procedure starts with subproblem 1 in the S_C, and then checks subproblem 2, and so forth. When using a language that support functions to modify created optimization models (e.g., CPLEX C++ API [16], AIMMS [17], and Gurobi C++ API [18]), we only have to create a model for subproblem 1 and can then modify this model to represent subproblem 2, and so forth.

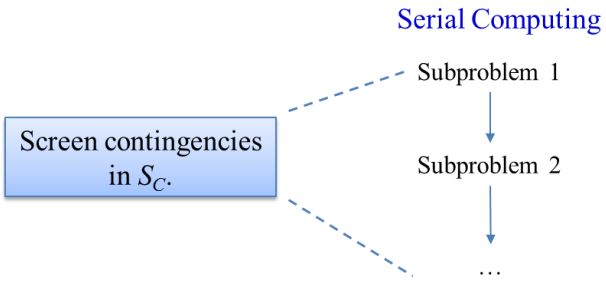

Fig. 5.2. Contingency screening procedure of our contingency filtering approach in serial computing.

To make the fewest modifications from one subproblem to another, we analyze structures of two subproblems corresponding to transmission contingencies *c* and *c'*. Software does not have to treat decision variables corresponding to these two contingencies differently, and the objective functions and most of the corresponding constraints are essentially the same between *c* and *c'*. The only places that differentiate *c* and *c'* are transmission constraints (5.1) and nodal flow balance constraints (5.6) as illustrated in Fig 5.3.

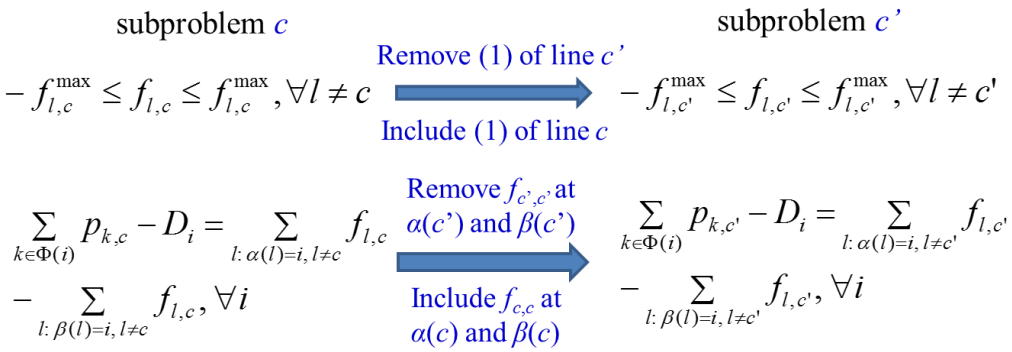

Fig. 5.3. Warm-start between two subproblems of transmission contingencies.

Under contingency *c*, the power flow at the tripped line $f_{c,c}$ is excluded from these constraints. A similar exclusion holds for contingency *c'*. Based on this observation, our method only removes two transmission constraints (for positive and negative directions) corresponding to line *c'* and then includes two corresponding to line *c*. Similarly, at most four nodal flow balance constraints are modified. This process

can start in the first iteration and continue for the remaining ones. As a result, we only need to create one model for all transmission contingency subproblems.

The numbers of operations of our warm-start are compared to those from creating models for all subproblems[10] in Table 5.1.

Table 5.1 Comparison between Our Warm-Start of Subproblem Models and Creating All Subproblem Models in Serial Computing

Constraints	Creating all models	Our new warm start method	
	# of constraints created	# of constraints created	# of constraints modified
(5.1)	$2(L-1) \times L$	$2(L-1)$	$4 \times (L-1)$
(5.3)	$2K \times L$	$2K$	0
(5.6)	$I \times L$	I	$4 \times (L-1)$
(5.8)	$2K \times L$	$2K$	0

The total number of operations to create and modify constraints is significantly reduced. Our warm-start of subproblem models is similar for generator contingencies and is not presented for conciseness.

5.4.2 Parallel Computing

Even after the reduction of overhead, it can still be time-consuming to solve a large number of contingency subproblems. Solving them in parallel can reduce the time.

Commercial solvers, such as CPLEX and Gurobi, directly provide the functionality of multithreaded parallelization [16], [18], where an optimization problem is solved in parallel on multiple threads of a local

[10] All models have to be created in languages that do not support modifications of created models, such as OPL [16].

computer. When applied to the corrective SCED problem, multithreaded parallelization solves each subproblem on multiple threads, while different subproblems are still solved in serial (illustrated in Fig. 5.2).

A different parallelization scheme solves multiple subproblems on different threads in parallel. To implement this parallelization, we adopt the "remote object for distributed parallel optimization" [19] (referred as the "remote object" for the rest of the chapter) provided by CPLEX. One master process is used to solve the master SCED problem and control the algorithm flow, and multiple worker processes are used to solve subproblems. Multithreaded parallelization can also be applied within the remote object, so each subproblem is solved in multiple threads at a lower level, and multiple subproblems are parallelized at an upper level.

Supported communication protocols between the master and each worker include Secure Shell (SSH), Message Passing Interface (MPI), and Transmission Control Protocol/Internet Protocol (TCP/IP). As discussed in Section 5.3, our approach only communicates a minimum amount of information between the master process and workers.

The new warm start method can also be applied in such a parallelization scheme. The contingency screening procedure is illustrated in Fig. 5.4, assuming W workers. For each worker, the new warm start method of subproblem models is applied (see Table 5.2). The new warm start method still significantly reduces the overhead in the usual situation where W is much smaller than L. For example, when there are thousands of contingencies, there may be 100 cores available for parallel computing.

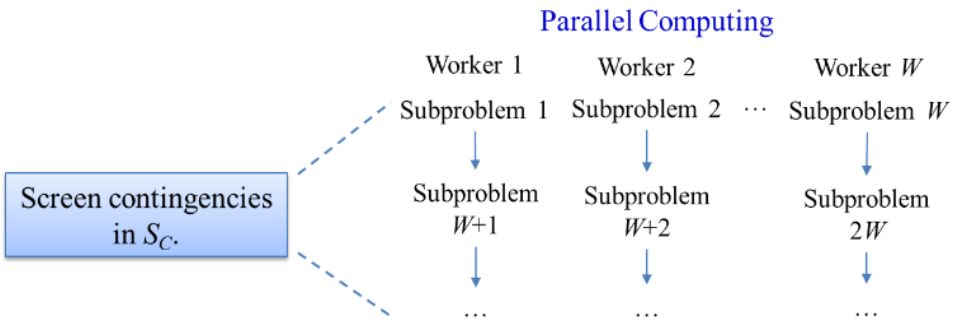

Fig. 5.4. Contingency screening procedure of our contingency filtering approach in parallel computing.

Table 5.2. Comparison between Our Warm-Start of Subproblem Models and Creating All Subproblem Models in Parallel Computing

Constraints	Creating all subproblem models	Our novel warm-start	
	# of constraints created	# of constraints created	# of constraints modified
(5.1)	$2(L-1)\times L$	$2(L-1)\times W$	$4\times(L-W)$
(5.3)	$2K\times L$	$2K\times W$	0
(5.6)	$I\times L$	$I\times W$	$4\times(L-W)$
(5.8)	$2K\times L$	$2K\times W$	0

5.5 Numerical Results

Two problems are tested to demonstrate properties of our contingency filtering approach. In Example 1, the IEEE RTS with three areas is tested to illustrate that our approach is able to manage feasible islanding contingencies. In Example 2, the Polish 2383-bus system is tested to validate that the option to keep Type 2 contingencies offered by our approach can increase the system reliability. It also demonstrates the computational efficiency of our approach with enhancements developed in Section 5.4. Example 1, and Cases 1 and 2 of Example 2 are tested on a laptop with an Intel i7-6920HQ 2.90GHz CPU (4 cores and 8

threads), 32GB memory, and Windows 10, where CPLEX 12.6.1 is called by using OPL. In Case 3 of Example 2, the Storrs HPC cluster [20] is utilized with CPLEX 12.6.1 called by its C++ API. [11]

5.5.1 Example 1

The IEEE RTS with three areas [21] is tested. There are 120 transmission lines, 72 conventional units, and 192 resulting "$N-1$" contingencies. The penalty factor M is set at \$5,000/MWh in our approach. For benchmarking, the direct approach is tested by solving the full-size LP problem.

It turns out that there is no active or infeasible contingency. The total costs of two approaches are the same, \$74,441. The direct approach takes 5.26 seconds of wall clock time, while our approach converges at the 1st iteration in 4.09 seconds.

To better illustrate our approach, ramp rates of all units are reduced to 7.7% of their original values to make some of the contingencies active. In this case, both approaches have the same cost \$78,229. The direct approach takes 8.41 seconds of wall clock time and identifies three active contingencies: 144, 168, and 192, corresponding to Units 24, 48, and 72, respectively. Our approach takes 8.80 seconds and converges in two iterations. The set of active contingencies, S_A, is empty at the 1st iteration. At the 2nd iteration, S_A contains two transmission contingencies (49 and 87) and 17 generator contingencies (140-144, 157, 158, 164-168, and 188-192). The three true active ones, 144, 168, and 192, are included in S_A.

One important finding of this case is that Contingencies 49 and 87 have islanding issues. However, they are feasible and should be kept in the contingency filtering process. If this is not the case, the base-case solution could be positioned such that unnecessary infeasibilities would occur under these two

[11] Testing data and results are available at http://www.engr.uconn.edu/msl/J1_IEEE.htm.

contingencies. This illustrates that our approach can increase the reliability by managing feasible islanding contingencies.

5.5.2 Example 2

The Polish 2383-bus system at winter peak [22] is tested. There are 327 units and 2896 transmission lines.

Case 1. Options between keeping and removing Type 2 contingencies in our approach are compared. Contingencies 2801-2900 are tested, including 96 transmission contingencies and four generator contingencies.

In our approach, the barrier method without crossover, as the fastest LP algorithm provided by CPLEX according to our testing results and consistent with [7], is used to solve the master problem and subproblems. The threshold of the total violation in Step 6 to terminate our approach is 0.001 MW.

After optimization, simulation is conducted to evaluate the consequences of keeping or removing Type 2 contingencies within the algorithm. In this simulation process, base-case ED decisions are fixed at the solution corresponding to each option and one more contingency screening procedure is conducted to solve subproblems of all contingencies that are not Type 1. Results are summarized in Table 5.3.

Table 5.3. Optimization and Simulation Results of Case 1 in Example 3

		Keep Type 2	Remove Type 2
Optimization	Wall clock time (s)	35	36
	Total cost (k$)	4,244.24	1,855.99
	Penalty cost (k$)	2,326.11	0
Base-case ED cost (k$)		1,918.12	1,855.99
Simulation	Total cost (k$)	4,244.24	6,917.39
	Penalty cost (k$)	2,326.11	5,061.40

In optimization, our approach with the option of keeping Type 2 contingencies takes 35 seconds to converge in two iterations. S_A is {2898, 2899, 2900}, S_1 contains 15 transmission contingencies, and S_2 is {2900}. Our approach with Type 2 contingencies removed takes 36 seconds to converge in three iterations, among which the 2nd iteration is a small one that only solves the master problem and removes Contingency 2900, as illustrated by the smaller loop in Fig 5.1. The total cost when keeping Type 2 contingencies is much higher than that when removing them. This outcome is caused by Contingency 2900, which has a high penalty cost and raises the base-case ED cost. The benefit of removing Type 2 contingencies is that the base-case ED cost is reduced.

In the simulation, keeping Type 2 contingencies incurs a lower penalty cost (and resulting total cost) than removing them. This validates that keeping Type 2 contingencies can increase the system reliability when contingency happens. There is a tradeoff between reliability and the base-case cost when making an option on how to treat Type 2 contingencies. Based on experience, when a Type 2 contingency is likely to happen or has high impacts, the operator tends to keep it. Otherwise, the operator tends to remove it.

Case 2. The ability of our approach to identify multiple Type 2 contingencies simultaneously is illustrated. The same contingencies are tested as in the previous case, while ramp rates of all units are reduced by half to create more conflicting contingencies.

Our approach converges in two iterations at 36 seconds when keeping Type 2 contingencies, and converges in three iterations at 37 seconds when removing them. At the 2nd iteration with either option, two Type 2 contingencies, 2899 and 2900, are identified at the same time.

Case 3. Performance enhancements of our approach as developed in Section 5.4 are tested. All 2896 transmission contingencies are considered in this case.

The direct approach is tested by using OPL for benchmarking. The pre-screening step as in [7] is used to identify and remove Type 1 contingencies and some of Type 2 contingencies that are conflicting with

the base case. The SCED problem considering the base case and the remaining contingencies are then solved as a large LP problem.

The optimal objective value is $1,859.85k. The pre-screening step takes 26 minutes and 30 seconds, and identifies 539 Type 1 contingencies. The large LP problem has a peak memory usage of 22 GB, and takes the wall clock time of 17 minutes, where the CPU time is 9 minutes and 32 seconds, and the overhead time 7 minutes and 28 seconds. The pre-screening step is time-consuming, and since there is no decomposition, it is impossible to apply performance enhancements such as warm-start of subproblem models and the remote object to the direct approach.

Our approach is tested in four configurations with their specifications and computational performance summarized in Table 5.4. There is no Type 2 contingency, so there is no difference between whether Type 2 ones are kept or removed for all configurations.

Table 5.4. Computational Performance on Laptop of Case 3 in Example II

Configuration	a	b	c	d
Language	OPL	C++	C++	C++
Subproblem models	Creating all	Creating all	Warm-start	Warm-start
Parallelization	Multi-threaded	Multi-threaded	Multi-threaded	Remote object
Wall clock time	40min08s	2h11min30s	8min34s	3min20s
CPU time	5min30s	18min17s	8min25s	3min03s[12]
Overhead time	34min38s	1h53min13s	9s	17s
Overhead/CPU time ratio	629.70%	619.23%	1.78%	9.29%
Speedup ratio of wall clock time	3.28	1	15.35	39.45

[12] This CPU time is the sum of the CPU time of the slowest subproblem in each group.

Configuration a is the same as previous testing. Configurations b, c and d are implemented in C++; c and d adopt the warm start of subproblems; d exploits the remote object with one thread as the master process, seven as worker processes, and communication via SSH.

For all configurations, the algorithm converges in three iterations. The optimal objective value and the number of Type 1 contingencies are the same as corresponding ones obtained by the direct approach. There are 8 active contingencies in S_A: 474, 544, 1075, and 1798 are identified in the 1st iteration, and 20, 396, 474, and 1798 in the 2nd iteration.

The overhead/CPU time ratio of Configurations a and b are more than 600%, indicating that creating models for all subproblems is a big burden for the entire solution process. In contrast, by using our warm-start of subproblem models, Configuration c only has 9 seconds of overhead, which is 1.78% of the CPU time and is negligible in the wall clock time. This leads to a speedup ratio of 15.35 and demonstrates the benefit of our new warm start method.

When the remote object is used for parallelization, the speedup ratio is increased to 39.45, demonstrating that the remote object is more efficient than multi-threaded parallelization for this case. Meanwhile, the overhead time is longer than that of Configuration c, since seven subproblems are created for workers in Configuration d.

To further accelerate the solution process, 24 cores (2.60GHz CPU, one thread per core) at one compute node with 128 GB memory and the Linux operating system in the Storrs HPC Cluster [20] is utilized. Results are summarized in Table 5.5, where Configuration d uses one core as the master process, 23 as worker processes, and communication via MPI. Configuration a is not tested, because the graphical interface to use OPL is not allowed in our HPC system.

Table 5.5. Computational Performance on HPC of Case 3 in Example 2

Configuration	b	c	d
Wall clock time	21min42s	7min53s	1min51s
CPU time	16min07s	7min52s	1min45s
Overhead time	5min35s	1s	6s
Overhead/CPU time ratio	34.64%	0.21%	5.71%
Speedup ratio of wall clock time	1	2.75	11.73

Although the overhead times at the HPC environment are shorter than corresponding ones at the PC environment, our warm-start can still significantly reduce the overhead time from Configuration b to c. In c, the one second overhead time is only 0.21% of the related CPU time. Furthermore, Configuration d exploiting the remote object can solve the problem in one minute and 51 seconds. This performance demonstrates the computational efficiency of our approach for practical use in real-time operations.

Our approach is able to solve the above cases of the IEEE RTS and the Polish 2383-bus system within 2 to 3 iterations in short amounts of time, demonstrating its scalability.

5.6 Conclusion

This chapter develops a new contingency filtering approach to manage "$N-1$" transmission and generator contingencies in real-time corrective SCED via decomposition and coordination. Our approach provides system operators an important option to keep conflicting contingencies for increased reliability, or remove them for reduced base-case costs. The performance is enhanced by new warm-start of subproblem models and by parallel computing. Our approach solves the Polish 2383-bus system with all transmission contingencies within two minutes, demonstrating its computational efficiency for practical use in real-time operations.

References

[1] A. J. Wood, B. F. Wollenberg, and G. B. Sheble, *Power Generation, Operation and Control*, 3rd ed. Hoboken, NJ, USA: Wiley, 2013.

[2] O. Alsac and B. Stott, "Optimal load flow with steady-state security," *IEEE Transactions on Power Apparatus and Systems*, vol. PAS-93, no. 3, pp. 745-751, May 1974.

[3] NERC, System Operating Limit Definition and Exceedance Clarification, Jan 2015. [Online]. Available: http://www.nerc.com/pa/Stand/Prjct201403RvsnstoTOPandIROStndrds/2014_03_fifth_posting_white_paper_sol_exceedance_20150108_clean.pdf

[4] ISO New England Operating Procedure No. 19 - Transmission Operations, June 2016. [Online]. Available: http://www.iso-ne.com/rules_proceds/operating/isone/op19/op19_rto_final.pdf

[5] A. Monticelli, M. V. F. Pereira, and S. Granville, "Security-constrained optimal power flow with post-contingency corrective rescheduling," *IEEE Transactions on Power Systems*, vol. 2, no. 1, pp. 175-180, 1987.

[6] Q. Jiang and K. Xu, "A novel iterative contingency filtering approach to corrective security-constrained optimal power flow," *IEEE Trans. Power Syst.*, vol. 29, no. 3, pp. 1099-1109, May 2014.

[7] Y. Liu, M. C. Ferris, and F. Zhao, "Computational study of security constrained economic dispatch with multi-stage rescheduling," *IEEE Trans. Power Syst.*, vol. 30, no. 2, pp. 920-929, March 2015.

[8] F. Capitanescu, J. L. M. Ramos, P. Panciatici, D. Kirschen, A. M. Marcolini, L. Platbrood, and L. Wehenkel, "State-of-the-art, challenges, and future trends in security constrained optimal power flow," *Electric Power Systems Research*, vol. 81, no. 8, pp. 1731-1741, 2011.

[9] B. Stott, O. Alsac and A. J. Monticelli, "Security analysis and optimization," *Proc. IEEE*, vol. 75, no. 12, pp. 1623-1644, Dec. 1987.

[10] F. Capitanescu and L. Wehenkel, "A new iterative approach to the corrective security-constrained optimal power flow problem," *IEEE Trans. on Power Syst.*, vol. 23, no. 4, pp. 1533-1541, Nov. 2008.

[11] D. Phan and J. Kalagnanam, "Some efficient optimization methods for solving the security-constrained optimal power flow problem," *IEEE Trans. Power Syst.*, vol. 29, no. 2, pp. 863-872, March 2014.

[12] I. Lelic, "Introduction to Wholesale Electricity Markets (WEM 101): Unit Commitment and Dispatch," ISO New England, April 2014, [Online]. Available: http://www.iso-ne.com/static-assets/documents/2016/04/20160404-06-wem101-unit-commitment-dispatch.pdf

[13] PJM Energy Market, http://www.pjm.com/markets-and-operations/energy.aspx

[14] NERC, Standard BAL-002-0 – Disturbance Control Performance, April 2015. [Online]. Available: http://www.nerc.com/files/bal-002-0.pdf

[15] ISO New England Operating Procedure No. 8 Operating Reserve and Regulation, May 2015. [Online]. Available: http://www.iso-ne.com/rules_proceds/operating/isone/op8/op8_rto_final.pdf

[16] IBM ILOG CPLEX Optimization Studio V12.6.1 documentation. [Online]. Available: http://www.ibm.com/support/knowledgecenter/SSSA5P_12.6.1/ilog.odms.studio.help/Optimization_Studio/topics/COS_home.html

[17] AIMMS. [Online]. Available: http://aimms.com/

[18] Gurobi Optimization. [Online]. Available: http://www.gurobi.com/

[19] S. Rux, "Applications and Use Cases of the CPLEX Remote API," IBM Software Group, Dec 2014. [Online]. Available: http://www-01.ibm.com/support/docview.wss?uid=swg27044403

[20] Storrs HPC Cluster, http://becat.uconn.edu/hpc/hpc-specs/.

[21] IEEE RTS Task Force of APM Subcommittee, "The IEEE reliability test system-1996," *IEEE Trans. Power Syst.*, vol. 14, no. 3, pp. 1010-1020, Aug 1999.

[22] Polish 2383-bus system at winter peak (case2383wp). [Online]. Available: http://www.neos-guide.org/content/optimal-power-flow